INTERNATIONAL CONFERENCE

MEĐUNARODNA KONFERENCIJA

MEETING POINT OF THE SCIENCE AND PRACTICE IN THE FIELDS OF CORROSION, MATERIALS AND ENVIRONMENTAL PROTECTION

STECIŠTE NAUKE I PRAKSE U OBLASTIMA KOROZIJE, ZAŠTITE MATERIJALA I ŽIVOTNE SREDINE

PROCEEDINGS

KNJIGA RADOVA

Under the auspicies of the
MINISTRY OF SCIENCE, TECHNOLOGICAL DEVELOPMENT AND INNOVATION OF THE REPUBLIC OF SERBIA

Pod pokroviteljstvom
MINISTARSTVO NAUKE, TEHNOLOŠKOG RAZVOJA I INOVACIJA REPUBLIKE SRBIJE

https://doi.org/10.65614/uisk_yucorr.2025.26

November 3-5, 2025, Palić, Serbia

CIP - Каталогизација у публикацији
Народна библиотека Србије, Београд

620.193/.197(082)(0.034.2)
621.793/.795(082)(0.034.2)
667.6(082)(0.034.2)
502/504(082)(0.034.2)
66.017/.018(082)(0.034.2)

МЕЂУНАРОДНА конференија YuCorr (26 ; 2025 ; Палић)
Meeting point of the science and practice in the fields of corrosion, materials and environmental protection [Elektronski izvor] : proceedings = Stecište nauke i prakse u oblastima korozije, zaštite materijala i životne sredine : knjiga radova / XXVI YuCorr International Conference, November 3-5, 2025, Palić, Serbia = XXVI YuCorr Međunarodna konferencija ; [organized by] Serbian Society of Corrosion and Materials Protection ... [et al.]] = [organizatori Udruženje inženjera Srbije za koroziju i zaštitu materijala ... [et al.] ; [editors, urednici Miroslav Pavlović, Marijana Pantović Pavlović]. - Beograd : Serbian Society of Corrosion and Materials Protection UISKOZAM = Udruženje inženjera Srbije za koroziju i zaštitu materijala UISKOZAM, 2025 (Beograd : UISKOZAM). - 1 elektronski optički disk (CD-ROM) ; 12 cm
Sistemski zahtevi: Nisu navedeni. - Nasl. sa naslovne strane dokumenta. - Radovi na engl. i srp. jeziku. - Tiraž 200. - Bibliografija uz većinu radova. - Abstracts.

ISBN 978-86-82343-33-2

a) Премази, антикорозиони -- Зборници b) Превлаке, антикорозионе -- Зборници v) Антикорозиона заштита -- Зборници g) Животна средина -- Заштита -- Зборници d) Наука о материјалима -- Зборници

COBISS.SR-ID 181188617

XXVI YUCORR – International Conference | *Međunarodna konferencija*

PUBLISHED BY | *IZDAVAČ*
SERBIAN SOCIETY OF CORROSION AND MATERIALS PROTECTION (UISKOZAM)
UDRUŽENJE INŽENJERA SRBIJE ZA KORZIJU I ZAŠTITU MATERIJALA (UISKOZAM),
Kneza Miloša 7a/II, 11000 Beograd, Srbija, tel/fax: +381 11 3230 028, *office@uiskozam.rs; www.uiskozam.rs*

FOR PUBLISHER | *ZA IZDAVAČA* *Dr MIROSLAV PAVLOVIĆ, predsednik UISKOZAM*

EDITORS | *UREDNICI:* *Dr Miroslav Pavlović, Dr Marijana Pantović Pavlović*
SCIENTIFIC AREA | *OBLAST:* CORROSION AND MATERIALS PROTECTION **|** *KOROZIJA I ZAŠTITA MATERIJALA*
PAGE LAYOUT | *KOMPJUTERSKA OBRADA I SLOG:* *Dr Marijana Pantović Pavlović*
DOI OBTAINED BY | *DOI BROJEVI:* *Studio Grma, Nikole Lunjevice 3D, 32300 Gornji Milanovac*
CIRCULATION | *TIRAŽ:* **200** copies **|** *primeraka*
REPRODUCER | *UMNOŽAVA:* UISKOZAM
PUBLICATION YEAR | *GODINA IZDANJA:* **2025**
ISBN 978-86-82343-33-2

Synthesis : : Materials : : Corrosion : : Environment : : Energy

XXVI YuCorr

Analyse : : Discover : : Coat : : Green : : Protect : : Save : : Sustain

November 3-5, 2025, Palić, Serbia

Ovaj PDF fajl sadrži elektronsku Knjigu radova prezentovanih u okviru Međunarodne konferencije **XXVI YuCorr.** U knjizi su **plavom bojom** obeleženi aktivni linkovi ka pojedinim njenim delovima, iz Sadržaja do naznačenih stranica.

This PDF file contains Proceedings presented on the **XXVI YuCorr** International Conference. It can be easily navigated through the book contents by a single click on the appropriate links in Contents (**showed in blue**).

Autori snose punu odgovornost za sadržaj, originalnost, jezik i gramatičku korektnost sopstvenih radova.

Authors bear full responsibility for the content, originality, language and grammatical correctness of their own works.

XXVI YUCORR IS ORGANIZED BY
ORGANIZATORI XXVI YUCORR-a

SERBIAN SOCIETY OF CORROSION AND MATERIALS PROTECTION

Udruženje Inženjera Srbije za Koroziju i Zaštitu Materijala

INSTITUTE OF CHEMISTRY, TECHNOLOGY AND METALLURGY, UNIVERSITY OF BELGRADE

Institut za Hemiju, Tehnologiju i Metalurgiju, Univerzitet u Beogradu

INSTITUTE OF GENERAL AND PHYSICAL CHEMISTRY, BELGRADE

Institut za Opštu i Fizičku Hemiju

UNION OF ENGINEERS AND TEHNICIANS OF SERBIA, BELGRADE

Savez Inženjera i Tehničara Srbije

ENGINEERING ACADEMY OF SERBIA

Inženjerska Akademija Srbije

XXVI YUCORR IS ORGANIZED UNDER THE AUSPICIES OF THE

MINISTRY OF SCIENCE, TECHNOLOGICAL DEVELOPMENT AND INNOVATION OF THE REPUBLIC OF SERBIA

XXVI YUCORR JE FINANSIJSKI POMOGLO

MINISTARSTVO NAUKE, TEHNOLOŠKOG RAZVOJA I INOVACIJA REPUBLIKE SRBIJE

GENERAL SPONSOR | *GENERALNI SPONZOR*

JADRAN d.o.o., Beograd

SPONSORs | *SPONZORi*

INTERNATIONAL SOCIETY OF ELECTROCHEMISTRY, Switzerland

ALFATERM d.o.o., Čačak

FIRESTOP INTERNACIONAL d.o.o., Nova Pazova

SURTEC ČAČAK d.o.o., Čačak

PPG, Amsterdam, Holandija

KANSAI HELIOS, Gornji Milanovac

INSTITUT ZA PREVENTIVU d.o.o., Novi Sad

INSTITUT ZA OPŠTU I FIZIČKU HEMIJU, Beograd

INSTITUT ZA PUTEVE, Beograd

SAVEZ INŽENJERA I TEHNIČARA SRBIJE, Beograd

Contents

PLENARY LECTURES
PLENARNA PREDAVANJA

Surfactants in corrosion cleaning products

Površinski aktivne materije u sredstvima za uklanjanje korozije

Stevan Blagojević*

Institute of general and physical chemistry, Studentski Trg 12/V, Belgrade, Serbia

https://doi.org/10.65614/uisk_yucorr.2025.26.ch1

**sblagojevic@iofh.bg.ac.rs*

Abstract

Surfactants are indispensable components in modern cleaning and corrosion control formulations. Their amphiphilic molecular structures allow them to interact simultaneously with hydrophobic contaminants and metal surfaces, providing cleaning, wetting, emulsifying, and corrosion-inhibiting functions. The selection of surfactant type, concentration, and synergistic additives determines both the cleaning efficiency and the degree of surface protection. This paper reviews the fundamental mechanisms of surfactant action in corrosion and cleaning products, discusses structure–property relationships, and summarizes current trends in environmentally friendly and multifunctional surfactant systems.

Keywords: *surfactants; corrosion; cleaning products; acid cleaners*

Izvod

Površinski aktivne materije (surfaktanti) predstavljaju neizostavne komponente savremenih formulacija za čišćenje i kontrolu korozije. Njihova amfifilna molekulska struktura omogućava istovremenu interakciju sa hidrofobnim nečistoćama i metalnim površinama, čime obezbeđuju efekte čišćenja, kvašenja, emulgovanja i inhibicije korozije. Izbor tipa surfaktanta, njegove koncentracije i prisustvo sinergističkih aditiva određuju i efikasnost čišćenja i stepen zaštite površine. U ovom radu analiziraju se osnovni mehanizmi delovanja surfaktanata u proizvodima namenjenim čišćenju i zaštiti od korozije, razmatraju se relacije između strukture i svojstava, kao i savremeni trendovi u razvoju ekološki prihvatljivih i multifunkcionalnih sistema površinski aktivnih materija.

Ključne reči: *surfaktanti; korozija; proizvodi za čišćenje; kisela sredstva za čišćenje*

Introduction

Corrosion and surface contamination represent major challenges in industrial maintenance, transportation, and household cleaning. The global market for industrial and institutional cleaners exceeds 50 billion USD annually, with surfactants comprising up to 30% of the total formulation cost. In addition to their cleaning role, surfactants influence corrosion by altering interfacial properties, forming protective films, and mediating the adsorption of inhibitors on metallic substrates.

Surfactants are amphiphilic molecules consisting of a hydrophilic head group (ionic or nonionic) and a hydrophobic tail (alkyl or aryl chain). This dual nature enables them to adsorb at solid–liquid interfaces, lower surface tension, and promote emulsification of soils and oils. Depending on their charge, surfactants are classified as anionic, cationic, nonionic, or amphoteric. Each class exhibits specific behavior toward metal surfaces and corrosion mechanisms.

Mechanism of Action in Cleaning Formulations

The cleaning process involves several concurrent phenomena: wetting of the solid surface, penetration of the contaminant layer, emulsification or solubilization of oily soils, and suspension of particles to prevent redeposition.

Anionic surfactants, such as linear alkylbenzene sulfonates (LAS) or alkyl sulfates, are widely used for their strong detergency and foaming properties. They provide excellent removal of organic soils but may increase corrosion rates on aluminum and mild steel if used without inhibitors.
Nonionic surfactants—such as alcohol ethoxylates, amine oxides, and alkylpolyglucosides (APG)—exhibit lower critical micelle concentrations (CMC) and are less sensitive to water hardness. Their mildness and compatibility with corrosion inhibitors make them preferred for neutral or mildly alkaline cleaning formulations.
Amphoteric surfactants, e.g., cocamidopropyl betaine, adjust their charge with pH and can improve both cleaning and anticorrosion properties through synergistic adsorption on metal surfaces.

Surfactants and Corrosion Mechanisms

Corrosion is an electrochemical process involving oxidation of metals and reduction of oxidizing species such as oxygen, hydrogen ions, or water. Surfactants can significantly modify these reactions by forming adsorbed films on metallic surfaces, altering surface charge, and changing the local environment at the metal/electrolyte interface.
The adsorption of surfactant molecules follows classical Langmuir or Temkin isotherms, depending on molecular orientation and surface coverage. The hydrophilic head group interacts with the metal surface through electrostatic attraction or chemisorption, while the hydrophobic tail extends into the solution, forming a compact barrier that limits the diffusion of corrosive agents such as Cl^-, SO_4^{2-}, or dissolved oxygen.
Cationic surfactants, particularly those based on quaternary ammonium or imidazolinium structures, are among the most effective corrosion inhibitors in acidic and neutral environments. They tend to adsorb strongly on negatively charged steel or copper surfaces, forming densely packed monolayers that suppress both anodic dissolution and cathodic hydrogen evolution. Experimental results have shown that certain alkyltrimethylammonium bromides reduce corrosion current density by more than 90 % in 1 M HCl solution.
Anionic surfactants, although primarily used for cleaning, can also act as inhibitors in alkaline media by forming insoluble complexes with metal cations. For example, alkyl sulfonates and carboxylates may precipitate as protective salts on steel, depending on the pH and ionic strength of the solution.
Nonionic surfactants influence corrosion more indirectly. By reducing surface tension and improving wettability, they ensure uniform distribution of inhibitors and removal of microbubbles or residues that may initiate localized pitting. Additionally, their ability to form mixed micelles with corrosion inhibitors enhances dispersion stability and prolongs protective film lifetime.
Synergistic systems combining surfactants with inorganic inhibitors (e.g., sodium molybdate, zinc phosphate, silicates) or organic compounds (e.g., benzotriazole, fatty amines) are widely applied in industrial cleaning and cooling-water treatment. The surfactant molecules facilitate adsorption of inhibitors on micro-defects of the metal surface, thus increasing the protective efficiency even at lower inhibitor concentrations.
Molecular modeling and quantum chemical calculations (DFT) have recently been employed to predict surfactant–metal interactions, allowing the design of tailor-made molecules with optimal charge density, dipole moment, and adsorption energy. Such computational approaches accelerate the development of next-generation corrosion inhibitors compatible with sustainable “green chemistry” principles.

Environmental and Green Chemistry Considerations

The environmental impact of surfactants has become a key driver of innovation. Biodegradability, aquatic toxicity, and low foaming are essential criteria in modern formulations. Biosurfactants—including rhamnolipids, sophorolipids, and surfactin—show promise as renewable and biodegradable alternatives with intrinsic anticorrosion properties.

Recent studies demonstrate that certain biosurfactants form dense monolayers on steel surfaces, reducing corrosion current density by more than 70%. Additionally, surfactants derived from fatty acids, amino acids, or sugar-based head groups can replace traditional petroleum-based agents.

Industrial Applications

Surfactants are present in virtually all corrosion-related cleaning processes: metal degreasing and pretreatment, pipeline cleaning, automotive cleaning, and household detergents for metallic surfaces. The integration of surfactants with nanoparticle additives (e.g., silica, ZnO, TiO2) is a recent trend to create self-healing or photocatalytically active protective films.

Conclusion

Surfactants play a dual role in cleaning and corrosion protection: they are essential for removing contaminants but can either promote or inhibit corrosion depending on their structure and formulation environment. Understanding the adsorption mechanisms, micellar behavior, and synergistic effects with inhibitors enables the design of multifunctional and environmentally compatible cleaning products. The future of surfactant technology lies in bio-based, low-toxicity, and smart self-assembling systems tailored for specific industrial needs.

Acknowledgements

A short acknowledgement section can be written between the conclusion and the references. Sponsorship and financial support acknowledgments should be included here. Acknowledging the contributions of other colleagues who are not included in the authorship of this paper is also added in this section. If no acknowledgement is necessary, this section should not appear in the paper.

References

1. Rosen, M. J. & Kunjappu, J. T. Surfactants and Interfacial Phenomena, 5th Ed., Wiley, 2023.
2. Myers, D. Surfactant Science and Technology, 4th Ed., Wiley-Interscience, 2020.
3. Singh, A. K., Quraishi, M. A. Effect of surfactants on corrosion inhibition of mild steel in acidic solution, Corrosion Science, 53 (2011) 3398–3410.
4. Holmberg, K. et al. Handbook of Applied Surface and Colloid Chemistry, Wiley-VCH, 2002.
5. Pereira, M. R., Freitas, R. F. S. Role of amphoteric surfactants in corrosion inhibition, Journal of Surfactants and Detergents, 22 (2019) 1331–1342.
6. U.S. EPA, Safer Chemical Ingredients List: Surfactants, 2024.
7. García, M. T. et al. Biosurfactants and green corrosion inhibitors, Colloids and Surfaces A, 657 (2023) 129876.
8. OECD Guidelines for Testing of Chemicals, Section 301: Ready Biodegradability, 2019.

Efficient Approach to Ship Hull Corrosion Monitoring: Paving the Way for Future Vessels

Špiro Ivošević*

University of Montenegro, Faculty of Maritime Studies Kotor, Put I Bokeljske brigade 44, Kotor, Montenegro

https://doi.org/10.65614/uisk_yucorr.2025.26.ch2

*spiroi@ucg.ac.me

Abstract

Although collisions, groundings and fires are among the dominant accidental causes of casulties to ships in operation, corrosion still remains the key monotonous degradation process that affects the structural integrity of the ship's hull in the long term. Despite the development and implementation of international standards promoted by the International Maritime Organization (IMO), Flag States and Classification societies, and the introduction of systems such as the Safety Management System, Common Structural Rules (CSR) and Performance Standard for Protective Coatings (PSPC), corrosion damage still represents a significant challenge in maintaining the expected life cycle of a ship of about 25 years.

Contemporary trends in the digitalization of the maritime industry and the development of advanced sensor and autonomous technologies enable a more efficient and proactive approach to corrosion monitoring. The integration of smart sensors, digital twins, real-time data analytics and artificial intelligence opens new possibilities for predictive maintenance, identification of critical degradation zones and optimization of inspection intervals. Special attention is drawn to underwater remotely operated vehicles (ROVs) and aerial drones, which, thanks to high-resolution cameras and advanced image processing algorithms, thickness measuring devices, represent a safer, faster and more economical alternative to traditional human inspections.

The subject of research in this paper are underwater remotely operated vehicles (ROV), autonomous underwater vehicles (AUV) and aerial drones which, in addition to enabling visual detection of corrosion zones and analysis of surface damage in real time, as wel las to measure the thickness of ship's hull structural elements. Although robotic systems offer increased safety, reliability of data compared to conventional inspections that require the work of human personnel in hazardous conditions, this investigation answers whether these advantages also apply to the thickness measurement and corrosion assessment of ship's hull structural elements.

Keywords: *corrosion; surface protection; rules and regulations; digitalization; remote inspection technique*

Izvod

Iako su sudari, nasukanja i požari među dominantnim slučajnim uzrocima oštećenja brodova u plovidbi, korozija i dalje ostaje ključni monotoni degradacioni proces koji dugoročno utiče na strukturnu cjelovitost brodskog trupa. Uprkos razvoju i implementaciji međunarodnih standarda koje promovišu International Maritime Organization (IMO), države zastave i klasifikaciona društva, te uvođenju sistema kao što su Safety Management System, Common Structural Rules i Performance Standard for Protective Coatings (PSPC), koroziona oštećenja i dalje predstavljaju značajan izazov u održavanju predviđenog životnog ciklusa broda od oko 25 godina.

Savremeni trendovi u digitalizaciji pomorske industrije i razvoju naprednih senzorskih i autonomnih tehnologija omogućavaju efikasniji i proaktivniji pristup praćenju korozije. Integracija pametnih senzora, digitalnih blizanaca, analitike podataka u realnom vremenu i vještačke inteligencije otvara nove mogućnosti za prediktivno održavanje, identifikaciju kritičnih zona degradacije i optimizaciju

intervala inspekcija. Posebnu pažnju privlače podvodna daljinski upravljana vozila (ROV) i aerodroni, koji, zahvaljujući visokorezolutivnim kamerama i naprednim algoritmima obrade slike, uređajima za mjerenje debljine, predstavljaju sigurniju, bržu i ekonomičniju alternativu tradicionalnim inspekcijama koje sprovodi čovjek.

Predmet istraživanja u ovom radu su podvodna daljinski upravljanih vozila (ROV), autonomna podvodna vozila (AUV) i aerodroni koji pored toga što omogućavaju vizuelnu detekciju korozionih zona i analizu površinskih oštećenja u realnom vremenu, koriste i za mjerenje debljine strukturnih elemenata brodskog trupa. Njihova integracija s digitalnim blizancima i sistemima zasnovanim na vještačkoj inteligenciji omogućava stvaranje prediktivnih modela degradacije i pravovremeno donošenje odluka o popravkama, čime se značajno doprinosi produženju životnog vijeka i strukturnoj otpornosti broda. Iako robotizovani sistemi nude povećanu sigurnost, pouzdanost podataka u poređenju s konvencionalnim inspekcijama koje zahtijevaju rad ljudskog osoblja u opasnim uslovima, ovaj rad daje odgovore da li se ove prednosti odnose i na mjerenje debljine i procjenu korozije strukturnih elemenata broda.

Keywords: *korozija; površinska zaštita; pravila i propisi; digitalizacija; tehnika daljinske inspekcije*

Radioecology: from early studies to modern challenges, with a focus on Serbia

Branislava M. Mitrović*, Jelena Matković

Faculty of veterinary medicine University of Belgrade, Bulevar oslobođenja 18, Belgrade, Serbia

https://doi.org/10.65614/uisk_yucorr.2025.26.ch3

*slavatab@vet.bg.ac.rs

Abstract

Radioecology is an interdisciplinary scientific field that studies the migration of radionuclides in the environment, their interactions with ecosystems, and the biological effects of ionizing radiation on non-human biota. Since its origins in the late 19th century, radioecology has evolved in response to nuclear testing, industrial activities, and major nuclear accidents such as Chernobyl and Fukushima. This paper explores both natural and anthropogenic radionuclides, their environmental pathways, and bioavailability, and a methodological approach for asseing the effects of ionizing radiation on non-human biota. Particular emphasis is placed on radioecology in Serbia, covering historical research developments, contamination sources, including depleted uranium, detection techniques for radionuclides and the principles of radiological protection. Through a systematic review of available data, this study highlights the importance of an integrated approach to protecting ecosystems from radiological contamination.

Keywords: *radioecology; NORM; nuclear accidents; reference animals and plants; Serbia*

Izvod

Radioekologija je interdisciplinarna naučna oblast koja proučava migraciju radionuklida u životnoj sredini, njihovu interakcije sa ekosistemima i biološke efekte jonizujućeg zračenja na živi svet. Od svog nastanka krajem 19. veka, radioekologija se razvijala kao odgovor na nuklearna testiranja, industrijske aktivnosti i velike nuklearne nesreće poput Černobilja i Fukušime. Ovaj rad istražuje prirodne i antropogene radionuklide, njihovu migraciju kroz životnu sredinu, uključivanje u karike lanca hrane i metodološki pristup za procenu dejstva jonizujućeg zračenja na živi svet. Poseban naglasak je stavljen na radieokološka ispitivanja u Srbiji, istorijski razvoj, izvore kontaminacije, uključujući osiromašeni uranijum, tehnike detekcije radionuklida i principe radiološke zaštite. Kroz sistematski pregled dostupnih podataka, ova studija ističe važnost integrisanog pristupa zaštiti ekosistema od radioaktivne kontaminacije.

Ključne reči: *radioekologija; NORM; nuklearni akcidenti; referentne životinje i biljke; Srbija*

Introduction

Radioecology is a scientific discipline that investigates the migration of radionuclides within the biosphere, the impacts of ionizing radiation on living organisms in their natural habitats, and the broader ecosystem. By integrating knowledge from multiple scientific fields, radioecology examines how natural or anthropogenic radionuclides move through ecosystems and affect organisms. Researchers study their distribution in air, water, and soil, as well as their influence on non-human biota, tracking their pathways and bioavailability through food chains. Understanding these processes provides crucial insights into the fate and long-term biological and environmental consequences of radionuclides [1-4]. Addressing these complex challenges requires collaboration among experts in physics, chemistry, geochemistry, biology, fostering a multidisciplinary approach to radioecological research.

Radioecology, as a subfield of ecology, emerged after the discovery of ionizing radiation in the late 19th century. One of the earliest studies, conducted in 1896 by scientist Tarkhanov, examined the

effects of X-rays on aquatic plants and animals, laying the foundation for both radiobiology and radioecology [5]. The term "radioecology" was introduced in the 1950s by American researchers Eugene Odum and Stanley Auerbach, alongside Soviet scientists Aleksandr Mikhailovich Kuzin and Aleksey Alekseyevich Peredelsky [3].

The end of World War II, marked by the dropping of the atomic bombs on Hiroshima and Nagasaki, as well as a large number of nuclear tests conducted in the post-war period, led to a major development of radioecology, which was accompanied by the development of new techniques for radionuclide detection. At the end of the 20th century, a nuclear accident occurred in Chernobyl (1986), resulting in widespread radioactive contamination [6]. These events highlighted the vital role of veterinary science in the case of nuclear accidents [7, 8]. Specifically, veterinary expertise is essential for protecting animal health and ensuring the production of radiologically safe food of animal origin.

Radionuclides in environment

All living organisms on Earth are continuously exposed to ionizing radiation due to the presence of radioactive elements in the environment, including soil, water, and air. These elements can be classified as natural or anthropogenic. There are two groups of natural radionuclides, primordial and cosmogenic. Primordial radionuclides, also referred to as terrestrial radionuclides, consist of the parent isotopes of three radioactive decay series: ^{238}U, ^{232}Th, and ^{235}U (Table 1), along with their decay products, as well as ^{40}K and ^{87}Rb [9].

According to the International Atomic Energy Agency [10], Naturally Occurring Radioactive Materials (NORM) are defined as materials containing radionuclides of natural origin where human activities have increased the likelihood of exposure compared to their natural state. This includes cases where radionuclide concentrations remain unchanged or are elevated, the latter often termed Technologically Enhanced Naturally Occurring Radioactive Materials (TENORM). Activities such as mining, fossil fuel combustion, the phosphate industry, and oil and gas extraction can concentrate or redistribute these radionuclides, posing heightened risks to both the environment and human health. Taking into account the current considerations of lithium exploitation in Serbia, it is necessary to highlight the potential exposure to NORM that accompanies this process. Lithium is an industrial resource, but its extraction and processing can lead to exposure to naturally occurring radionuclides originating from the decay series of ^{238}U and ^{232}Th. People can be exposed through the inhalation of dust contaminated with alpha particles, the inhalation of radon and thoron with their decay products, the ingestion of drinking water containing alpha and beta emitters, as well as direct gamma radiation. These radioactive elements are inherent in the geological formations being mined for lithium [11].

Depleted uranium (DU) is a by-product or waste material generated during the enrichment of uranium for nuclear reactors. It is produced from natural uranium ore through industrial processes and has been utilized in various applications. Notably, DU has been used in military contexts, such as armor-piercing munitions and vehicle shielding. Its use in conflicts, including the First Gulf War (Iraq, 1991), the Bosnian War (1995), and the Kosovo conflict (Yugoslavia/Serbia, 1999), has raised significant environmental and health concerns due to its radioactive properties [12, 13].

Cosmogenic radionuclides are formed in the Earth's atmosphere through the interaction of primary cosmic radiation with air atoms (Table 1) [9, 14]. The most common cosmogenic radionuclides are present in Table 1. Only ^{3}H and ^{14}C are significant in terms of the dose to humans and non-human biota.

Table 1. Natural radionuclides in environment [9]

Radionuclide	Half-life	Radionuclide	Half-life
Primordial radionuclides			
^{238}U	4.47×10^{9} years	^{40}K	1.28×10^{9} years
^{232}Th	1.41 x 10^{10} years	^{87}Rb	4.75×10^{10} years

^{235}U	74 x 10^8 years		
Cosmogenic radionuclides			
^{3}H	12.3 years	^{35}S	87.51 days
^{7}Be	53.3 days	^{32}P	14.3 days
^{14}C	5730 years	^{33}P	25.3 days
^{22}Na	2.60 years	^{33}S	87.5 days

Nuclear fission, nuclear fusion and neutron activation are the main physical processes that lead to the creation of artificial radionuclides. Nuclear testing and accidents at nuclear power plants have led to widespread contamination of the environment with artificial radionuclides. Among more than 300 different radionuclides produced by nuclear fission, the most important for living organisms are the isotopes caesium, strontium, ruthenium, cerium, iodine, plutonium and americium (Table 2) [15-17]. Radioactive isotopes of caesium and strontium are chemically similar to potassium and calcium, respectively. This similarity arises because they belong to the same groups in the periodic table. The caesium and the potassium are alkali metals (Group 1), while the strontium and the calcium are alkaline earth metals (Group 2). Due to this chemical similarity, when these radioactive isotopes enter a living organism, they can mimic the behavior of their non-radioactive analogues.

Table 2. The most significant artificial radionuclides [15]

Radionuclide	Half-life	Radionuclide	Half-life
^{89}Sr	50.53 days	^{137}Cs	30.17 years
^{90}Sr	28.79 years	^{141}Ce	32.51 days
^{106}Ru	373.59 days	^{144}Ce	284.91 days
^{131}I	8.02 days	^{239}Pu	2.41 x 10^4 years
^{134}Cs	2.06 years	^{241}Am	432.2 years

Chernobyl and Fukushima Nuclear Disasters

The Chernobyl disaster in 1986 and the Fukushima Daiichi nuclear accident in 2011 are the only two nuclear accidents classified as Level 7 on the International Nuclear Event Scale (INES) [18], representing the most severe level. Although both events caused significant environmental pollution and public concern, they were significantly different in their causes, like the radioactive releases and in the extent of their effects.

The Chernobyl accident (April 26, 1986) was primarily attributed to human error during a poorly planned and executed safety test. The operational staff violated several safety procedures, leading to an uncontrolled power surge that resulted in the catastrophic destruction of the reactor. This led to an uncontrolled nuclear chain reaction that caused a steam explosion, instantaneously destroying the reactor and its building. The explosion was followed by a graphite fire that burned for over ten days, leading to a prolonged and substantial release of a wide range of radioactive materials into the atmosphere [19 - 20] (Table 3). According to the Kashparov report [21], one of the characteristics of the accident was the dispersal of hot particles in the radioactive fallout. The microscopic particles were made of a matrix predominantly composed of uranium oxides, but also of various other materials that were part of the reactor fuel. These distinctive fuel particles were found near the Chernobyl site and in Finland, Sweden, Germany and other European countries [21].

Table 3. Main radionuclides, released into the atmosphere (TBq) following the nuclear accidents at Chernobyl [21-22] and Fukushima [23*-24**]

Radionuclide	Chernobyl	Fukushima

^{131}I	1760	100 – 500**
^{134}Cs	47	8.3 – 50*
^{137}Cs	85	6 – 20**
^{90}Sr	4	0.003 – 0.14*

The Fukushima Daiichi accident, which occurred on March 11, 2011, was the result of a natural disaster. A strong earthquake of magnitude 9.0 struck off the east coast of northern Japan, triggering a massive tsunami that subsequently struck the east coast. At the Fukushima Daiichi Nuclear Power Plant, the tsunami flooded the facility, resulting in the total loss of both off-site grid power and on-site emergency power supply. This power failure shut down the cooling systems of three of the six reactor units. Without cooling, the residual heat caused the reactor cores in these units to gradually overheat, oxidise, and eventually melt over an extended period. These damages led to radioactive material being released into the surrounding region. Unlike Chernobyl, the release of radioactive material at Fukushima occurred over an extended timeframe [23, 24].

The total radioactive release from the Chernobyl accident (5300 PBq, excluding noble gases) was much higher than of Fukushima Daiichi (520 PBq, from 340 PBq to 800 PBq), which represented 10% to 40% of the Chernobyl emissions [19]. Approximately 80% of the radionuclides released during the Fukushima Daiichi accident were transported to marine environments through multiple pathways. These included atmospheric fallout of radioactive particles, as well as direct releases and leakage of contaminated cooling water into the Pacific Ocean [19, 25].

The high radiation levels caused morbidity and mortality among plants and animals in highly contaminated zones around Chernobyl. Within a radius of 7 km around the reactor, the pine trees have been exposed to extreme radioactive contamination from the mixed release of radioactive materials (combining both short and long-lived isotopes). Intense radiation exposure was fatal to vegetation, with gamma radiation doses exceeding 5 mGy per hour during the initial period of exposure. Pine needles absorbed cumulative gamma doses of 80 Gy to 100 Gy, leading to a rapid deforestation of forests. This heavily contaminated area has become known as the Red Forest because of the characteristic brown-red color of the dying trees - one of the most visible biological effects of acute radiation exposure [6, 26]. In addition, the numerous studies have shown elevated mutation rates, chromosomal aberrations, and genetic damage in various in various non-human species (birds, mammals, insects) within the Exclusion Zone (30 km) [27-29]. Following the Chernobyl disaster, significant environmental contamination has been observed within 30 km of the Chernobyl Nuclear Power Plant, with long-lived radioactive materials, such as ^{90}Sr, ^{241}Am, and plutonium isotopes [30].

The nuclear accident at Fukushima, Japan, resulted in the release of significant quantities of water containing radioactive materials into the Pacific Ocean. The high levels of radioactive deposition were reported in the evacuation zone of 20 km, but significant contamination was also detected in regions beyond this immediate area [24]. The surface area contaminated with more than 185 kBq/m² of ^{137}Cs in the Fukushima region has been estimated at approximately 1,700 km² [19]. According to UNSCEAR [24], in areas with enhanced radiation levels, various cytogenetic, physiological, and morphological effects (at the sublethal, individual level) in plant and animal species were observed. The Japanese red pine and Japanese fir trees exhibited developmental abnormalities after the Fukushima accident that were comparable to those observed in Chernobyl [31-33], strongly suggesting that radiation exposure during development was the primary cause of these aberrations. However, the underlying genetic and physiological mechanisms responsible for these radiation-induced developmental effects in conifers remain largely unknown. Also, contrary to expectations, a study on field mice exposed to high radioactive contamination near the Fukushima nuclear power plant showed no detrimental effects on spermatogenesis, underscoring the need for further research into taxonomic variations in radiation sensitivity [34]. Despite the appearance of radiation-induced

base-exchanges in mDNA, masu salmon collected from the radioactively contaminated Mano River showed no phenotypically significant alterations in the sampled population [35].

The Reference Animals and Plants (RAPs)

To support environmental protection, the International Commission on Radiological Protection (ICRP) established a system of Reference Animals and Plants (RAPs), analogous to the concept of the "Reference Man" used in human radiological protection [15]. This framework provides a scientific basis for understanding the relationships between radiation exposure, absorbed dose, and resulting biological effects in selected animal and plant species [36]. The selection of RAPs [36, 37] follows clear ecological and radiological criteria. Chosen species are ecologically important, widely distributed, and representative of both terrestrial and aquatic environments. The process considers various life stages, habitat types, and the organism's potential to accumulate radionuclides. RAPs are also expected to have relatively high exposure levels and sensitivity to radiation. In addition, they should be well studied biologically to allow accurate modelling of radiation dose and effects.

In the field of radioecology, the assessment of the effects of ionizing radiation on non-human biota requires a structured and integrated framework consisting of five key elements [24]. The first element, exposure characteristics, involves analyzing the spatiotemporal dynamics of radionuclide distribution in the environment, understanding of species-specific uptake pathways and bioaccumulation processes, and the internal distribution of radionuclides within organisms, to enable accurate dose estimation. The second element recognizing the diversity of non-human biota, is essential to select suitable reference organisms (Table 4) that are representative of the ecosystems under study and relevant to the geographical area of interest. The selection should be based on ecological relevance, data availability, and, where applicable, conservation status.

The third element, dosimetry modelling, plays a crucial role in the accurate estimation of absorbed dose, either to the whole organism or specific target tissues. Dosimetric calculations should include geometric corrections to account for the size, shape, and internal anatomy of the organism, as these factors influence energy deposition and dose distribution. The use of appropriate relative biological effectiveness (RBE) values is necessary to account for differences in the biological impact of various radiation qualities. The fourth element is the definition of ecologically significant endpoints in radiological assessment, which emphasize population-level deterministic effects like mortality and reproductive capacity, as well as the formulation of corresponding reference dose levels. The fifth element, a comprehensive understanding of the effects of radiation on biota, requires a clear link between individual radiation-induced responses and their potential impact on population dynamics. This involves considering the ecological relevance of observed biological effects, such as changes in survival, reproduction, or behavior, and evaluating whether these responses are likely to result in measurable impacts at the population scale. It is also necessary to take into account the role of background radiation and natural biological variability within and between populations, both of which can affect the sensitivity and resilience of species to radiological stressors [24].

Table 4. The Reference Animals and Plants (RAPs) [24]

Reference organism	Description
Earthworm	soil invertebrate
Rat	burrowing mammal
Bee	above ground invertebrate
Wild grass	grasses, herbs and crops
Pine tree	tree
Deer	herbivorous mammal

Duck	bird
Frog	amphibian
Brown seaweed	microalgae
Trout	pelagic fish
Flatfish	benthic fish
Crab	crustaceans

In radioecological assessments, threshold doses, dose rate limits, and Derived Consideration Reference Levels (DCRLs) are used to assess the radiological risk to non-human biota [24, 36]. A threshold dose refers to the minimum absorbed dose of ionizing radiation required to induce a measurable biological effect in an organism. This value is typically determined from laboratory or field studies that examine endpoints such as mortality, reduced reproduction, developmental abnormalities, or behavioral changes. Threshold doses are often used in dose–response analyses and expressed in gray (Gy) or milligray (mGy) [24].

A dose rate limit is a fixed value of radiation absorbed per unit time (typically in μGy/h) that serves as a screening criterion in radiological assessments. Below this limit, adverse effects at the population level are not expected, and no further detailed evaluation is usually required. For example, the ERICA Tool [38, 39] and FASSET framework [40] propose generic screening dose rates of 10 μGy/h (0.24 mGy/day) for terrestrial and freshwater organisms and 40 μGy/h 0.96 mGy/day] for marine organisms These limits are developed to ensure a high level of protection across taxa.

In 2008, the International Commission on Radiological Protection (ICRP) introduced the concept of Derived Consideration Reference Levels (DCRLs) [36], which define bands of dose rates within which there is a probability of detecting radiation-induced effects in Reference Animals and Plants (RAPs). For instance, ICRP [41] reports that dose rates between 0.1 mGy/day and 1 mGy/day may cause limited effects on sensitive endpoints in some organisms. From 10 mGy/day to 100 mGy/day, effects become likely for many endpoints across diverse biota; however, sensitivity varies considerably among RAPs, for example, bees, crabs, and earthworms generally show lower sensitivity [41]. DCRLs are not strict regulatory limits but help inform decision-making for environmental radiation protection. If estimated dose rates are within or exceed a DCRL band, a more detailed, site-specific ecological assessment should be carried out to evaluate whether protective measures are needed [36]. The establishment of RAPs and associated dose assessment frameworks represents a significant advancement in environmental radiological protection. By providing standardized reference points, these instruments enable consistent assessment of radiation effects on non-human biota, with the aim of protecting environmental integrity.

Radionuclide Detection Techniques in Radioecology

In radioecological investigations the determining the content of radionuclides is fundamental to assess their distribution, transfer, and potential impacts on non-human biota and the environment. One of the most common techniques used in radionuclide detection is gamma spectrometry. Its primary benefit, besides wide accessibility, is the ability to simultaneously identify and quantify multiple radionuclides in a single measurement [42, 43]. The technique is non-destructive, allowing for the analysis of samples without altering their physical or chemical properties [44]. However, it has limited sensitivity for low-energy gamma emitters [45]. Furthermore, the resulting spectra can be complex, making additional analysis and interpretation challenging and requiring specific skills and experience [46].

Alpha spectrometry, not so widely accessible as gamma spectrometry, due to limited application only on alpha emitters and requirement specialized equipment and expertise. Sample preparation requires specialized instrumentation and analytical expertise [43, 47]. Nonetheless, alpha spectrometry is

highly sensitive to alpha-emitting radionuclides, allowing for the detection of low concentrations. It can also provide information regarding specific radionuclides in a sample and precise quantification of alpha-emitting isotopes [48].
Liquid Scintillation Counting (LSC) is another useful technique, particularly for beta-emitting radionuclides, and it has proven effective for low-energy beta emitters. LSC can be used for a variety of samples, including biological tissues and liquids. However, without additional research, LSC provides limited insight into the specific radionuclides present [49].
In many academic disciplines, such as the biological sciences, agriculture, industry, and food and nutrition, Neutron Activation Analysis (NAA) is frequently used due to its high level of accuracy and sensitivity for trace elements (<0.01%). NAA can also analyze multiple elements from a single sample [50].
Mass spectrometry is another common analytical method encountered in radioecology. Its main advantages are high precision and sensitivity, leading to versatile applications. Mass spectrometry is very efficient in determining isotopic ratios, which are important for tracing the origin of radionuclides. Some disadvantages include high cost and relatively complex sample preparation. Additionally, mass spectrometry provides limited information about the chemical and molecular structure of compounds [51-53].

Radioecology investigation in Serbia

The radiation protection legislation in the Federal People's Republic of Yugoslavia was established in 1947 with the adoption of the Rulebook on Protective Measures during Work with X-ray Devices and Radioactive Substances [54, 55]. This pioneering regulation established fundamental safety standards for the use of radioactive materials in both medical and industrial settings. It marked the beginning of a structured approach to radiation protection, later expanded through the adoption of the Law on Protection from Ionizing Radiation in 1959. Further legislative development followed in 1965 with the adoption of the Basic Law on Ionizing Radiation Protection in the Socialist Federal Republic of Yugoslavia (SFRY), forming the core of the national radiation safety framework.
The Yugoslav Society for Radiation Protection was founded on October 11, 1963, during the Yugoslav Symposium on Radiological Protection held in Portorož. In 1969, the society became a full member of the International Commission on Radiological Protection (ICRP). Between 1972 and 2003, the organization underwent several changes in response to evolving political circumstances, ending in the establishment of the Society for Radiation Protection of Serbia and Montenegro in 2005.
The development of radioecological research within the territory of the former Yugoslavia, presently Serbia, can be most effectively tracked by examining the number of publications presented at the conferences of the Society for Radiation Protection. Research conducted by Todorović et al. [56] indicated a significant increase in the number of published works in the field of radioecology after 1975. Notably, the conference proceedings published in 1996, marking a decade since the Chernobyl accident, with 50% of the papers focused on radioecology, and those from 2016, commemorating its 30th anniversary, with 95% of contributions in this area, stand out. In addition to their participation in symposia, scientists have published a considerable number of papers in both domestic and international journals. Numerous studies have investigated the levels of radionuclides in various environmental compartments in Serbia. Regarding soil, studies have measured natural radionuclides such as 40K, 238U,226Ra, 232Th, across different regions [56 - 58], including the cities of Belgrade and Novi Sad [59] as well as mountain regions [60, 61]. The artificial radionuclide 137C was also detected in Serbian soils, resulting from the Chernobyl accident and historical atmospheric nuclear weapons testing [62 - 66]. Moreover, studies across Serbia have used the fallout radionuclide ^{137}Cs to quantify soil erosion rates [67, 68]. The non-human biota of Serbia also contains measurable levels of radionuclides. Studies on plants, particularly medicinal herbs, have reported the presence of 40K, 238U, 226Ra, 232Th, and 137Cs [69 - 71]. In animals, including fish, livestock, and game meat, the

40K is the primary contributor to radiation exposure, while ^{137}Cs was also frequently detected [60, 4]. Researchers have also employed tools like ERICA and RESRAD to assess radiation exposure to both human and non-human biota in the Serbian environment [72, 73].

During the 1999 Kosovo conflict, NATO aircraft deployed depleted uranium (DU) weapons against specific targets in Kosovo, Southern Serbia, and Montenegro. NATO confirmed to the United Nations that over 30,000 DU rounds were used in Kosovo, more than 2,500 rounds in Serbia, and 300 rounds in Montenegro [78]. According to the SEPA [76], an estimated 15 tons of DU were used during the NATO bombing of Kosovo. The use of DU weapons has raised significant concerns about the long-term environmental and health impacts on the affected regions. Depleted uranium, while less radioactive than natural uranium, can still pose serious health risks due to its chemical toxicity and potential to cause kidney damage and cancer. Efforts to clean up contaminated sites have been ongoing [77], but the full extent of the contamination and its effects on local populations are still being studied. To assess DU contamination in soil, water, air, and bioindicators, environmental monitoring has been carried out [78 - 81]. After the NATO attack, in certain regions, elevated uranium levels and non-natural isotopic ratios have been found. Between 2002 and 2007, the Vinča Institute of Nuclear Sciences carried out cleanup operations in southern Serbia to remediate DU-contaminated sites [77]. Due to the use of depleted uranium weapons and the targeting of industrial facilities such as large power plants, chemical plants, and oil refineries, the bombing of the former Yugoslavia caused serious environmental harm. This resulted in the release of numerous toxic chemical substances into the atmosphere, hydrosphere, and lithosphere. Consequently, these pollutants entered the biosphere via natural cycles and trophic pathways, accumulating in living organisms. A number of these substances have been shown to cause genetic mutations, cancer, and developmental abnormalities. Since pollutants are expected to have long-term effects on human health, non-human biota, and the ecosystem as a whole, a multidisciplinary scientific team must collaborate to fully evaluate the environmental effects of the bombing [82].

The environmental radioactivity monitoring program in Serbia uses systematic and ongoing measurements of the radionuclide content of different environmental samples to track the level of radioactivity in the country's environment. This monitoring covers air, precipitation, soil, surface waters, drinking water, food products of plant and animal origin, milk, and animal feed. The legal basis for this monitoring is established by the Rulebook for establishing a programme of systematic environmental radioactivity examination [83]. The Serbian Radiation and Nuclear Safety and Security Directorate (SRBATOM) is the primary authority responsible for overseeing and implementing these monitoring activities. SRBATOM also publishes annual reports detailing the levels of population exposure to ionizing radiation from the environment. These reports are available from 2010 to 2024, with specific reports for 2016 and 2017 focusing on locations affected by depleted uranium. To ensure timely response in case of radiological emergencies, Serbia has established a Programme of early warning of emergency [84]. Furthermore, Serbia actively participates in the European Radiological Data Exchange Platform (EURDEP), facilitating the real-time exchange of environmental radiation monitoring data with other European countries. Radioactivity monitoring has also been carried out in previous periods. Between 1965 and 1987, the Federal Committee for Labour, Health and Social Welfare Yugoslavia released yearly reports on environmental radioactivity under the title “Radioactivity of the Environment in Yugoslavia” [55].

The radioecological investigations in Serbia provide data on the state of radioactivity in the environment, the presence of natural and anthropogenic radioactive elements and their impact on living beings. This research will allow a broader understanding of the behavior of radioactive substances in complex ecosystems. Future studies will likely focus on refining dose assessment models, mitigating long-term contamination effects, and strengthening environmental protection strategies to protect the ecological integrity.

Conclusion

Radioecology has developed into an important interdisciplinary field that addresses the transport, bioavailability, and ecological effects of radionuclides in the environment. The historical evolution of this discipline has been shaped by nuclear energy production, accidental releases of radionuclides, and industrial activities, all of which have necessitated methodological advancements in radionuclide detection and radiological risk assessment. The environmental impacts of nuclear disasters, such as Chernobyl and Fukushima, highlight the need for continuous monitoring and improved radiological protection measures. In Serbia, radioecological research has played a crucial role in assessing contamination levels from both natural sources and anthropogenic activities, including the legacy of depleted uranium usage. Researchers provide valuable insights into the state of radioactivity in the environment and radiological safety by integrating international standards, dose assessment models, and advanced detection techniques. The findings emphasise the importance of sustained scientific collaboration, environmental policy development, and further refinement of methodologies for assessing radiation effects on non-human biota. Future research should focus on improving dosimetric models, refining ecological risk assessment frameworks, and exploring mitigation strategies to ensure effective environmental radioprotection.

Acknowledgements

The study was supported by the Ministry of Science, Technological Development and Innovation of the Republic of Serbia (Contract number 451-03-136/2025-03/200143).

References

1. W.E., Martin, Radioecology and the Study of Environmental Radiation Published by: Torrey Botanical Society. Bulletin of the Torrey botanical club, 91(4), 283–323, 1964.
2. C. M. Vandecasteele, 2004. Environmental monitoring and radioecology: A necessary synergy, J. Environ. Radioact., 72 1–2), 17–23, 2004.
3. M. R. Alexakhin, “Radioecology: History and state-of-the-art at the beginning of the 21st century” in Radiation Risk Estimates in Normal and Emergency Situations, 159–168. Springer, 2006.
4. B. Salbu, Challenges in radioecology. J. Environ. Radioact., 100(12), 1086–1091, 2009.
5. I. Tarkhanov, Experiments on Roentgen X-ray effects on a living organism. Bull. St-Petersburg Biological Laboratory, 1(3), 47–52, 1896 (in Russian).
6. International Atomic Energy Agency (IAEA). Environmental consequences of the Chernobyl accident and their remediation: twenty years of experience. Report of the Chernobyl Forum Expert Group “Environment”. IAEA, Vienna 2006.
7. D. Waltner-Toews, Food safety in a nuclear crisis: The role of the veterinarian, Can. Vet. J., 31, 361-366, 1990.
8. World Association of Veterinary Food Hygienists WAVFH. Report on International Round Table Conference "Accidental Radiation Contamination of Foodof Animal Origin" Volume I. Stockholm, Sweden, 1987.
9. National Research Council (NRC). Evaluation of Guidelines for Exposures to Technologically Enhanced Naturally Occurring Radioactive Materials. Washington, DC: The National Academies Press, 1999. https://doi.org/10.17226/6360.
10. International Atomic Energy Agency (IAEA). *Extent of Environmental Contamination by Naturally Occurring Radioactive Material (NORM) and Technological Options for Mitigation*, Technical Reports Series No. 419, IAEA, Vienna, 2003.
11. D. Gbondo, M. Pham, Y. Zhao, N. Tsurikov, K. Rumchev, Radioactivity and exposure to radiation in lithium mining in Western Australia, *J. Hazard. Mater*, 18100652, 2025.
12. J. P. McLaughlin, "Exposure potential of depleted uranium ammunition in the environment – a review," in *The Natural Radiation Environment VII: VIIth Int. Symp. On the NRE*, Elsevier. 95–104, 2005.
13. Y. Wang, K. Von Gunten, B. Bartova, N. Meisser, M. Astner, M. Burger, R. Bernier-Latmani, Products of in Situ Corrosion of Depleted Uranium Ammunition in Bosnia and Herzegovina Soils. *Environ. Sci. Technol.*, **50(22),** 12266–12274, 2016.

14. UNSCEAR, *Sources and Effects of Ionising Radiation*. United Nations Scientific Committee on the Effects of Atomic Radiation, New York, 2000.
15. The International Commission on Radiological Protection (ICRP), *Nuclear Decay Data for Dosimetric Calculations*. ICRP Publication 107. *Ann. ICRP*, 38, 3, 2008.
16. J. Masarik, "Origin and distribution of radionuclides in the continental environment," in *Environmental Radionuclides: Tracers and Timers of Terrestrial Processes*, K. Froehlich, Ed. Elsevier, pp. 1–25, 2009.
17. Т. А. Макаревич. *Радиоэкология.* Минск: БГУ, 2013.
18. International Atomic Energy Agency (IAEA). *INES The international nuclear and radiological event scale, user's manual*. IAEA, Vienna, 2008.
19. G. Steinhauser, A. Brandl, T.E. Johnson, Comparison of the Chernobyl and Fukushima nuclear accidents: A review of the environmental impacts, *Sci. Total Environ.,* **470–471**, 800–817, 2014.
20. T. Imanaka, G. Hayashi, S. Endo, Comparison of the accident process, radioactivity release and ground contamination between Chernobyl and Fukushima. *J. Radiat. Res.*, **56**, i56–i61. 2015.
21. V. Kashparov, *Report Chernobyl: 30 Years of Radioactive Contamination Legacy*. Ukrainian Institute of Agricultural Radiology (UIAR) o National University of Life and Environmental Sciences of Ukraine (NUBiP of Ukraine), Kyiv, 2016. Available: https://inis.iaea.org/records/5cqh2-5rp06.
22. B. Howard, "Environmental pathways of radionuclides to animal products in different farming and harvesting systems" in *Nuclear and radiological emergencies inanimal production systems preparedness, response and recovery*. Naletoski I, Luckins AG, Viljoen G, editors. Berlin (DE): Springer; 2021. Available from: https://www.ncbi.nlm.nih.gov/books/NBK585721/ doi: 10.1007/978-3-662-63021-1
23. International Atomic Energy Agency (IAEA), *The Fukushima Daiichi accident*. IAEA, Vienna, 2015.
24. UNSCEAR, Sources, Effects and Risks of Ionizing Radiation: United Nations Scientific Committee on the Effects of Atomic Radiation 2020/2021. Report to the General Assembly, with Scientific Annexes, vol. II, Scientific Annex B. United Nations, New York, 2022.
25. Y. Inomata, M. Aoyama, T. Tsubono, D. Tsumune, D., K. Hirose, Spatial and temporal distributions of ^{134}Cs and ^{137}Cs derived from the TEPCO Fukushima Daiichi Nuclear Power Plant accident in the North Pacific Ocean by using optimal interpolation analysis. Environ. Sci.: Process. Impacts, **18(1),** 126–136, 2016.
26. D. Holiaka, S. Fesenko, V. Kashparov, V. Protsak, S. Levchuk, M. Holiaka, Effects of radiation on radial growth of Scots pine in areas highly affected by the Chernobyl accident, J. Environ. Radioact., **222**, 106320, 2020.
27. T. G. Hinton, R. Alexakhin, M. Balonov, N. Gentner, J. Hendry, B. Prister, P. Strand, D. Woodhead, Radiation-induced effects on plants and animals: Findings of the United Nations Chernobyl forum, Health Phys., **93(5),** 427–440, 2007.
28. A. P. Møller, I. Nishiumi, H. Suzuki, K. Ueda, T. A. Mousseau, Differences in effects of radiation on abundance of animals in Fukushima and Chernobyl, Ecol. Indic., 24, 75–81, 2013.
29. C. Adam-Guillermin, T. Hertal-Aas, D. Oughton, L. Blanchard, F. Alonzo, O. Armant, N. Horemans, "Radiosensitivity and transgenerational effects in non-human species," *Ann. ICRP*, **47(3-4)**, 327-341, 2018. doi:10.1177/0146645318756844.
30. D. Bugai, S. Kireev, M. A. Hoque, Y. Kubko, J. Smith, Natural attenuation processes control groundwater contamination in the Chernobyl exclusion zone: evidence from 35 years of radiological monitoring, *Scientific Reports*, **12(1)**, 1–16, 2022.
31. Y. Watanabe, M. Kubota, J. Hoshino, Y. Kubota, K. Maruyama, S. Fuma, et al., Morphological defects in native Japanese fir trees around the Fukushima Daiichi Nuclear Power Plant, *Sci. Rep.*, 5, 3232, 2015.
32. V. Yoschenko, K. Nanba, S. Yoshida, Y. Watanabe, T. Takase, N. Sato, et al., Morphological abnormalities in Japanese red pine (Pinus densiflora) at the territories contaminated as a result of the accident at Fukushima Dai-Ichi Nuclear Power Plant, *J. Environ. Radioact.*, **165(60–67),** 2016.
33. T. A. Mousseau and A. P. Møller, Plants in the light of ionizing radiation: What have we learned from Chernobyl, Fukushima, and other 'hot' places? *Frontiers in Plant Science*, **11(1–9),** 2020.
34. T. Okano, H. Ishiniwa, M. Onuma, J. Shindo, Y. Yokohata, Effects of environmental radiation on testes and spermatogenesis in wild large Japanese field mice (Apodemus speciosus) from Fukushima, *Nature Publishing Group*, 1–8, March, 2016.
35. M. F. Bin Yusof, G. Kawada, M. Enomoto, A. Tomiya, M. Watanabe, D. Morishita, S. Izumi, M. Nakajima, "Mutations Observed in Mitochondrial DNA of Salmon Collected in Mano River, Fukushima

Prefecture, Japan," in *Low-Dose Radiation Effects on Animals and Ecosystems: Long-Term Study on the Fukushima Nuclear Accident*, M. Fukumoto, Ed. Singapore: Springer Singapore, 89–98, 2020.
36. International Commission on Radiological Protection (ICRP), *Environmental Protection - the Concept and Use of Reference Animals and Plants*. ICRP Publication 108. Ann. ICRP, 38, 4-6, 2008.
37. International Atomic Energy Agency (IAEA), Approaches for modelling of radioecological data to identify key radionuclides and associated parameter values for human and wildlife exposure assessments. Vienna, 2021.
38. J. E. Brown, B. Alfonso, R. Avila, N. A. Beresford, D. Copplestone, G. Pröhl, and A. Ulanovsky, The ERICA Tool, *J. Environ. Radioact.*, **99(9),** 1371–1383, 2008.
39. J. E. Brown, B. Alfonso, R. Avila, N. A. Beresford, D. Copplestone, A. Hosseini, A new version of the ERICA tool to facilitate impact assessments of radioactivity on wild plants and animals, *J. Environ. Radioact.,* **153(141–148),** 2016.
40. C. M. Larsson, The FASSET framework for assessment of environmental impact of ionising radiation in European ecosystems-an overview, *J. Radiol. Prot.*, **24(4A),** A1-12, 2004
41. International Commission on Radiological Protection (ICRP), *Protection of the environment under different exposure situations.* ICRP Publication 124. Ann. ICRP 43(1), 2014.
42. J. Qiao, S. Nielsen, Radiochemical methods-Radionuclide Monitoring, in *Encyclopedia of Analytical Science*, Elsevier, 2019, 31-39.
43. S. Pommé, Radionuclide metrology: confidence in radioactivity measurements, *J. Radioanal. Nucl. Chem.*, **331**, 4771-4798, 2022.
44. B. Salbu, O. C. Lind, Analytical techniques for charactering radioactive particles deposited in the environment, *J. Environ. Radioact.,* **211**, 106078, 2020.
45. S. Song, J. Kim, J. H. Park, S. Kim, T. Lim, J. H. Kim, S. Kim, B. Lee, Measurements of low dose rates of gamma-rays using position-sensitive plastic scintillation optical fiber detector, *Nuclear Engineering and Technology*, **54(9),** 3398-3402, 2022.
46. K. Buchtela, Radiochemical methods. Gamma-Ray Spectrometry, in *Encyclopedia of Analytical Science*, Eds. Elsevier, 2005 ,72-79.
47. N. Vajda, R. Pöllänen, P. Martin, C.-K. Kim, Alpha spectrometry, in *Handbook of Radioactivity Analysis* M. F. L'Annunziata, Ed. Academic Press, 2020, 493-573.
48. A. Suckow, Analysis of Radionuclides, in *Radioactivity in the Environment*, K. Froehlich, Ed. Elsevier, 2009, 363-406.
49. X. Hou, Liquid scintillation counting for determination of radionuclides in environmental and nuclear application, *J. Radioanal. Nucl. Chem.*, **318**, 1597–1628, 2018.
50. M. F. L'Annunziata, Introduction: Radioactivity and Our Well-Being, in *Radioactivity*, M. F. L'Annunziata, Ed. Elsevier Science B.V, 2007, 1-45.
51. W. Bu, J. Zheng, M. E. Ketterer, S. Hu, S. Uchida, X. Wang, Development and application of mass spectrometric techniques for ultra-trace determination of ^{236}U in environmental samples - A review, *Anal. Chim. Acta*, **995**, 1-20, 2017.
52. A. Quemet, A. Hubert, A. M. Sánchez Hernández, M. Crozet, G. Bailly, A. Dobney, G. Duhamel, J. Hiess, U. Repinc, S. Mialle, B. Boulet, R. Escoube, C. Bouvier-Capely, F. Pointurier, S. Picart, An isotope dilution mass spectrometry overview: tips and applications for the measurement of radionuclides, *J. Anal. At. Spectrom.,* **39(7),** 1665-1699, 2024.
53. A. El-Aneed, A. Cohen, J. Banoub, Mass Spectrometry, Review of the Basics: Electrospray, MALDI, and Commonly Used Mass Analyzers, *Appl. Spectrosc. Rev.*, **44(3),** 210–230, 2009.
54. I. Avramović, "Regultativa na simpzijumima Društva za zaštitu od zračenja," in DZZ SCG 2019, 575–583.
55. B. Mitrović, Udžbenik iz radiobiologije sa radijacionom higijenom. Beograd, 2021.
56. I. Bikit, M. Veskovi, J. Slivka, M. Krmar, Lj. Čonkić, S. Ćuk, The Radioactivity of Vojvodina Agricultural Soil, Archive of oncology, **9(4),** 202–212, 2001.
57. S. Dragović, L. J. Mandić, M. Momčilović, A. Onjia, Population doses from terrestrial gamma exposure in Serbia, Archive of Oncology, **15(3–4),** 78–80, 2007.
58. I. Bikit, S. Forkapic, J. Nikolov, N. Todorovic, D. Mrdja, Radioactivity of the Agricultural Soil in Northern Province of Serbia, Vojvodina, WASET, International Journal of Environmental and Ecological Engineering, **5(4),** 298–303, 2011.

59. Lj. Janković Mandić, I. Jelić, M. Rajačić, J. Krneta Nikolić, I. Vukanac, S. Dimović, N. Sarap, M. Šljivić-Ivanović, Distribution of natural radionuclides and ^{137}Cs in urban soil samples from the city of Novi Sad, Serbia-Radiological Risk Assessment, Toxics**, 11(345),** 2023.
60. B. M. Mitrović, O. Vitorović, J. Ajtić, B. Vranješ, Radioactivity in the environment and food chain at Mt. Maljen, Serbia, Rom. Rep. Phys., **72(4),** 1–11, 2020.
61. B. M. Mitrović, D. Todorović, J. Ajtić, B. Vranješ, A review: natural and artificial radionuclides and radiation hazard parameters in the soil of mountain regions in Serbia, J. Agric. Sci., **65**(1), 1–18, 2020.
62. Lj. Janković Mandić, R. Dragović, S. Dragović, Distribution of lithogenic radionuclides in soils of the Belgrade region (Serbia), *J. Geochem. Explor.*, **105(1–2),** 43–49, 2010.
63. D. Popović, P. D. Todorović, V. Spasić Jokić, Contents of radionuclides in soils in Serbia: dose calculations and environmental risk, *Adv. Environ. Res.*, **6**, 2009.
64. S. Forkapic, J. Vasin, I. Bikit, D. Mrdja, K. Bikit, S. Milić, Correlations between soil characteristics and radioactivity content of Vojvodina soil, *J. Environ. Radioact.,* **166**, 104–111, 2017.
65. Lj. Janković Mandić, R. Dragović, M. Djordjević, M. Djolić, A. Onjia, S. Dragović, G. Bacić, Spatial variability of ^{137}Cs in the soil of Belgrade region (Serbia), *Hemijska industrija*, **68(4),** 449–455, 2014.
66. J. Petrović, M. Ćujić, M. Đorđević, R. Dragović, B. Gajić, Š. Miljanić, S. Dragović, Spatial distribution and vertical migration of 137Cs in soils of Belgrade (Serbia) 25 years after the Chernobyl accident, *Environ Sci Process Impacts*, **15(6),** 1279, 2013.
67. A. Čupić, I. Smičiklas, M. Manić, M. Đokić, R. Dragović, M. Đorđević, M. Gocić, M. Jović, D. Topalović, B. Gajić, S. Dragović, ^{137}Cs-based assessment of soil erosion rates in a morphologically diverse catchment with varying soil types and vegetation cover: relationship with soil properties and RUSLE model predictions, *Water (Switzerland)*, **17(4),** 1–25, 2025.
68. J. Petrović, S. Dragović, R. Dragović, M. Dordević, M. Dokić, B. Zlatković, D. Walling, Using ^{137}Cs measurements to estimate soil erosion rates in the Pčinja and South Morava River Basins, southeastern Serbia, *J. Environ. Radioact.,* **158–159**, 71–80, 2016.
69. B. M. Mitrović, B. R. Vranješ, O. A. Kostić, V. S. Perović, M. M. Mitrović, P. Pavlović, Radionuclides and heavy metals in soil, vegetables, and medicinal plants in suburban areas of the cities of Belgrade and Pančevo, Serbia, *Nucl. Techn. & Rad. Protect.*, **34(3),** 278–284, 2019.
70. B. M. Mitrović, S. N. Grdović, G. S. Vitorović, D. P. Vitorović, G. K. Pantelić, G. A. Grubić, ^{137}Cs and ^{40}K in some traditional herbal teas collected in the mountain regions of Serbia, *Isot. Environ. Health Stud*, **50(4),** 2014.
71. I. Kandić, A. Kandić, I. Čeliković, M. Gavrilović, P. Janaćković, Activity concentrations of ^{137}Cs, ^{40}K, and ^{210}Pb radionuclides in selected medicinal herbs from Central Serbia and their effective dose due to ingestion, *Science of the Total Environment*, **701**, 2020.
72. B. Milenkovic, J. M. Stajic, N. Stojic, M. Pucarevic, S. Strbac, Evaluation of heavy metals and radionuclides in fish and seafood products, *Chemosphere*, **229**, 324–331, 2019.
73. M. Ćujić, S. Dragović, Assessment of dose rate to terrestrial biota in the area around coal fired power plant applying ERICA tool and RESRAD BIOTA code, *J. Environ. Radioact.,* **188**, 108-114, 2018.
74. B. Mitrović, J. Ajtić, M. Lazić, V. Andrić, N. Krstić, B. Vranješ, M. Vićentijević, M., 2016. Natural and anthropogenic radioactivity in the environment of Kopaonik mountain, Serbia. *Environmental Pollution*, **215**, 273–279, 2016.
75. UNEP, Depleted *Uranium in Serbia/Montenegro Post-Conflict Environmental Assessment*. UNEP, 2002.
76. Serbian Environmental Protection Agency (SEPA), *Environment in Serbia: an indicator – based review.* SEPA, Belgrade, 2007.
77. S. Raicevic, J. Raicevic, Remediation of uranium contaminated sites: clean-up activities in Serbia, *Proceedings of the Fifth Yugoslav Nuclear Society Conference YUNSC*, Belgrade, 2004, 377-380.
78. J. Petrović, M. Đorđević, R. Dragović, B. Gajić, S. Dragović, Assessment of radiation exposure to human and non-human biota due to natural radionuclides in terrestrial environment of Belgrade, the capital of Serbia, *Environ. Earth Sci.*, **77,** 290, 2018.
79. D. Popovic, D. Todorovic, M. Frontasyeva, J. Ajtic, M. Tasic, S. Rajsic, Radionuclides and heavy metals in Borovac, Southern Serbia, *Environ. Sci. Pollut. Res*, **15(6),** 509–520, 2008.
80. N. B. Sarap, M. M. Janković, D. J. Todorović, J. D. Nikolić, M. S. Kovačević, Environmental radioactivity in southern Serbia at locations where depleted uranium was used, *Arhiv za Higijenu Rada i Toksikologiju*, **65(2),** 189–197, 2014.

81. M. Esposito, P. Polić, P. Bartolomei, V. Benzi, M. Martellini, O. Cvetković, V. Damjanov, M. Simić, Z. Źunić, B. Živančević, S. Simić, V. Jovanović, Survey of natural and anthropogenic radioactivity in environmental samples from Yugoslavia, *J. Environ. Radioact.,* **61**(3), 271–282, 2002.
82. S. Bakrač, E. Klem, M. Milanović, Ekološke posledice NATO bombardovanja Republike Srbije 1999. godine, *Vojno delo*, **70(4)**, 475–492, 2018.
83. Official Gazette of RS, *Rulebook for establishing programme of systematic environmental radioactivity examination,* No. 100/2010.
84. Official Gazette of RS, Rulebook for establishing programme of early warning of emergency, No. 70/2011.

INVITED LECTURES
PREDAVANJA PO POZIVU

Investigation of mirror bright metal coatings and electrolytically produced copper powders on turn of the century at Department of Electrochemistry, ICTM

Nebojša D. Nikolić*

University of Belgrade, Institute of Chemistry, Technology and Metallurgy, Njegoševa 12, 11 000 Belgrade, Serbia

https://doi.org/10.65614/uisk_yucorr.2025.26.ch4

*nnikolic@ihtm.bg.ac.rs

Abstract

Some fundamental and applied aspects of formation of mirror bright metal coatings and copper powder production by electrolysis are presented. These investigations are performed in a period between 1995 and 2000, at University of Belgrade, Institute of Chemistry, Technology and Metallurgy, Department of Electrochemisty, partly under supervisor of Prof. Dr. Miomir G. Pavlović, long-standing president of Serbian Society of Corrosion and Materials Protection (UISKOZAM). The coatings of chrome, copper and zinc are explored and the working conditions (the current density, temperature, the types of electroplating bath and cathode, addition agents for levelling and brightness, ...) which enable their mirror bright appearance were defined. The electrolytic production of copper powders desired the apparent density, as well as their stabilisation to prevent corrosion were widely investigated, too. Some of these investigations were conducted for companies in the Republic of Serbia (mirror bright chrome coatings - Župa, Kruševac, and copper powder - RTB Bor, d.d. "Topionica i rafinacija", Bor).

Keywords: *metal coatings; powder; electrolysis; chrome; copper; zinc*

Izvod

Predstavljeni su neki fundamentalni i primenjeni aspekti formiranja ogledalasto sjajnih metalnih prevlaka i proizvodnje bakarnog praha elektrolizom. Ova istraživanja su izvedena u periodu između 1995. i 2000. godine na Univerzitetu u Beogradu, Institutu za hemiju, tehnologiju i metalurgiju, Centru za elektrohemiju, delimično pod rukovodstvom prof. dr Miomira G. Pavlovića, dugogodišnjeg predsednika Udruženja inženjera Srbije za koroziju i zaštitu materijala (UISKOZAM). Istraživane su prevlake hroma, bakra i cinka i radni uslovi (gustina struje, temperatura, vrste kupatila za galvanizaciju i katode, dodaci za poravnavanje i sjajnost površina, ...) koji omogućavaju njihov ogledalasti sjaj su definisani. Takođe je široko istraživana elektrolitička proizvodnja bakarnih prahova željene nasipne mase, kao i njihova stabilizacija u cilju zaštite od korozije. Neka od ovih istraživanja su vršena za preduzeća u Republici Srbiji (ogledalasto sjajne prevlake hroma - Župa, Kruševac, i bakarni prah - RTB Bor, d.d. "Topionica i rafinacija", Bor).

Ključne reči: *metalne prevlake; prah; elektroliza; hrom; bakar; cink*

Energy-Saving Microwave-Assisted Synthesis of PLA for PU/PLA Hybrid Multifunctional Coatings in Drug Release

Vladan Mićić[1, *], Marija Krstic[2], Darko Manjenčić[3], Suzana Cakić[4], Ivan Ristić[2]

[1] *Faculty of Technology Zvornik, University of East Sarajevo, Karakaj 34A, 75400 Zvornik, Republic of Srpska, Bosnia and Herzegovina*

[2] *University of Novi Sad, Faculty of Technology Novi Sad, Boulevard cara Lazara 1, 21101 Novi Sad, Serbia*

[3] *Academy of Kruševac, Department of Technical and Technological Studies, Kosančićeva 36, 37000 Kruševac, Serbia*

[4] *University of Niš, Faculty of Technology, Bulevar oslobođenja 124, 16000 Leskovac, Serbia*

https://doi.org/10.65614/uisk_yucorr.2025.26.ch5

[*]*micicvladan1971@gmail.com*

Abstract

The development of multifunctional polymeric coatings that combine biodegradability, stability, and controlled release capacity is of great importance in modern materials science. In this study, polylactic acid (PLA) was synthesized via an energy-saving microwave-assisted polycondensation route, providing an efficient and sustainable alternative to conventional synthesis methods. The obtained PLA was processed into nanofibrous mats by electrospinning and subsequently deposited onto polyurethane (PU) films to form hybrid multilayer coatings. FTIR spectroscopy indicated the absence of significant chemical interactions between PLA and PU, confirming the preservation of the individual polymer structures. DSC analysis showed the reduction in melting enthalpy which suggests effective integration of the electrospun PLA onto PU substrate and the reduced crystallinity of the hybrid PU/PLA system. SEM micrographs revealed a uniform fibrous morphology of the electrospun PLA layer, providing a coherent and stable coverage of the PU substrate. Mechanical testing of the hybrid coating revealed a tensile strength of 2.9 MPa and an elongation at break of 57%, indicating a balanced combination of strength and flexibility. Beyond pharmaceutical applications, the proposed approach demonstrates potential for environmentally friendly protective and functional coatings in biomedical and packaging technologies. The combination of microwave-assisted synthesis and electrospinning thus represents a sustainable and versatile pathway toward advanced polymer-based multifunctional coatings.

Keywords: *biodegradable polymers; controlled drug release; hybrid PU/PLA coatings; microwave-assisted synthesis*

Introduction

Biodegradable and bio-based polymers are increasingly important for biomedical applications such as wound dressings [1-3], drug delivery [4], and protective coatings. Polylactic acid (PLA) is a biodegradable aliphatic polyester derived from renewable resources, offering high strength and biocompatibility, but its brittleness limits flexibility. Polyurethane (PU), especially when synthesized with bio-based polyols such as polyricinoleate, provides elasticity, toughness, and tenable phase morphology. Hybrid PU/PLA coatings are promising since they integrate the toughness and flexibility of PU with the biodegradability and rigidity of PLA. Moreover, microwave-assisted polymerization represents energy-efficient and sustainable alternative for polymer synthesis, while

electrospinning of PLA nanofibers yields high-surface-area coatings suitable for controlled drug release [5].
Electrospinning has emerged as a versatile technique for fabricating nanofibrous polymer mats with high surface area, porosity, and tunable fiber morphology [6-8]. Such properties are highly beneficial for drug delivery applications, since drugs can be loaded either within the nanofibers or adsorbed on their surface, allowing sustained or stimuli-responsive release. When electrospun fibers are deposited directly onto a flexible polymer substrate, the resulting system can mimic a patch-like configuration, suitable for external applications such as wound dressings or transdermal delivery systems.
In this work, PLA was electrospun directly onto bio-based PU films, yielding PU/PLA hybrid coatings that combine the mechanical flexibility of PU with the biodegradability and nanostructured morphology of PLA. The aim of this study was to develop such a hybrid PU/PLA system using energy-efficient microwave-synthesized PLA and bio-based PU, and to thoroughly characterize its chemical, thermal, morphological, and mechanical properties for advanced coating applications. Moreover, microwave-assisted synthesis routes were employed to ensure sustainability and efficiency in polymer production, aligning with current trends in green materials development.

Experimental

Synthesis of Bio-Based PU

As a soft segment for the preparation of PU, polycatprolactone (Mn=2000 g/mol, from Sigma Aldrich) and polyricinoleate diol synthesized by high-temperature polycondensation of ricinoleic acid with diethylene glycol in the presence of $Ti(iPrO)_4$ catalyst, were used. PU samples were then prepared via a one-pot two-step polymerization using polyricinoleate/PCL (1:1 mol/mol) blends as soft segments and diphenylmethane diisocyanate (MDI) with 1,4-butanediol as chain extender. PU was synthesized with 60% of soft segment content, mixing all components in tetrahydrofuran, as solvent, at 60 °C for 3 hours. The obtained thermoplastic PU was purified and vacuum-dried.

Microwave-assisted synthesis of PLA

Microwave polymerization of L-lactide monomer involves the addition of the dry monomer (5 g) in the evaporating bowls, followed by the addition of tin(II) 2-ethylhexanoate solution (2.81 mg in 1 mL toluene). After the mixture became homogenized toluene was evaporated at 60 °C in vacuum for 6 h. The reaction mixture was then moved to a glass ampoule. Polymerization was performed in a microwave reactor at the frequency of 2.45 GHz. The temperature regulation was carried out by the infrared in-mass measuring system and was maintained at 100 °C. Very short polymerization time was 15 minutes. The obtained PLA was characterized by a yield of 92% and a number-average molecular weight (M_n) of 81,000 g/mol.

Fabrication of Hybrid PU/PLA Coatings

PLA solutions were electrospun into nanofibrous mats and directly deposited onto PU films, yielding PU/PLA multilayer coatings. For electrospinning of pure PLA, 15 wt% solutions of PLA in solvent mixture DCM/DMF (in ratio 4:3 v/v) were prepared. Solutions were homogenized 24 hours on magnetic stirrer at room conditions before electrospinning.
Machine Fluidnatec LE-10 by BioInicia was used for electrospinning. Feed rate 5 ml/h, distance from tip to collector 15 cm and voltage 16 kV were process parameters used for preparation of non-wovens.

Characterization

Fourier transform infrared spectra (FTIR) were recorded by Bomem Hartmann & Braun MB-series, in the wave band range from 400 to 4.000 cm^{-1}. Obtained polymers were milled with KBr before the preparation of tablets under vacuum press.

Differential scanning calorimetry (DSC) measurements were performed using a TA Instruments Q20 DSC (software Universal Analysis from TA Instruments) instrument in the temperature range from 25 to 200°C under nitrogen atmosphere at a heating rate of 10 °C min^{-1}.
PLA nanofiber morphology was analysed on SEM. Scanning electron microscopy (SEM) imaging was done on a SEM Lyra (Tescan) operated at 25 kV.
Mechanical properties of electrospun non-wovens were determined using Tensile Testing Machine Instron 1122, where speed was 1 mm min^{-1} at room conditions. Samples were cut from prepared nonwoven mats in the form of rectangle; with approximate dimensions 10x50 mm.

Results and Discussion

FTIR Analysis

The chemical composition of the polyurethanes, based on polyricinoleate and PCL soft segments, is indicated by a carbonyl band at 1728 cm^{-1}, attributed mainly to free ester C=O of the soft segments but possibly overlapping with free urethane C=O. Ester C–O vibrations appear in the 1100–1200 cm^{-1} region. Characteristic urethane absorptions include an N–H stretching band at 3323–3340 cm^{-1} and an amide II band at 1530 cm^{-1}, Figure 1. The N–H bands were shifted to lower wavenumbers suggesting hydrogen bonding either between the hard segments or between hard segments and soft segments. The peak centered at 1703 cm^{-1} is ascribed to the vibration of hydrogen-bonded carbonyls from both triglyceride ester and urethane groups. FTIR spectrum shows the asymmetrical valence vibrations of the ester C-O-C bond of the aliphatic chain as strong band with a position at 1168 cm^{-1} and symmetrical valence vibrations of C–O–C of the aliphatic chain at 1066 and 1100 cm^{-1}. Other bands that characterize the structure of the used polyester polyols are overlapped by polyurethane bands.

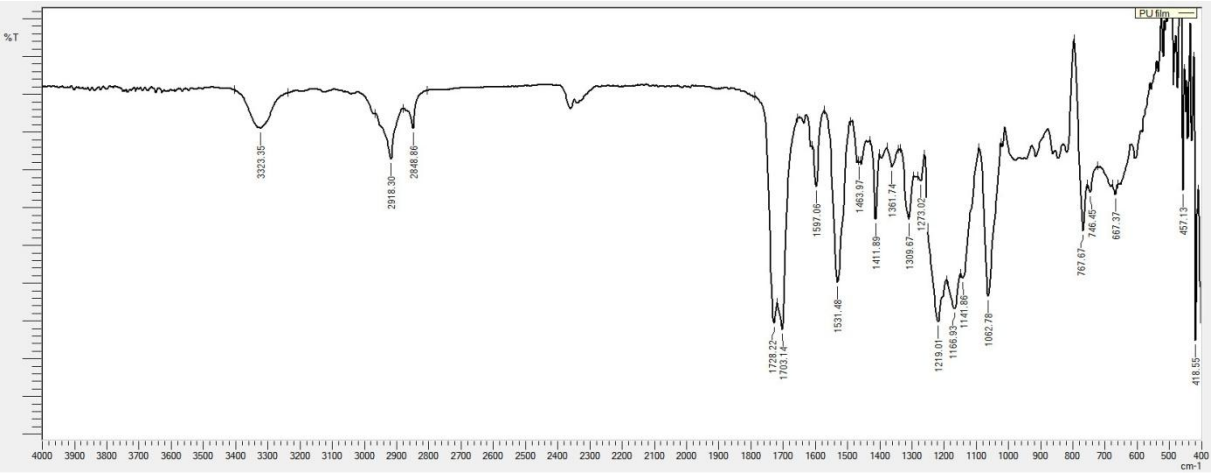

Figure 1. *FTIR spectrum of PU sample.*

The molecular structures of synthesized PLA were estimated by FTIR spectroscopy, Figure 2. Bands at 1751 cm^{-1} (cyclicdilactone C=O valence vibration), 1445 and 1382 cm^{-1} (asymmetric and symmetric bending vibration of C–H from CH_3, respectively) and 930 cm^{-1} (COO ring breathing mode) are characteristic for the FTIR spectra of monomer L-lactide, with band at 1260 cm^{-1} from asymmetric valence vibrations of C–O–C in the lactonic ring and band at 1100 cm^{-1} from symmetric valence vibrations of C–O–C in the lactonic ring. The broad absorption band of the hydroxyl (OH) stretching vibration between 3200 and 3600 cm^{-1} were presented in spectra of synthesized poly(lactide) sample. Bands at 2960 and 2830 cm^{-1} from asymmetric and symmetric valence vibrations of C–H were presented in polymer spectra. The band at 2880 cm^{-1} was attributed to the symmetric valence vibration of C–H from CH_3. As it can be seen from the FTIR spectrum of PLA

the asymmetrical valence vibrations of C–O–C of the aliphatic chain were shifted at 1182 and 1207 cm^{-1}, and symmetrical valence vibrations of C–O–C of the aliphatic chain 1082 and 1100 cm^{-1}, compared with bands at1267 and 1099 cm^{-1}, which appeared in monomer lactide. Band at 1751 cm^{-1} emerges from the valence vibration of C=O of aliphatic ester, whereas the bands at 1454 and 1382 cm^{-1} originated from asymmetric and symmetric bending vibration of C–H from CH_3, respectively. The band at 1260 cm^{-1} from the overlap of C–H bending vibration and C–O–C stretching vibration, was also detected.

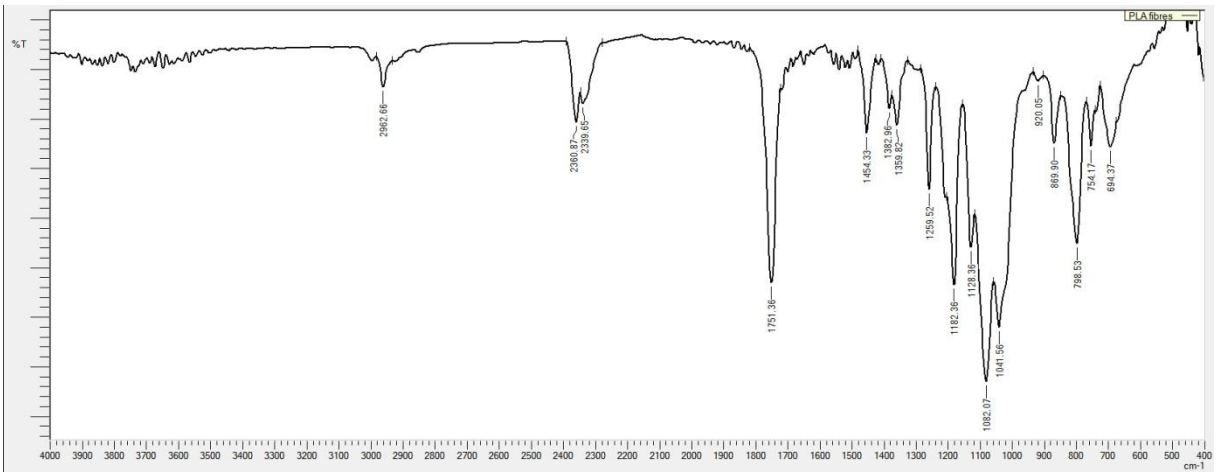

Figure 2. *FTIR spectrum of PLA sample.*

DSC Analysis

The glass transition of the soft segment in PU films was observed at approximately –17 °C, confirming the high chain mobility of the flexible polyester-based domains. However, the glass transitions of the MDI/BDO hard segments were not clearly distinguishable, suggesting that a significant portion of the hard domains remained amorphous. This behavior can be attributed to the use of fatty acid–based polyricinoleate polyols, which introduce dangling chains into the structure. These chains increase the miscibility of hard and soft phases and hinder the formation of well-ordered crystalline hard domains, leading to smaller and more imperfectly packed hard segment regions.

Interestingly, the *Tg* of electrospun PLA fibers (in hibrid PU/PLA materials) was not clearly distinguishable, most likely due to the thin nanofiber morphology and partial amorphous character of the electrospun mats, which suppress the detection of a distinct glass transition. Complex endothermic peak with a maximum at 165 °C was detected, corresponding to the melting of crystalline poly(L-lactide) fibres in hybrid sample, Figure 3. For the PU/PLA hybrid coatings, the overall melting enthalpy was significantly reduced (ΔH_m = 1.42 J/g), indicating that the PLA nanofiber layer contributed only partially to the total crystallinity of the hybrid system. The reduction in melting enthalpy further suggests effective integration of the electrospun PLA within the PU substrate, which limits the extent of crystallization while preserving structural stability.

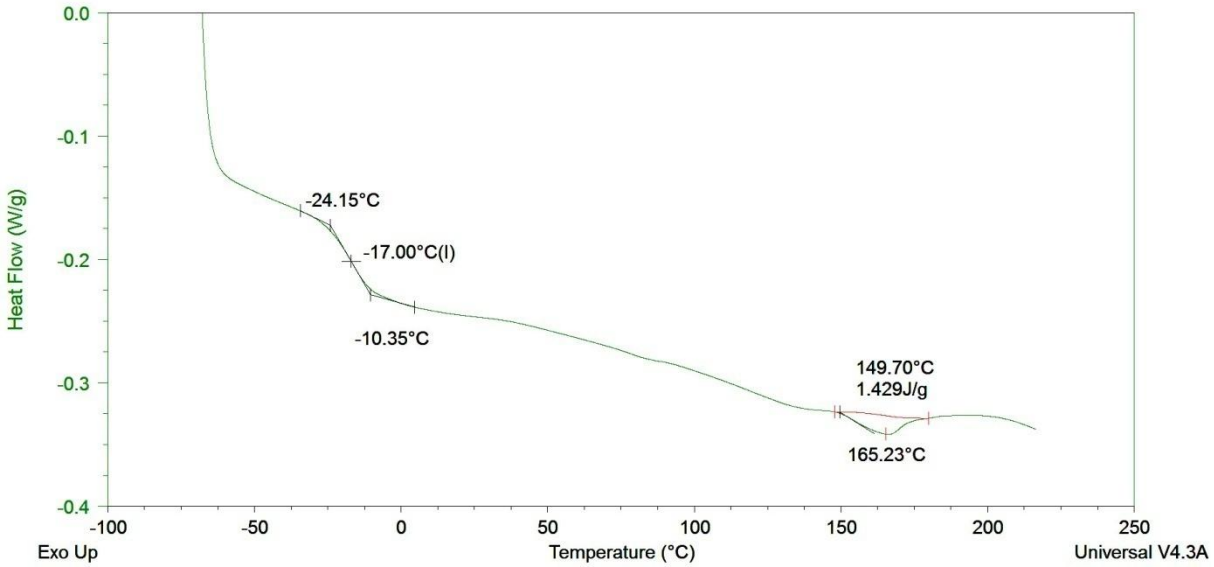

***Figure 3. DSC** thermogram of PU/PLA hybrid sample.*

Morphological analysis

Electrospun PLA nanofibers exhibited uniform fibrous morphology and coherent coverage on PU films, providing a stable substrate with high surface area, favourable for drug release. It can be seen that smooth and uniform fibers without beads and drops were obtained using appropriate process parameters, Figure 4.

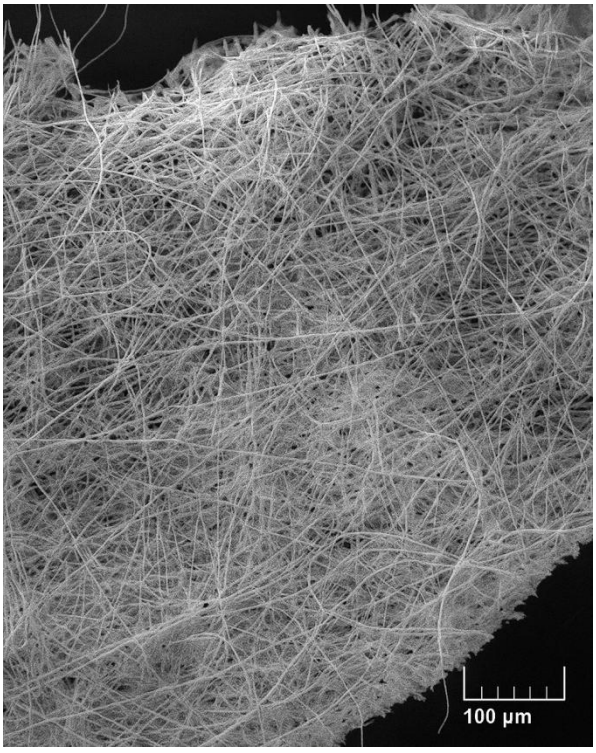

***Figure 4.** SEM micrograph of hybrid PU/PLA sample.*

Analysis of Mechanical Properties

The mechanical performance of the individual polymer components—polyurethane (PU) and polylactic acid (PLA)—was evaluated to understand their contribution to the hybrid PU/PLA system.

Tensile testing revealed the distinct mechanical profiles of the two materials. The PU sample exhibited a tensile strength of approximately 5 MPa and a very high elongation at break of nearly 400%. This behavior is characteristic of a tough and highly elastic material, resulting from the mobility of the long polymer chains in the soft segments.
In contrast, the fibres of pure synthesized PLA demonstrated a tensile strength of 1.6 MPa but a drastically lower elongation at break of less than 10%, confirming its inherently brittle nature. This rigidity is a direct consequence of PLA's semi-crystalline structure and restricted chain mobility, as further confirmed by thermal analysis.
The hybrid PU/PLA material, fabricated by electrospinning PLA nanofibers onto a PU film, exhibited a promising combination of these properties. The mechanical behavior of the hybrid is a synergistic interplay between the two layers. The PU substrate provides the primary flexibility, enabling the entire structure to withstand significant deformation. Upon stretching, the hybrid structure demonstrated a desirable failure mechanism. The initial deformation led to the alignment and unravelling of the PLA nanofibers rather than their immediate fracture. This process allows for efficient stress transfer and energy dissipation. Ultimately, the hybrid material achieved an elongation at break of 57% and a tensile strength of 2.9 MPa. Failure was defined by the fracture of the PLA nanofiber network at this point, which was taken as the ultimate tensile strength of the hybrid construct. It is important to note that the underlying PU film itself, with its much higher inherent elasticity (~400% elongation), had not yet reached its rupture point. This indicates that the electrospun PLA layer provides a reinforcing effect, increasing the strength of the pure PU film, while the PU matrix imparts flexibility to the otherwise brittle PLA fibers, creating a composite material with balanced and satisfactory mechanical properties for advanced coating applications. This indicates that the ductile PU matrix imparts flexibility, while the PLA nanofibers provide strengthening, creating a composite material with balanced and satisfactory mechanical properties for advanced coating applications..
The combination of elastic PU films and rigid electrospun PLA layers resulted in coatings with complementary properties: flexibility, biodegradability, structural stability, and nanostructured morphology suitable for controlled drug release and wound healing.

Conclusion

This study demonstrated that microwave-assisted polymerization provides an energy-efficient route for the synthesis of PLA with controlled crystallinity, while bio-based PU derived from polyricinoleate offers tunable flexibility and toughness. FTIR and DSC analyses confirmed the expected structural features and thermal transitions, including the suppressed glass transition of PLA nanofibers and the reduced crystallinity of the hybrid PU/PLA system. SEM imaging revealed uniform nanofiber morphology with coherent coverage of PU substrates, while mechanical testing highlighted the synergistic performance of the hybrid, combining the ductility of PU with the reinforcing effect of PLA fibers. The hybrid coating exhibited a tensile strength of 2.9 MPa and an elongation at break of 57%, demonstrating a successful compromise between the mechanical properties of its individual components. The developed PU/PLA hybrid coatings can be regarded as patch-like systems, offering both flexibility and controlled drug release capacity. Such materials hold strong potential for biomedical applications, particularly in wound dressings and transdermal delivery platforms, while also supporting sustainability goals through the use of energy-saving synthesis methods and renewable resources.

Acknowledgements

This work was supported by the Ministry of Scientific and Technological Development and Higher Education of theRepublic of Srpska, through the project ''Development of New Systems for Controlled Drug Delivery based on Biodegradable Polymers'', contact number 19.032/961-91/24,

and the NATO SPS program, project G6031-"Wearable Smart Patches for Multimodal Wound Healing - DRESWOUTRE" for financial support.

References

1. Gültekin, G., Atalay-Oral, Ç., Erkal, S., Şahin, F., Tantekin-Ersolmaz, S. B., & Güner, F. S. (2019). Fatty acid-based polyurethane films for wound dressing applications. *Journal of Materials Science: Materials in Medicine 20*, 421–43 https://doi.org/10.1007/s10856-019-6244-8
2. Filatova, K., Domincova Bergerova, E., Kazantseva, N., Masar, M., Suly, P., Sopik, T., Cisar, J., Durpekova, S., & Sedlarik, V. (2023). Design and fabrication of electrospun PLA-based silica-modified composite nanofibers with antibacterial properties for perspective wound treatment. *Polymers, 15*(17), 3500. https://doi.org/10.3390/polym15173500
3. Abolhassani, S., Alipour, H., Alizadeh, A., Nemati, M. M., Najafi, H., & Alavi, O. (2022). Antibacterial effect of electrospun polyurethane-gelatin loaded with honey and ZnO nanoparticles as potential wound dressing. *Journal of Biomaterials Applications*. Advance online publication. https://doi.org/10.1177/15280837211069871
4. Gajić, I., Stojanović, S., Ristić, I., Ilić-Stojanović, S., Pilić, B., Nešić, A., Najman, S., Dinić, A., Stanojević, L., & Urošević, M. (2022). *Electrospun Poly(lactide) fibers as carriers for controlled release of Biochanin A*. *Pharmaceutics, 14*(3), 528. https://doi.org/10.3390/pharmaceutics14030528
5. Nikolic, L., Ristic, I., Adnadjevic, B., Nikolic, V., Jovanovic, J., Stankovic, M. (2010). Novel Microwave-Assisted Synthesis of Poly(D,L-lactide): The Influence of Monomer/Initiator Molar Ratio on the Product Properties. *Sensors*, *10*(5), 5063-5073. https://doi.org/10.3390/s100505063
6. Magiera, A., Markowski, J., Menaszek, E., & others. (2017). PLA-based hybrid and composite electrospun fibrous scaffolds as potential materials for tissue engineering. *Journal of Nanomaterials*, 2017, Article 9246802. https://doi.org/10.1155/2017/9246802
7. Yan, L., Si, S., Chen, Y., Yuan, T., Fan, H., Yao, Y., Zhang, Q. (2011). Electrospun in-situ hybrid polyurethane/nano-TiO_2 as wound dressings. *Fibers and Polymers, 12*(2), 207-213. https://doi.org/10.1007/s12221-011-0207-0
8. Pahlevanneshan, Z., Deypour, M., Kefayat, A., Rafienia, M., Sajkiewicz, P., Esmaeely Neisiany, R., & Enayati, M. S. (2021). Polyurethane-nanolignin composite foam coated with propolis as a platform for wound dressing: synthesis and characterization. *Polymers, 13*(18), 3191. https://doi.org/10.3390/polym13183191

Electrochemical and Electrocatalytic Behavior of Pd-based Electrodes in Alkaline Media

Jelena D. Lović*, Milica G. Košević, Nebojša D. Nikolić

Department of Electrochemistry, Institute of Chemistry, Technology and Metallurgy, University of Belgrade, Serbia

https://doi.org/10.65614/uisk_yucorr.2025.26.ch6

*jelena.lovic@ihtm.bg.ac.rs

Abstract

During the late 20th and early 21st centuries, palladium began to be used in electrocatalysis as a more economical substitute for platinum, especially in situations where CO resistance, such as in fuel cells, is an essential consideration. Additionally, Pd-based catalysts, in particular when alloyed with other metals, often exhibit higher tolerance to certain poisons, a common challenge faced in polymer electrolyte membrane fuel cells (PEMFCs). The role of ethanol as the anode reaction of PEMFCs is well recognized. Key performance indicators for effective electrocatalysts in the ethanol oxidation reaction (EOR) consist of high activity (characterized by low onset potential and elevated current density), outstanding selectivity (favouring the desired products such as C1 species), and remarkable durability (ability to resist deactivation and poisoning over time). Strategies for catalyst design that enhance performance include the appropriate morphology, optimization of electronic structures through the incorporation of non-precious or transition metals, and the utilization of two-dimensional materials. Apart from catalyst design, the choice of electrolyte greatly affects the EOR by influencing mass transport, charge transfer, and the stability of reaction intermediates. In such way electrolyte engineering may be an effective method for improving performance. Recent studies on Pd and Pd-Sb catalysts have shown that the interactions between the alkaline electrolyte and the electrocatalyst have a significant impact on the electrocatalytic properties indicating that selection of the proper electrolyte also plays an active role in electrocatalytic behaviour.

Keywords: *electrooxidation of ethanol; direct alcohol fuel cells; electrodeposition; surface morphology; alkali metal cations*

Izvod

Krajem 20. i početkom 21. veka, paladijum je počeo da se koristi u elektrokatalizi kao ekonomičnija zamena za platinu, posebno u situacijama gde je otpornost na CO, kao što je u gorivnim ćelijama, bitna stvar. Pored toga, katalizatori na bazi Pd, posebno kada su legirani sa drugim metalima, često pokazuju veću toleranciju na određene otrove, što je izazov sa kojim se suočavaju gorivne ćelije sa polimernim elektrolitnim membranama (PEMFCs). Uloga etanola kao anodne reakcije PEMFC-a je poznata. Ključni indikatori za efikasne elektrokatalizatore u reakciji oksidacije etanola (EOR) obuhvataju visoku aktivnost (koju karakteriše nizak početni potencijal i povišena gustina struje), izuzetnu selektivnost (koja favorizuje željene proizvode kao što su C1 vrste) i izuzetnu izdržljivost (sposobnost da se ne deaktiviraju i ne truju tokom vremena). Strategije za dizajn katalizatora koje poboljšavaju performanse uključuju odgovarajuću morfologiju, optimizaciju elektronskih struktura kroz ugradnju neplemenitih ili prelaznih metala i korišćenje dvodimenzionalnih materijala. Pored dizajna katalizatora, izbor elektrolita značajno utiče na EOR delovanjem na transport mase, prenos naelektrisanja i stabilnost reakcionih intermedijera. Na taj način, inženjering elektrolita može biti efikasan metod za poboljšanje performansi. Nedavne studije o Pd i Pd-Sb katalizatorima pokazale su da interakcije između alkalnog elektrolita i elektrokatalizatora imaju značajan uticaj na elektrokatalitička svojstva, što ukazuje da izbor odgovarajućeg elektrolita takođe igra aktivnu ulogu u elektrokatalitičkom ponašanju.

Ključne reči: *elektrookidacija etanaola; direktno alkoholne alkalne gorivne ćelije; elektrohemijsko taloženje; površinska morfologija; katjoni alkalnih metala*

Acknowledgements

This research was funded by the Ministry of Science, Technological Development and Innovation of the Republic of Serbia (Contract No. 451-03-66/2024-03/200026).

Pt-based thin film catalysts as the model system for real catalysts

Tankoslojni katalizatori na bazi platine kao model sistemi za realne katalizatore

Dušan Tripković*, Dragana Milošević, Sanja Stevanović

University of Belgrade - Institute of Chemistry, Technology and Metallurgy, Njegoševa 12, 11000 Belgrade, Serbia

https://doi.org/10.65614/uisk_yucorr.2025.26.ch7

*dusan@ihtm.bg.ac.rs

Abstract

The opportunity to use the structure-function relationship in electrocatalyst design is based on a fundamental understanding of physicochemical processes at the very top of the surface. Electrochemical reaction rates are highly sensitive to the geometric configuration of surface atoms, primarily due to variations in adsorbate binding strengths across different crystallographic facets. Platinum (Pt) thin films, prepared using different substrates and deposition processes, were systematically studied for the electrooxidation of small organic molecules, specifically formic acid and methanol. The low-index Pt single crystal electrodes were employed for reactivity benchmarking, which later guided the thermal annealing procedure leading to the fine-tuning of the ratio between (111) and (100) surface facets on Pt thin films. The oxidation activity for both methanol and formic acid is significantly increased due to the modified thin film structure, confirming the efficacy of the method. This exmerimental procedure could eventually lead to the invention of superior new catalysts that will enable the full commercialization of the fuel cell technology.

Keywords: *Pt thin films; thermal treatment; formic acid; methanol; electrooxidation*

Izvod

Mogućnost korišćenja odnosa morfologije i aktivnosti prilikom dizajniranja elektrokatalizatora zasniva se na fundamentalnom razumevanju fizičko-hemijskih procesa na samoj površini. Elektrohemijske reakcije su veoma osetljive na geometrijsku konfiguraciju površinskih atoma, prvenstveno zbog varijacija u jačini vezivanja adsorbata na različitim kristalografskim fasetama. Tanki filmovi platine (Pt), pripremljeni korišćenjem različitih podloga i procesa taloženja, sistematski su proučavani za elektrooksidaciju malih organskih molekula, posebno mravlje kiseline i metanola. Monokristalne elektrode Pt korišćene su za procenu aktivnosti specifičnih struktura, što je poslužilo kao osnova da se postupkom termičkog tretmana postigne fino podešavanje odnosa između (111) i (100) faseta na površini tankih filmova Pt. Aktivnost katalizatora i za metanol i za mravlju kiselinu je značajno povećana usled modifikovane strukture tankog filma, što potvrđuje efikasnost metode. Ovakav eksperimentalni pristup bi u bliskoj budućnosti mogao dovesti do pronalaska superiornih novih katalizatora koji će omogućiti potpunu komercijalizaciju tehnologije gorivnih ćelija.

Ključne reči: *Pt tanki filmovi; termički tretman; mravlja kiselina; metanol; elektrooksidacija*

Influence of processing-induced changes on the performance of Ti-based alloy in biological systems

Uticaj promena izazvanih procesnim postupcima na performanse Ti-legure u biološkim sistemima

Slađana Laketić[1,*], Miloš Momčilović[1], Jovan Ciganović[1], Jelena Bajat[2], Vesna Kojić[3], Dejan Zagorac[1], Ivana Cvijović-Alagić[1]

[1] *Vinča Institute of Nuclear Sciences - National Institute of the Republic of Serbia, University of Belgrade, P.O. Box 522, 11001 Belgrade, Serbia*

[2] *Faculty of Technology and Metallurgy, University of Belgrade, Karnegijeva 4, Belgrade, Serbia*

[3] *Oncology Institute of Vojvodina, Put doktora Goldmana 4, Sremska Kamenica, Serbia*

https://doi.org/10.65614/uisk_yucorr.2025.26.ch8

[*]*sladjana.laketic@vin.bg.ac.rs*

Abstract

This work explores the impact of high-pressure torsion (HPT) and laser surface modification on the microstructure, surface features, mechanical properties, corrosion resistance, and biological response of the Ti-45Nb (mass%) alloy, considering its potential for biomedical application. HPT processing resulted in significant grain refinement, producing an ultrafine-grained alloy. Microstructural characterization revealed two phases, β-Ti and Ti_4Nb, present in both the coarse- and ultrafine-grained alloy microstructures, consistent with theoretical investigations. Subsequently, laser scanning of the Ti-45Nb alloy in both microstructural states produced uniform linear surface micropatterns accompanied by changes in surface chemistry (increased oxygen content and oxide layer formation) and surface topography (increased surface roughness). Mechanical testing showed that the elastic modulus, hardness, and plasticity increased in both microstructural variants after laser surface modification, with higher values observed in the ultrafine-grained alloy. Additionally, theoretical investigations confirmed these findings and highlighted the impact of both structural and surface modifications on the alloy's mechanical behavior. Furthermore, corrosion testing demonstrated that all alloy samples exhibited high corrosion resistance, which was attributed to the formation of a dual-layer oxide film. The ultrafine-grained alloy developed a thicker inner barrier layer, whereas the coarse-grained alloy exhibited a thicker outer porous layer. Specifically, the best corrosion resistance was observed in the coarse-grained alloy prior to laser modification and in the ultrafine-grained alloy following laser modification. Finally, biological tests confirmed excellent cytocompatibility of the alloy in both microstructural states, before and after surface modification. In vitro tests further showed that laser surface modification enhances the attachment, adhesion, and proliferation of fibroblast cells on all alloy sample surfaces, indicating excellent biocompatibility, especially pronounced in the ultrafine-grained alloy. Overall, the combined influence of microstructural and surface modifications significantly enhanced the Ti-45Nb alloy's performance, highlighting its strong potential for application in biological systems.

Keywords: *Ti-45Nb alloy; high-pressure torsion; laser surface modification; mechanical properties; corrosion resistance; biocompatibility*

Izvod

Ovaj rad istražuje uticaj postupka uvijanjanja pod visokim pritiskom (HPT) i laserske površinske modifikacije na njenu mikrostrukturu, površinske karakteristike, mehanička svojstva, otpornost prema koroziji i biološki odgovor Ti-45Nb (mas.%) legure, uzimajući u obzir njen potencijal za

primenu u biomedicini. Primena HPT procesa rezultirala je značajnom rafinacijom zrna, pri čemu je formirana sitnozrna legura. Mikrostrukturna karakterizacija otkrila je prisustvo dve faze, β-Ti i Ti_4Nb, u mikrostrukturama krupnozrne i sitnozrne legure, u skladu s teorijskim istraživanjima. Nakon toga, lasersko skeniranje Ti-45Nb legure u oba mikrostrukturna stanja proizvelo je uniformne linearne površinske mikroobrazce, uz promene u hemijskom sastavu površine (povećan sadržaj kiseonika i formiranje oksidnog sloja) i topografiji površine (povećana hrapavost). Mehanička ispitivanja pokazala su da su se vrednosti modula elastičnosti, tvrdoće i plastičnosti povećale kod obe mikrostrukturne varijante nakon laserske površinske modifikacije, pri čemu su veće vrednosti zabeležene kod sitnozrne legure. Takođe, teorijsko istraživanje potvrdilo je ove rezultate, ukazujući na uticaj i strukturnih i površinskih modifikacija na mehaničko ponašanje legure. Pored toga, ispitivanja korozije pokazala su da se svi uzorci legure odlikuju visokom otpornošću prema koroziji, što se pripisuje formiranju dvoslojnog oksidnog filma. Sitnozrna legura se odlikuje debljim unutrašnjim barijernim slojem, dok je krupnozrna legura pokazala deblji spoljašnji porozni sloj. Konkretno, najveća otpornost prema koroziji primećena je kod krupnozrne legure pre laserske modifikacije, odnosno kod sitnozrne legure nakon laserske modifikacije. Na kraju, biološki testovi potvrdili su odličnu citokompatibilnost legure u oba mikrostrukturna stanja i pre i nakon površinske modifikacije. In vitro ispitivanja su dodatno pokazala da laserska modifikacija površine poboljšava vezivanje, adheziju i proliferaciju fibroblastnih ćelija na površinama svih uzoraka legure, što ukazuje na izvanrednu biokompatibilnost, pri čemu je ovaj efekat najizraženiji kod sitnozrne legure. U celini, kombinovani uticaj mikrostrukturne i površinske modifikacije značajno je poboljšao ponašanje Ti-45Nb legure, ističući njen veliki potencijal za primenu u biološkim sistemima.

Ključne reči: *Ti-45Nb legura; uvijanje pod visokim pritiskom; laserska modifikacija površine; mehanička svojstva; otpornost prema koroziji; biokompatibilnost*

Acknowledgements

This work was financially supported by the Ministry of Science, Technological Development and Innovation of the Republic of Serbia through Contract No. 451-03-136/2025-03/ 200017. Authors would also like to acknowledge the help of Dr. Anton Hohenwarter from the Department of Materials Science, Montanuniversität, Leoben, Austria, during the Ti-45Nb alloy HPT processing and Prof. Dr. Đorđe Veljović from the Faculty of Technology and Metallurgy, University of Belgrade, Serbia, during the Ti-45Nb alloy characterization.

ORAL PRESENTATIONS
USMENA SAOPŠTENJA

Advanced composite coatings on titanium with improved adhesion for use in medicine and dentistry

Katarina Đ. Božić[1,*], Marijana R. Pantović Pavlović[1], Miroslav M. Pavlović[1], Đorđe N. Veljović[2]

[1] *University of Belgrade, Institute of Chemistry, Technology and Metallurgy, Belgrade, Serbia*

[2] *University of Belgrade, Faculty of Technology and Metallurgy, Belgrade, Serbia*

https://doi.org/10.65614/uisk_yucorr.2025.26.ch9

[*]*katarina.bozic@ihtm.bg.ac.rs*

Abstract

The long-term performance of titanium-based implants largely depends on their ability to achieve strong interfacial bonding with surrounding tissue while maintaining structural stability under physiological conditions. Although titanium exhibits excellent mechanical properties, corrosion resistance, and biocompatibility, its inherently low bioactivity limits direct tissue integration. To address this challenge, recent research has focused on developing advanced composite surface coatings that combine inorganic bioactive phases with organic biopolymers to improve surface functionality, adhesion, and biological response.

This study investigates composite coatings engineered through a combined electrochemical and electrophoretic process designed to simultaneously modify the titanium surface and deposit a multifunctional hybrid layer. The approach enables the formation of a titanium-oxide-based intermediate structure that enhances coating adhesion, while the incorporated bioactive phases provide favorable chemical and structural conditions for cellular attachment and growth. Structural and chemical characterization techniques, including XRD, FTIR, SEM and adhesion testing, were employed to evaluate crystallinity, functional groups, and surface morphology. Results confirmed the successful formation of well-adhered composite layers with controlled microstructural features and well-developed porosity, which is beneficial for subsequent biological interactions.

Adhesion testing revealed high coating integrity, exceeding the performance typically observed for conventionally deposited ceramic layers. This improvement is attributed to synergistic interfacial bonding mechanisms arising from the combined contributions of the electrochemically formed oxide layer and the polymer–inorganic composite matrix.

Biocompatibility was assessed using fibroblast cell lines, demonstrating enhanced cell viability, proliferation, and metabolic activity on the composite-coated titanium surfaces compared to the unmodified substrate. These findings indicate that tailored composite coatings methodology can significantly improve the biological performance of implants, supporting more efficient tissue integration.

Overall, the results highlight the potential of hybrid organic–inorganic coatings obtained by coupled electrochemical–electrophoretic processing as a promising strategy for next-generation biomedical and dental implants. Their combination of strong adhesion, favorable surface morphology, and excellent cytocompatibility positions the investigated coatings as viable candidates for improving implant–tissue interactions and long-term clinical outcomes.

Keywords: *Titanium implants; Surface modification; Composite coatings; Bioactivity; Cytocompatibility*

POSTER PRESENTATIONS
POSTERSKA SAOPŠTENJA

Plant Extracts as "Green" Corrosion Inhibitors: A Mini Review

Biljni ekstrakti kao „zeleni"inhibitori korozije: Kratak pregledni rad

Nebojša Vasiljević[1,2,*], Marija Mitrović[1], Regina Fuchs-Godec[3], Dragan Tošković[1], Milorad Tomić[1,4]

[1] *University of East Sarajevo, Faculty of Technology Zvornik, 75400 Zvornik, Republic of Srpska,*

[2] *University of Novi Sad, Faculty of Technology, 21102 Novi Sad, Serbia,*

[3] *University of Maribor, Faculty of Chemistry and Chemical Engineering, 2000 Maribor, Slovenia,*

[4] *Engineering Academy of Serbia, Department of Technology and Metallurgy, 11000 Belgrade, Serbia*

https://doi.org/10.65614/uisk_yucorr.2025.26.ch10

[*]*nebojsa.vasiljevic@tfzv.ues.rs.ba*

Abstract

Plant extracts represent an alternative to conventional corrosion inhibitors, primarily due to their low cost and biodegradability. This review presents the results of 35 relevant studies from the Scopus and Web of Science databases in order to evaluate the application of plant extracts in this area. The analysis of the work shows that the most effective extracts are those containing high content of phenols, flavonoids, tannins, alkaloids and saponins. These compounds contain heteroatoms (N, S, O) and aromatic systems, which are easily adsorbed on metal surfaces and thus form a protective film. It is described in scientific papers that the inhibitory effect is most often attributed to physical and chemical adsorption, which is confirmed by Langmire/Freundlich adsorption models and changes in electrochemical behavior and surface morphology. The effectiveness of the inhibition itself depends on the type of plant, extraction method, extract concentration, temperature and exposure time; thus, in most studies, the corrosion efficiency is over 70%, while under optimal conditions it exceeds over 90%. However, for plant extracts to be used in industry, it is necessary to determine whether they remain effective on a large scale and over a long period of time.

Keywords: *adsorption; carbon steel; green corrosion inhibitors; plant extracts; protective film*

Izvod

Biljni ekstrakti predstavljaju alternativu konvencionalnim inhibitorima korozije, pre svega zbog svoje niske cene i biorazgradivosti. U ovom preglednom radu su predstavljeni rezultati 35 relevantnih studija iz baza podataka Scopus i Web of Science kako bi se procenila primena biljnih ekstrakata u ovoj oblasti. Analiza rada pokazuje da su najefikasniji ekstrakti oni koji sadrže fenole, flavonoide, tanine, alkaloide i saponine. Ova jedinjenja sadrže heteroatome (N, S, O) i aromatične sisteme, koji se lako adsorbuju na metalnim površinama i tako formiraju zaštitni film. U naučnim radovima je opisano da se inhibitorsko dejstvo najčešće pripisuje fizičkoj i hemijskoj adsorpciji, a koja se potvrđuje Langmirovim/Frojndlihovim modelima adsorpcije i promenama u elektrohemijskom ponašanju i morfologiji površine. Efikasnost same inhibicije zavisi od vrste biljke, metode ekstrakcije, koncentracije ekstrakta, temperature i vremena izlaganja; tako je u većini studija efikasnost korozije preko 70%, dok pod optimalnim uslovima prelazi preko 90%. Ipak, da bi se biljni ekstrakti koristili u industriji, potrebno je da se utvrdi da li ostaju efikasni u velikom obimu i tokom dužeg vremena.

Ključne reči: *adsorpcija; biljni ekstrakti; zaštitni film; ugljenični čelik; zeleni inhibitori korozije*

Protection of Steel Against Corrosion in 4% HCl Solution Using Thyme Extract

Zaštita čelika od korozije u 4% rastvoru HCl-a primenom ekstrakta majčine dušice

Milorad Tomić[1,2,*], Nebojša Vasiljević[1,3], Bojan Gorančić[1], Marija Mitrović[1], Regina Fuchs-Godec[4], Dragan Tošković[1]

[1] *University of East Sarajevo, Faculty of Technology Zvornik, 75400 Zvornik, Republic of Srpska,*

[2] *Engineering Academy of Serbia, Department of Technology and Metallurgy, 11000 Belgrade, Serbia*

[3] *University of Novi Sad, Faculty of Technology, 21102 Novi Sad, Serbia,*

[4] *University of Maribor, Faculty of Chemistry and Chemical Engineering, 2000 Maribor, Slovenia*

https://doi.org/10.65614/uisk_yucorr.2025.26.ch11

[*] *milorad.tomic@tfzv.ues.rs.ba*

Abstract

In this paper, the efficiency of the thyme extract as a "green" corrosion inhibitor for two types of steel in a 4% HCl solution was investigated. Measurements were performed without inhibitors and at different inhibitor concentrations (0.5, 1.0 and 1.5 g/L) and different exposure times (2, 4, 6, 8, 24, 48 and 168h). The responses in the study - corrosion rate (Km^-), depth corrosion indicator (π) and inhibitor efficiency (z) were analyzed using the statistical software MINITAB 21. In the absence of inhibitors, the corrosion rate (Km^-) was significantly higher, while in the presence of the extract there was a decrease in Km^- and a proportional increase in the inhibition efficiency z. The maximum values of inhibition efficiency reached ~90–97% under optimal conditions (for steel 2 the inhibition efficiency reached 96.8% at a inhibitor concentration of 1.0 g/L and a time of 2h, while for steel 1 the inhibition efficiency reached 93.99% at an inhibitor concentration of 0.5 g/L and a time of 48h). Such a high efficiency suggests that a protective film has formed on the surface of the steel and that the thyme extract can be used as a corrosion inhibitor in aggressive acidic environments, such as HCl solution.

Keywords: *ANOVA analysis; corrosion efficiency; green inhibitors; steel; thyme extract*

Izvod

U ovom radu ispitivana je efikasnost ekstrakta majčine dušice kao „zelenog“ inhibitora korozije za dve vrste čelika u 4% rastvoru HCl. Merenja su sprovedena bez inhibitora i pri različitim koncentracijama inhibitora (0,5, 1,0 i 1,5 g/L) i različitim vremenima izlaganja (2, 4, 6, 8, 24, 48 i 168h). Odgovori u studiji - brzina korozije (Km^-), dubinski pokazatelj korozije (π) i efikasnost inhibitora (z) analizirani su korišćenjem statističkog softvera MINITAB 21. U odsustvu inhibitora, brzina korozije (Km^-) je bila značajno veća, dok je u prisustvu ekstrakta došlo do smanjenja Km^- i proporcionalnog povećanja efikasnosti inhibicije z. Maksimalne vrednosti efikasnosti inhibicije dostigle su ~90–97% pod optimalnim uslovima (za čelik 2 efikasnost inhibicije dostigla je 96,8% pri koncentraciji inhibitora od 1,0 g/l i vremenu od 2 sata, dok je za čelik 1 efikasnost inhibicije dostigla 93,99% pri koncentraciji inhibitora od 0,5 g/l i vremenu od 48h). Tako visoka efikasnost sugeriše da se na površini čelika formirao zaštitni film i da se ekstrakt majčine dušice može koristiti kao inhibitor korozije u agresivnim kiselim sredinama, kao što je rastvor HCl.

Ključne reči: *ANOVA analiza; ekstrakt majčine dušice, efikasnost korozije; zeleni inhibitori; čelik*

Protection of Steel Against Corrosion in 4% HCl Solution Using Wild Oregano Extract

Zaštita čelika od korozije u 4% rastvoru HCl-a primjenom ekstrakta divljeg origana

Kristina Đerić[1,*], Marija Mitrović[1], Milorad Tomić[1,2], Nebojša Vasiljević[1,3]

[1] *University of East Sarajevo, Faculty of Technology Zvornik, 75400 Zvornik, Republic of Srpska,*

[2] *Engineering Academy of Serbia, Department of Technology and Metallurgy, 11000 Belgrade, Serbia*

[3] *University of Novi Sad, Faculty of Technology, 21102 Novi Sad, Serbia*

https://doi.org/10.65614/uisk_yucorr.2025.26.ch12

[*]*kristinadjeric8@gmail.com*

Abstract

In this study, the potential use of wild oregano extract as a green corrosion inhibitor for two types of steel in 4% HCl solution was investigated. Four solutions of 4% HCl were prepared: one without inhibitor (solution 1) and three with the addition of wild oregano extract at different concentrations (0.5, 1.0, and 1.5 g/L). Steel samples 1 and 2, with dimensions of 30 mm × 30 mm × 2 mm, were immersed in the prepared solutions for 2, 4, 6, 8, 24, 72, and 168 hours. Based on the weight loss of the steel samples before and after immersion, the negative mass corrosion index (Km^{-}), corrosion rate (π), and inhibition efficiency (z) were calculated. The obtained results indicate that the wild oregano extract exhibits corrosion inhibition properties and effectively slows down the corrosion of both steel types. For steel 1, the protection efficiency ranged from 83.78% to 97.56%, while for steel 2 it reached up to 79.68%. The optimal concentration of wild oregano extract in 4% HCl was determined to be 1 g/L, as at this concentration the protection efficiency for steel 1 ranged from 79.89% to 97.56%, and for steel 2 from 40.25% to 79.49% across all immersion times. The average corrosion rate for steel 2 in pure 4% HCl was 1.0836 mm/year, while for steel 1 it was 4.1359 mm/year. This indicates that steel 2 is more resistant and exhibits faster self-passivation than steel 1, which explains the somewhat lower, though still significant, inhibitory effect of wild oregano extract. The obtained results are in good agreement with those derived from electrochemical measurements of corrosion rate, including electrochemical impedance spectroscopy (EIS) and Tafel polarization plots. These findings suggest that wild oregano extract can serve as an effective and environmentally friendly corrosion inhibitor in acidic environments such as HCl solutions.

Keywords: *corrosion inhibitor; eco-friendly inhibitors; steel; wild oregano extract; inhibition efficiency*

Izvod

U ovom radu ispitivana je mogućnost korišćenja ekstrakta divljeg origana kao zelenog inhibitora korozije za dvije vrste čelika u 4% rastvoru HCl-a. Korišćena su četiri rastvora 4%HCl, jedan bez inhibitora (rastvor 1) i tri uz dodatak ekstrakta divljeg origana kao inhibitora korozije, različitih koncentracija (0.5, 1.0 i 1.5 g/L). Uzorci čelika 1 i 2 dimenzija (30mm x 30mm x 2mm) potapani su u pripremljene rastvore tokom 2, 4, 6, 8, 24, 72 i 168 sati. Na osnovu gubitka mase uzoraka čelika prije i poslije vremena provedenog u pripremljenim rastvorima računati su negativni maseni pokazatelj korozije (Km^{-}), dubinski pokazatelj korozije (π) i efikasnost inhibitora (z). Na osnovu dobijenih rezultata može se zaključiti da ekstrakt divljeg origana ima inhibitorsko dejstvo i da usporava koroziju oba korišćena čelika. Kod čelika 1 stepen zaštite se kreće od 83,78 -97,56%, dok kod čelika 2 stepen zaštite je do 79,68%. Na osnovu dobijenih rezultata optimalna koncentracija

ekstrakta divljeg origana u 4% HCl je 1g/L, jer kod čelika 1 stepen zaštite za sva vremena se kreće od 79,89-97,56%, a kod čelika 2 od 40,25-79,49%. Za čelik 2 srednji dubinski pokazatelj korozije π =1,0836mm/god u čistoj 4% HCl, a za čelik 1 π =4,1359mm/god. To ukazuje na činjenicu da je čelik 2 otporniji i brže se samopasivira od čelika 1, pa je zbog toga i i dejstvo ekstrakta divljeg origana manje izržen, ali je ipak značajno. Dobijeni rezultati se u velikoj mjeri slažu sa dobijenim rezultatima elektrohemijskih mjerenja brzine korozije: spektroskopije elektrohemijske impedanse (SEI) i Tafelovih polarizacionih dijagrama. Ovi rezultati sugerišu da ekstrakt divljeg origana može poslužiti kao efikasan i ekološki prihvatljiv inhibitor korozije u rastvoru HCl-a.

Ključne reči: *inhibitor korozije; ekološki inhibitori; čelik; ekstrakt divljeg origana; efikasnost inhibitora*

Inhibition Efficiency of 1-Butyl-3-methylimidazolium Bis(trifluoromethylsulfonyl)imide on AISI 316L in Strong Acid

Jan Vodenik[1], Marija Mitrović[2], Milorad Tomić[2], Regina Fuchs–Godec[1,*]

[1] *Faculty of Chemistry and Chemical Engineering, University of Maribor, Smetanova 17, Maribor*

[2] *Faculty of Technology Zvornik, University of Eastern Sarajevo, Karakaj bb, Republic of Srpska*

https://doi.org/10.65614/uisk_yucorr.2025.26.ch13

[*]*regina.fuchs@um.si*

Abstract

The corrosion inhibition performance of the ionic liquid 1-butyl-3-methylimidazolium fluoromethanesulfonate (BMIFMS) on AISI 316L stainless steel was examined in the hydrochloric acid environments (1.0 M and 0.5 M HCl). The effects of BMIFMS concentration and immersion time on electrochemical behaviour were evaluated using potentiodynamic polarisation techniques over a 5-day period. Results show that BMIFMS does not significantly reduce corrosion current in 1.0 M HCl, except at the highest tested concentration (0.5 wt%), where a marked decrease in anodic current density and corrosion rate was observed. In contrast, in 0.5 M HCl, BMIFMS demonstrated a substantial inhibitory effect, with corrosion current densities reduced by up to three orders of magnitude and inhibition efficiency exceeding 99% at 0.5 wt%. The inhibition is attributed to the formation of a stable adsorbed BMIFMS layer, which is particularly effective in less aggressive corrosive media. The study highlights the influence of medium aggressiveness and ionic liquid concentration on the efficiency of corrosion inhibition.

Keywords: *stainless-steel; HCl; ionic liquid; adsorption*

Introduction

Ionic liquids are a distinctive class of salts that remain liquid at room temperature. They comprise organic cations (such as imidazolium, pyridinium, or ammonium) and various anions (for example, tetrafluoroborate, hexafluorophosphate, or sulfate), which together form stable liquids with low volatility, high thermal and chemical stability, and good ionic conductivity. Owing to these properties, they are often described as “green solvents”, as they can replace volatile organic solvents and thus reduce environmental impact. The applications of ionic liquids are varied: they are used as solvents in chemical synthesis, in electrochemistry (such as in batteries and supercapacitors), for separation processes, as catalysts, and as heat transfer media. A particularly interesting and rapidly developing area is their use as corrosion inhibitors. In this role, ionic liquids adsorb their cations and anions onto metal surfaces, forming a protective layer that prevents direct contact between the metal and aggressive agents such as acids, chlorides, or moisture. Their unique molecular structures enable strong interactions with metallic surfaces, resulting in highly effective corrosion protection even in harsh environments. One of the main advantages of ionic liquids as corrosion inhibitors is that they can be tailored by carefully selecting the cation and anion, allowing their efficiency, solubility, and environmental safety to be optimised for specific applications. In addition, their low volatility makes them significantly safer for humans and the environment compared to conventional inhibitors. For these reasons, ionic liquids are increasingly recognised as a promising solution for protecting metals in industrial systems, oil and gas infrastructures, and energy storage devices [1-3].

The aim of this study was to investigate the inhibition performance of the selected imidazolium-based ionic liquid, 1-butyl-3-methylimidazolium bis(trifluoromethylsulfonyl)imide (BMIFMS), as an environmentally friendly corrosion inhibitor for stainless steel AISI 316L in aqueous hydrochloric acid solutions at concentrations of 0.5 M and 1.0 M. Various concentrations of the ionic liquid were

tested: 0.1 wt%, 0.2 wt%, 0.3 wt%, and 0.5 wt%. Corrosion measurements were conducted using the classical electrochemical method. The inhibitory effect of BMIFMS was monitored after 1 hour of immersion and after 1, 2, 3, 4, and 5 days of exposure to the corrosive medium. Fourier-transform infrared spectroscopy (FTIR) was used to analyse the adsorption layers formed by BMIFMS on the stainless-steel surface.

Experimental

The conventional three-electrode configuration was used for the potentiodynamic studies. All potentials were measured against the saturated calomel electrode (SCE), and the counter electrode was platinum. Measurements were conducted within a potential range of ±300 mV relative to the open circuit potential (OCP), with a scan rate of 1 mV s^{-1}. Polarisation plots were obtained 60 minutes after the working electrode was immersed in the solution, allowing the stationary potential to stabilise. All experiments were performed at 25 °C ± 1 °C. Potentiodynamic curve measurements were taken after 1 hour of immersion and after 1, 2, 3, 4, and 5 days of testing. The measurements were performed using a Gamry 600™ potentiostat/galvanostat controlled by electrochemical software. Data were collected and analysed using CorrView and CorrWare software developed by Scribner Associates, Inc.

Results and discussions

Electrochemical results

The effect of BMIFMS on the current–potential characteristics displayed by the polarisation curves of stainless-steel type AISI 316L in 1.0 M and 0.5 M HCl after 1, 2, 3, 4, and 5 days of testing, is presented in the Figs. 1a-e and Figs. 2a-e. From the potentiodynamic curves shown in Figures 1a–e, it is clear that the addition of BMIFMS does not produce a significant inhibitory effect, as the corrosion current value does not decrease substantially. This is evident from the Tafel curves, which mostly overlap over time without a distinct downward shift that, according to the extrapolation method, would indicate a notable reduction in corrosion current and, consequently, effective inhibition (Fig 1a.). The only exception is at the highest concentration of 0.5 wt% BMIFMS in the corrosive medium (Fig 1b.). Similarly, no significant decrease in the cathodic current density is observed, whereas the area under the anodic peak (charge under the oxidation curves), shown in Figures 1c–e, is noticeably reduced. To determine the charge under the oxidation curves, we integrated from the corrosion potential, where the current is minimal, up to the selected potential of –0.1 V (vs.SCE).

Table 1. Inhibition efficiency at selected concentrations of the BMIFMS ionic liquid over a period of 1 hour to 5 days of sample immersion in 1.0 M HCl, determined from the charge under the oxidation curves

	0.2 % BMIFMS	**0.3 % BMIFMS**	**0.5 % BMIFMS**
***t* [h]**	**η_a [%]**		
1	48.92	42.11	60.28
24	50.90	55.38	86.76
48	55.92	65.98	86.81
72	60.00	62.89	86.95
96	61.27	66.75	85.81
120	67.89	67.01	84.50

$$\eta_a = \frac{A - A'}{A} \cdot 100\% \quad (1)$$

where:

η_a – inhibition efficiency of the anodic part

A – area under the curve of the unprotected sample surface

A' – area under the curve of the inhibited sample surface

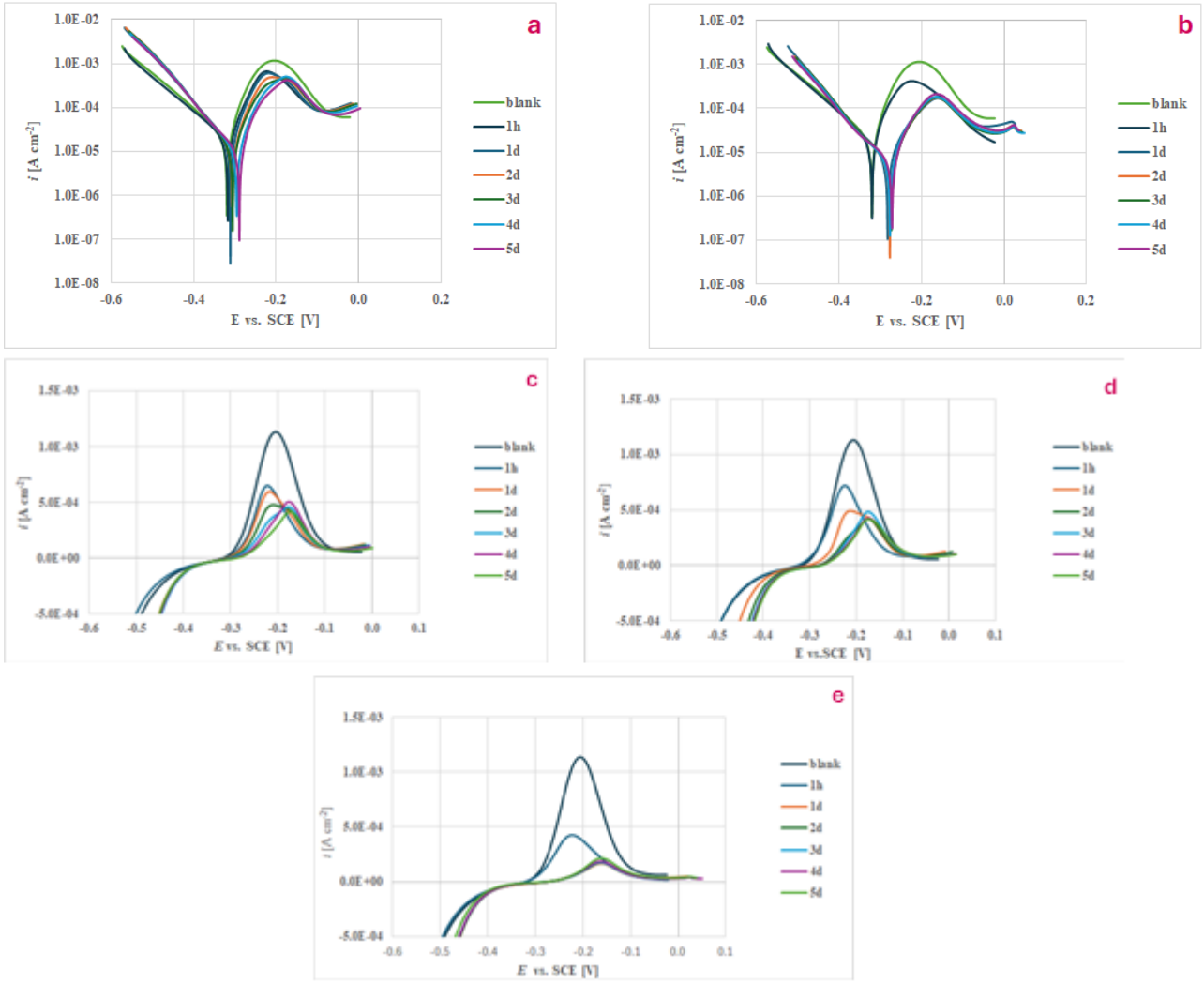

Figure 1. *Influence of the ionic liquid BMIFMS on the cathodic and anodic behaviour of AISI 316L in 1.0 M HCl at 25°C, after 1h, after 1, 2-, 3-, 4-, and 5-days duration test. a.) 0.2 wt% BMIFMS, b.) 0.5 wt% BMIFMS, c.) 0.2 wt% BMIFMS, d.) 0.3 wt% BMIFMS, e.) 0.5 wt% BMIFMS.*

Using Equation 1, the area of the inhibited region was compared with the area under the curve representing the response of the unprotected steel surface. In this way, the inhibition efficiency of the anodic part and its variations with time and BMIFMS concentration were determined, as summarised in Table.1. The difference in the reduction of the anodic current density/ charge under the oxidation curves shown in Figs. 1c and 1d is minimal or negligible. Therefore, this slight decrease in the anodic peak can be attributed primarily to the formation of a passive layer rather than to the adsorption of BMIFMS on the surface. In contrast, with the addition of 0.5 wt% BMIFMS, a pronounced decrease in the anodic peak and consequently in the anodic current density is clearly observed compared to the

responses in Figures 1c and 1d, which can be unequivocally attributed to the formation of an adsorbed BMIFMS layer. This is further confirmed by the increase in inhibition efficiency of the AISI 316L sample after 1 day of immersion, from 60% to more than 85%. While the use of 1.0 M HCl did not result in high inhibition efficiency of BMIFMS, except at the highest concentration added, significantly improved anticorrosion performance was observed in a solution that was twice as dilute (0.5 M HCl). This is confirmed by the reduction of the corrosion current density by up to three orders of magnitude. It can be concluded that the aggressiveness of the corrosive medium influences the adsorption efficiency of BMIFMS and, consequently, its inhibition performance. The high aggressiveness of the 1.0 M HCl medium likely causes the anodic reaction rate to dominate over the adsorption rate.

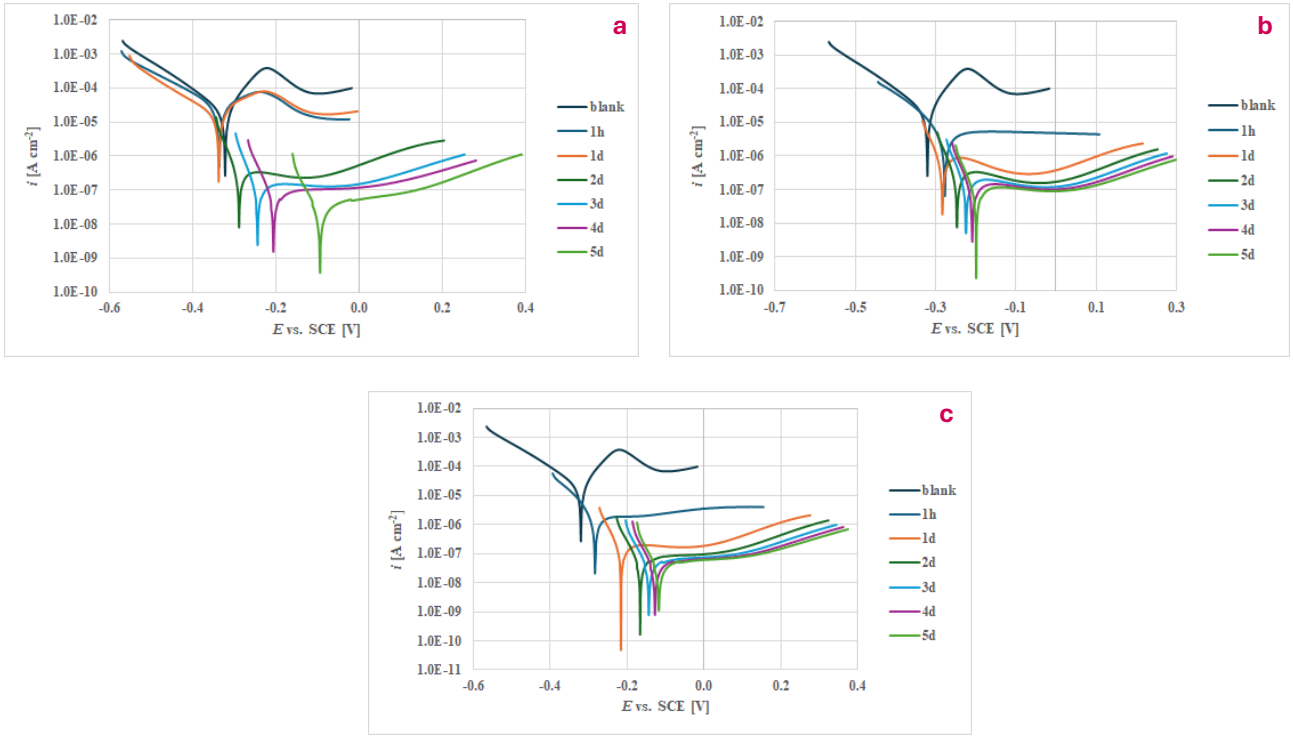

Figure 2. *Influence of the ionic liquid BMIFMS on the cathodic and anodic behaviour of AISI 316L in 0.5.0 M HCl at 25°C, after 1h, after 1, 2-, 3-, 4-, and 5-days duration test. a.) 0.2 wt% BMIFMS, b.) 0.3 wt% BMIFMS, c.) 0.5 wt% BMIFMS.*

Figures 2a–c illustrate the current–potential response as the concentration of added BMIFMS increases. At the lowest addition of 0.2 wt% BMIFMS, effective adsorption is observed only after 2 days of immersion. In contrast, for additions of 0.3 wt% and 0.5 wt% BMIFMS, a relatively high degree of adsorption is achieved after just 1 hour of immersion in the corrosive medium. The measurements further confirm that the adsorbed film remains stable even after 5 days of immersion in 0.5 M HCl, with inhibition efficiency exceeding 99.0%.

Table 2. Kinetic parameters for corrosion of SS AISI 316L for the bare surface after 1h, and for after 1, 2, 3, 4, and 5days duration test in the 0.5 M HCl at 25ºC at selected concentrations of the BMIFMS ionic liquid

time	β_C [V/dec]	β_A [V/dec]	i_{kor} [µA cm^{-2}]	R_p [kΩ cm^2]	E_{kor} [mV]	η_{ikor} [%]	η_{Rp} [%]
blank							
	0.133	0.077	26.96	0.746	-321.1	-	-
0.2 % BMIFMS							
1h	0.152	0.195	26.82	0.796	-335.9	0.50	6.28
1d	0.136	0.100	13.53	1.115	-337.0	49.81	33.12
2d	0.033	0.211	0.220	37.63	-288.7	99.18	98.02
3d	0.033	0.157	0.079	102.6	-242.4	99.71	99.27
4d	0.039	0.238	0.053	180.4	-206.3	99.80	99.59
5d	0.047	0.152	0.020	607.1	-92.53	99.93	99.88
0.3 % BMIFMS							
1h	0.063	0.179	2.418	5.565	-276.3	91.03	86.60
1d	0.040	0.190	0.560	17.53	-282.7	97.92	95.75
2d	0.037	0.176	0.196	47.32	-247.3	99.27	98.42
3d	0.037	0.167	0.111	80.79	-224.8	99.59	99.08
4d	0.037	0.153	0.077	114.4	-208.9	99.72	99.35
5d	0.036	0.143	0.059	140.3	-199.3	99.78	99.47
0.5 % BMIFMS							
1h	0.043	0.118	0.864	10.69	-284.8	96.79	93.02
1d	0.035	0.118	0.092	87.09	-217.4	99.66	99.14
2d	0.039	0.164	0.037	241.9	-165.1	99.86	99.69
3d	0.043	0.204	0.032	315.5	-144.2	99.88	99.76
4d	0.038	0.117	0.023	366.6	-128.4	99.91	99.80
5d	0.039	0.120	0.022	409.1	-117.7	99.92	99.82

Conclusion

The findings show that the corrosion inhibition efficiency of BMIFMS on AISI 316L stainless steel depends strongly on both the concentration of the ionic liquid and the aggressiveness of the corrosive medium. Minimal inhibition was observed in 1.0 M HCl, except at the highest concentration tested, whereas significant anticorrosive performance was achieved in 0.5 M HCl, even at lower BMIFMS concentrations. The improved performance in diluted acid is attributed to more favourable adsorption conditions, resulting in the formation of a stable protective film. Notably, the addition of 0.5 wt% BMIFMS provided over 99% inhibition efficiency after prolonged immersion. These results indicate that BMIFMS is a promising corrosion inhibitor for stainless steel, particularly in less aggressive acidic environments, where adsorption can effectively outcompete corrosion reactions.

Acknowledgements

This work was supported financially by the Slovenian Research Agency—ARRS, Ljubljana (www.aris-rs.si/sl) under the research project "Physico-Chemical Processes on the Surface Layers and Application of Nanoparticles" (P2-0006).

References

1. Y. L. Kobzar, K. Fatyeyeva, Ionic liquids as green and sustainable steel corrosion inhibitors: Recent developments, Chemical Engineering Journal, 425, 131480, 2021.
2. Fernicola, B. Scrosati, and H. Ohno, Potentialities of ionic liquids as new electrolyte media in advanced electrochemical devices, Ionics, 12(2), 95–102, 2006.
3. C. Verma, E. E. Ebenso, M.A. Quraishi, Ionic liquids as green and sustainable corrosion inhibitors for metals and alloys: An overview, Journal of Molecular Liquids, 233, 403–414, 2017.

Ionic Liquid-Modified Hydrophobic Layers for Enhanced Corrosion Inhibition

Regina Fuchs–Godec*, Jan Vodenik

Faculty of Chemistry and Chemical Engineering, University of Maribor, Smetanova 17, Maribor

https://doi.org/10.65614/uisk_yucorr.2025.26.ch14

*regina.fuchs@um.si

Abstract

The aim of this study was to investigate the potential of the ionic liquid 1-methyl-3-n-octylimidazolium bis(trifluoromethanesulfonyl)imide (M3OITF), in combination with stearic acid (SA), to form self-assembled hydrophobic protective layers SAHL on AISI 316L stainless steel. The corrosion resistance of the resulting layers were evaluated in 1.0 M and 0.5 M HCl solutions using potentiodynamic polarisation measurements. Results show that immersing steel samples in ethanolic solutions of SA containing various concentrations of M3OITF leads to the formation of a hydrophobic layer that effectively suppresses anodic dissolution. Increasing the M3OITF concentration significantly decreased the anodic current density and enhanced inhibition efficiency. In 1.0 M HCl, inhibition efficiencies above 85% were achieved for all concentrations tested, while in 0.5 M HCl, efficiencies close to 99.9% were obtained. Contact angle measurements confirmed the hydrophobic nature of the modified surfaces, remaining above 105° even after five days of immersion in 0.5 M HCl. These findings demonstrate that M3OITF, when combined with stearic acid, can effectively form durable and highly efficient self-assembled anticorrosive coatings.

Keywords: *stainless-steel; HCl; ionic liquid; SAHL*

Introduction

The development of green chemistry and sustainable chemical engineering promotes the search for non-toxic substances and environmentally friendly technological solutions. In this context, ionic liquids (ILs) have emerged as a promising alternative to traditional, environmentally harmful organic corrosion inhibitors. ILs are salts composed of cations and anions with melting points below 100 °C. Their liquid state at room temperature results from weak electrostatic interactions between ions, caused by large, asymmetric ionic species that prevent the formation of an ordered crystalline structure. Due to these structural characteristics, ILs do not crystallise but remain liquid, enabling their efficient use as solvents or functional components in various applications, including corrosion inhibition. Ionic liquids possess several environmentally beneficial properties, such as non-toxicity, non-flammability, high stability across wide pH and temperature ranges, and very low vapour pressures, which significantly reduce evaporation into the environment and consequently limit air pollution by volatile compounds. Moreover, ILs serve as sustainable solvents for a wide variety of inorganic and organic compounds. They are anhydrous liquids with low oxygen content and a high concentration of ionic species. The cationic parts act as electron-accepting sites, while the electron-rich functional groups serve as adsorption centres during corrosion inhibition. The anion contributes to interfacial stabilisation throughout the adsorption process [1,2].

A key advantage of ionic liquids is their molecular tunability—they can be synthesised to possess specific, tailored properties. The appropriate selection of cations and anions allows adjustment of the structure and functionality of ILs according to the desired medium, material, or environmental requirements. In this way, their specificity, efficiency, and environmental compatibility can be optimised. Among the most efficient modern approaches for preparing such customised ionic liquids is microwave-assisted synthesis, which provides a rapid and energy-efficient process. Despite their

many advantages, the broader application of ILs is currently limited by their relatively high cost compared to conventional organic inhibitors [3,4].
The aim of this study was to investigate the use of the ionic liquid 1-Methyl-3-n-octylimidazolium bis(trifluoromethanesulfonyl)imide (M3OITF) in combination with stearic acid (SA) for the formation of self-assembled hydrophobic protective layer. The corrosive media used were 1.0 M HCl and 0.5 M HCl. The inhibition efficiency of the coatings was evaluated using the classical potentiodynamic method, while FTIR spectroscopy and scanning electron microscopy (SEM) were used to characterise the self-assembled layer.

Experimental

The conventional three-electrode configuration was used for the potentiodynamic studies. All potentials were measured against the saturated calomel electrode (SCE), and the counter electrode was platinum. Measurements were conducted within a potential range of ±300 mV relative to the open circuit potential (OCP), with a scan rate of 1 mV s^{-1}. Polarisation plots were obtained 60 minutes after the working electrode was immersed in the solution, allowing the stationary potential to stabilise. All experiments were performed at 25 °C ± 1 °C. Potentiodynamic curve measurements were taken after 1 hour of immersion and after 1, 2, 3, 4, and 5 days of testing. The measurements were performed using a Gamry 600™ potentiostat/galvanostat controlled by electrochemical software. Data were collected and analysed using CorrView and CorrWare software developed by Scribner Associates, Inc. The samples intended for the formation of self-assembled coatings were immersed in an ethanolic solution of 0.05 M SA containing varying amounts of the ionic liquid M3OITF: (0.05 M SA + 1.0% M3OITF), (0.05 M SA + 2.0% M3OITF), and (0.05 M SA + 5.0% M3OITF). The specimens designated for electrochemical measurements in 1.0 M HCl were kept in these solutions for 24 hours. The same procedure was applied to another set of samples subsequently exposed to a 0.5 M HCl solution, which were also immersed for 24 hours in freshly prepared solutions. After immersion, the steel samples were carefully removed from the solutions using tweezers and dried with compressed air, resulting in a functionalised self-assembled surface layer.

Results and discussions

Electrochemical results

Figures 1a-c show the current–potential curves of AISI 316L steel in 1.0 M HCl, modified with a self-assembled coating prepared by immersing the metallic samples in an ethanolic solution of 0.05 M stearic acid (SA) with the addition of x wt% of the ionic liquid M3OITF. Measurements were performed after different immersion times (1 h, 2 days, 3 days, 4 days, and 5 days). All polarisation curves display a distinct anodic peak, indicating the material's susceptibility and the presence of anodic dissolution in the corrosive medium. After surface functionalisation with the self-assembled coating, the area under the anodic peak decreased significantly, suggesting improved corrosion resistance and reduced anodic activity. The formation of a hydrophobic layer by immersion in the ethanolic SA solution containing M3OITF effectively reduced surface hydrophilicity and enhanced the protective performance of the coating. Increasing the M3OITF concentration further decreased the anodic current, confirming higher inhibition efficiency of the coating at greater mass fractions of the ionic liquid. The inhibition efficiency was calculated according to Equation 1, based on integration of the area under the anodic peak of each polarisation curve, by comparing the untreated sample with those protected by the self-assembled coating. The integration limits were defined within the potential range between the open-circuit potential (OCP) and –0.1 V vs SCE.

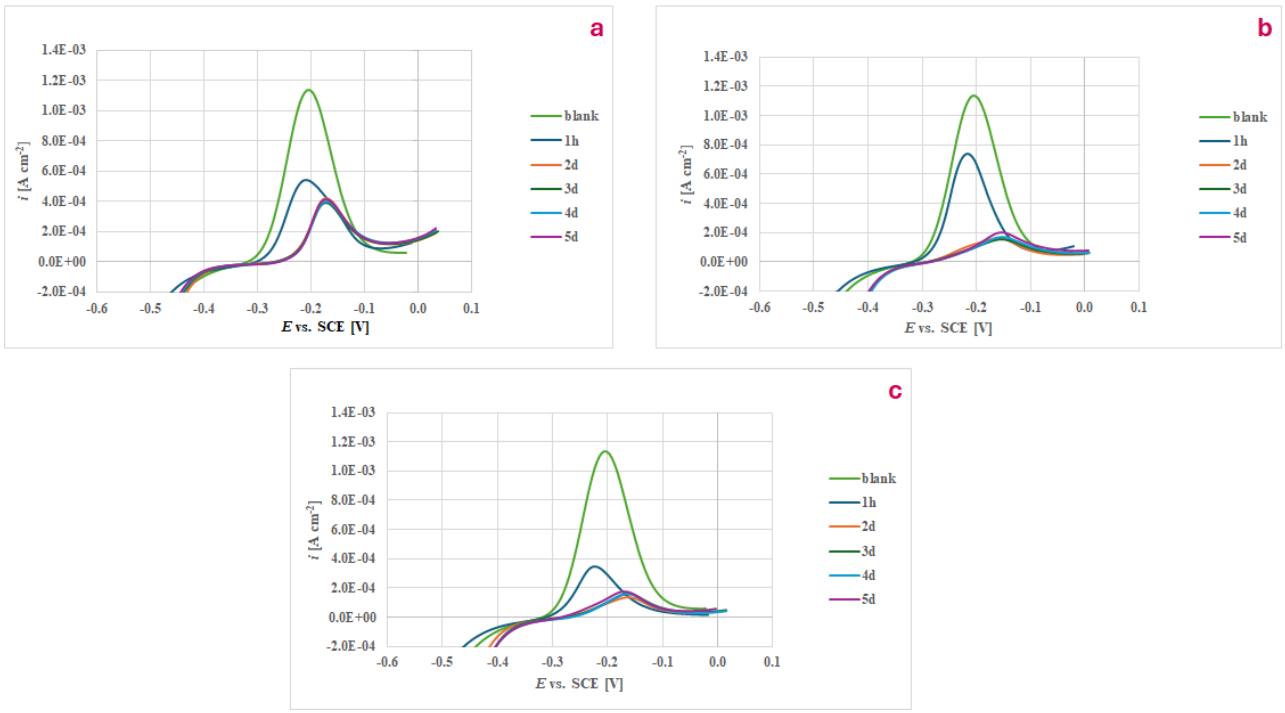

Figure 1. *Potentiodynamic polarisation curves (1 mVs^{-1}) of AISI 316L in 1.0 M HCl at 25°C, after 1h, after 2-, 3-, 4-, and 5-days duration test. a.) (0.05 M SA + 1.0% M3OITF), b.) (0.05 M SA + 2.0% M3OITF), c.) (0.05 M SA + 5.0% M3OITF).*

$$\eta_a = \frac{A - A'}{A} \cdot 100\% \qquad (1)$$

where:
η_a – inhibition efficiency of the anodic part
A – area under the curve of the unprotected sample surface
A' – area under the curve of the inhibited sample surface

Figure 2 shows that the self-assembled hydrophobic layers effectively inhibit the development and progression of anodic reactions after two days of immersion in the selected corrosive medium. The lowest addition of M3OITF forms a protective coating that inhibits dissolution of the steel sample by more than 70.0%. The two higher concentrations of ionic liquid achieve inhibition efficiencies above 85.0% in 1.0 M HCl. All three concentrations demonstrate the durability of the coatings even after five days, as there is no significant decrease in inhibition or increase in the area under the anodic peak. In addition, it can be concluded that a higher concentration does not result in a significant improvement in η.

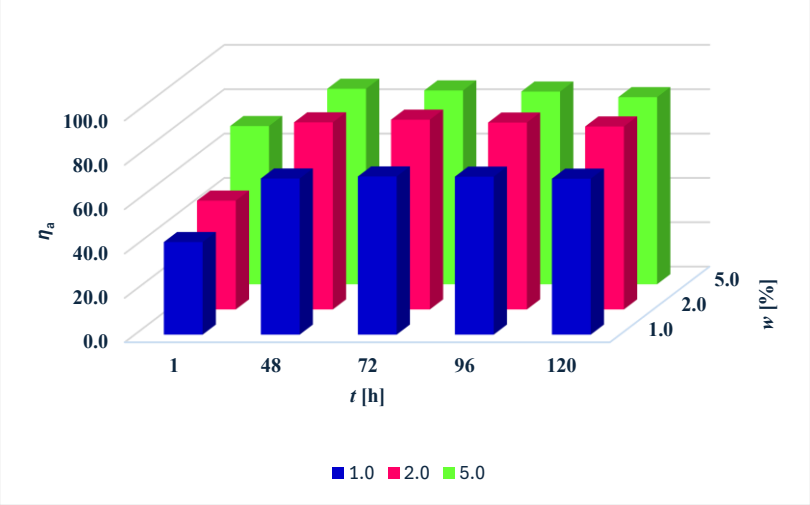

Figure 2. *Dependence of inhibitory effectiveness, determined from the charge involved in the surface anodic reaction, on time and concentration of M3OITF in 1.0 M HCl at 25°C, after 1h, after 2-, 3-, 4-, and 5-days duration test.*

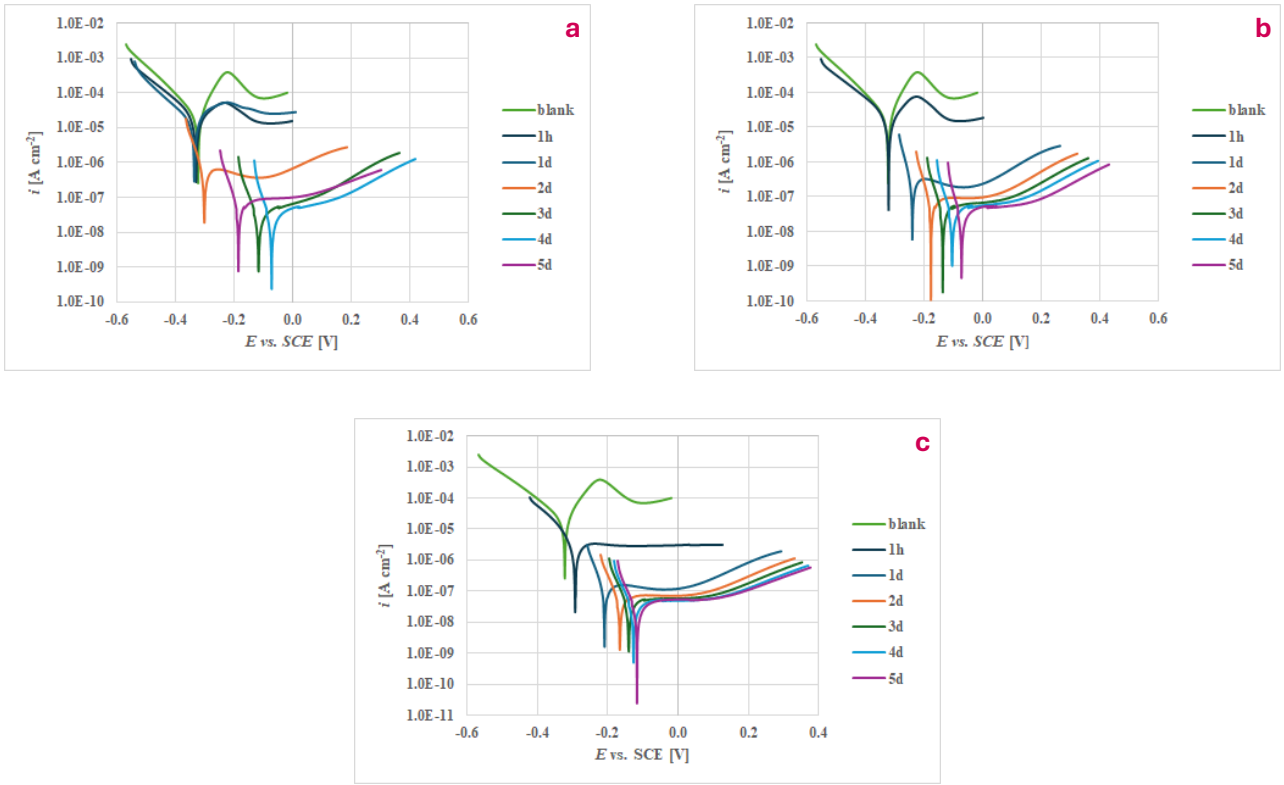

Figure 3. *Potentiodynamic polarisation curves (1 mVs^{-1}) of AISI 316L in 0.5 M HCl at 25°C, after 1h, after 1-, 2-, 3-, 4-, and 5-days duration test. a.) (0.05 M SA + 1.0% M3OITF), b.) (0.05 M SA + 2.0% M3OITF), c.) (0.05 M SA + 5.0% M3OITF).*

Table 1 presents the electrochemical parameters and the calculated inhibition efficiencies for three concentrations of M3OITF, which, together with SA, formed an anticorrosive self-assembled coating. The inhibitor concentrations were 1.0%, 2.0%, and 5.0%. The corrosive medium was 0.5 M HCl.

Table 1. Kinetic parameters for corrosion of SS AISI 316L obtained from potentiodynamic polarisation curves for the bare and modified surfaces in the 0.5 M HCl 25°C at

selected concentrations of M3OITF ionic liquid, after 1h, and after 1-, 2-, 3-, 4-, and 5-days duration test

time	β_C [V/dekada]	β_A [V/dekada]	i_{kor} [µA cm^{-2}]	R_p [kΩ cm^2]	E_{kor} [mV]	η_{ikor} [%]	η_{Rp} [%]
brez prevleke							
blank	0.133	0.077	26.96	0.746	-321.1	-	-
1.0 % M3OITF							
1h	0.145	0.225	21.17	1.167	-328.4	21.48	36.10
1d	0.134	0.128	13.22	1.328	-336.4	50.96	43.85
2d	0.045	0.488	0.512	24.37	-301.0	98.10	96.94
3d	0.047	0.157	0.022	534.0	-114.9	99.92	99.86
4d	0.042	0.139	0.018	612.4	-70.43	99.93	99.88
5d	0.043	0.271	0.050	210.5	-184.3	99.81	99.65
2.0 % M3OITF							
1h	0.146	0.155	20.20	1.178	-320.9	25.06	36.70
1d	0.032	0.165	0.195	40.6	-242.5	99.28	98.16
2d	0.034	0.226	0.055	154.6	-178.5	99.80	99.52
3d	0.038	0.201	0.033	272.0	-135.1	99.88	99.73
4d	0.039	0.142	0.024	375.2	-103.6	99.91	99.80
5d	0.035	0.150	0.021	410.1	-72.08	99.92	99.82
5.0 % M3OITF							
1h	0.067	0.457	2.53	6.469	-292.6	90.62	88.47
1d	0.035	0.207	0.095	93.17	-207.7	99.65	99.20
2d	0.039	0.269	0.044	222.8	-164.7	99.84	99.67
3d	0.041	0.182	0.030	335.3	-141.0	99.89	99.78
4d	0.041	0.169	0.024	412.0	-125.4	99.91	99.82
5d	0.039	0.147	0.021	461.5	-117.0	99.92	99.84

With 1.0% and 2.0% M3OITF incorporated into the self-assembled hydrophobic layer with stearic acid, we observed that one hour after exposure to 0.5 M HCl, there was almost no effect. However, with 5.0% M3OITF, an inhibition efficiency greater than 90.0% was achieved within one hour. As the inhibitor concentration increased, the time required for the coating to effectively suppress corrosion processes decreased. All concentrations of M3OITF reached similar inhibition efficiency values, around 99.9% (Fig.4). This indicates that the anticorrosive coating almost completely prevents corrosion of the metal sample.

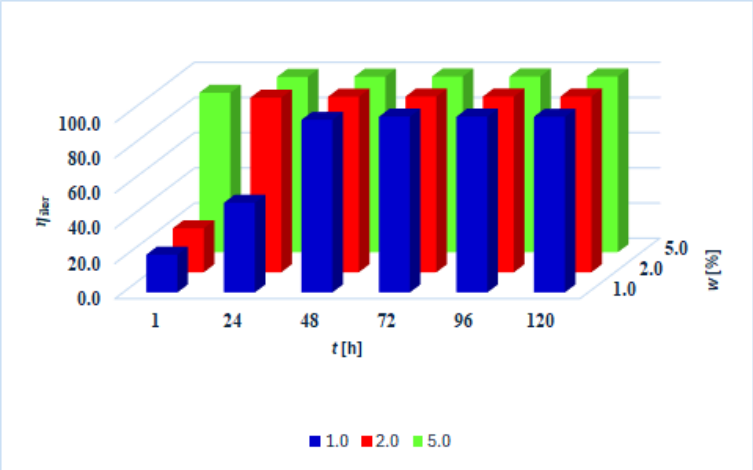

Figure 4. *Dependence of inhibitory effectiveness, on time and concentration of M3OITF in 1.0 M HCl at 25°C, after 1h, after 1-, 2-, 3-, 4-, and 5-days duration test.*

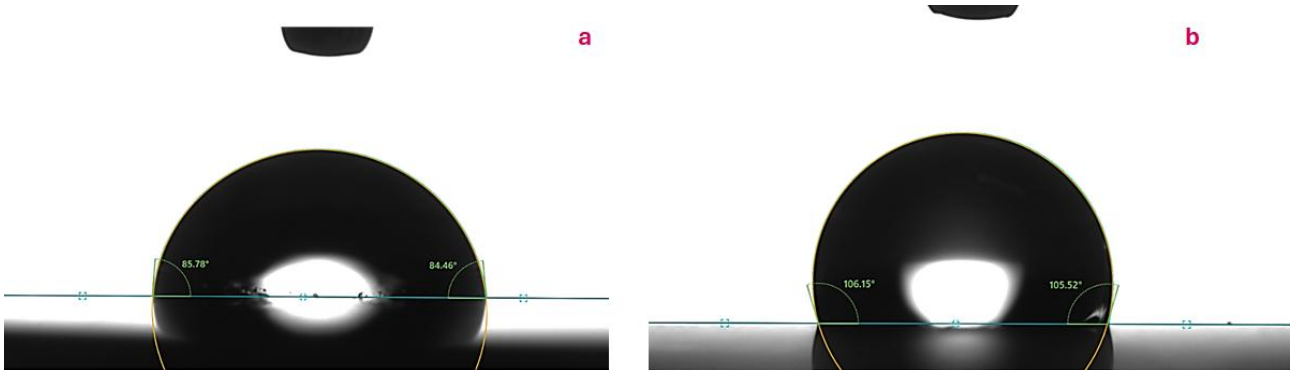

Figure 5. *a.) Contact angle of the polished sample surface of the AISI 316L, b.) Contact angle of the modified sample surface of the AISI 316L (0.05 M SA + 2.0% M3OITF).*

Figure 5a shows the measured contact angle of the polished surface of AISI 316L without a protective layer. As this angle is 85°, the sample surface exhibits hydrophilic properties. Figure 5b shows the measured contact angle of the SAHL coating containing 2.0% M3OITF after 5 days of immersion. After 5 days, the contact angle exceeds 105°, confirming that the surface of the modified sample retains its hydrophobic properties even after 5 days of immersion in 0.5 M HCl. This is also reflected in the high inhibition efficiency of over 99%.

Conclusions

- In 1.0 M HCl, the SAHL with M3OITF significantly reduced anodic dissolution, achieving inhibition efficiencies above 70% for 1.0% M3OITF and over 85% for 2.0% and 5.0% concentrations. The SAHL remained stable after five days of immersion.

In 0.5 M HCl, the SAHL showed superior performance. The 5.0% M3OITF layer achieved over 90% inhibition within one hour, while all concentrations reached efficiencies of around 99 % after five days, maintaining strong hydrophobicity (contact angle >105°).

- Overall, combining stearic acid with M3OITF enables the formation of durable, hydrophobic, and highly efficient anticorrosive self-assembled coatings for stainless steel in acidic environments.

Acknowledgements

This work was supported financially by the Slovenian Research Agency—ARRS, Ljubljana (www.aris-rs.si/sl) under the research project "Physico-Chemical Processes on the Surface Layers and Application of Nanoparticles" (P2-0006).

References

1. R.D. Rogers, G.A. Voth, Ionic Liquids, *American Chemical Society*, **40,** 1077–1078, 2007.
2. Y. L. Kobzar, K. Fatyeyeva, Ionic liquids as green and sustainable steel corrosion inhibitors: Recent developments, *Chemical Engineering Journal*, **425**, 131480, 2021.
3. L. Souza, E. Pereira, L. Matlakhova, V.A.F. Nicolin, S.N. Monteiro, A.R.G de Azevedo, Ionic liquids as corrosion inhibitors for carbon steel protection in hydrochloric acid solution: A first review. *Journal of Materials Research and Technology* **22,** 2186–2205, 2023.
4. A.O. Gadioli, L.M. de Souza, E.C. Pereira, S.N. Monteiro, A.R.G. Azevedo, Imidazolium-based ionic liquids as corrosion inhibitors for stainless steel in different corrosive media: An overview. *Journal of Materials Research and Technology*, **29**, 803–823, (2024).

Testing and verification of the quality of JET A-1 fuel and lubricants from the aspect of device operation and engine unit testing

Ispitivanje i verifikacija kvaliteta goriva JET A-1 i maziva sa aspekta rada uređaja i ispitivanja agregata motora

Danijela Jovičić, Zorica Ristić, Stanko Spasojević, Božidarka Arsenović*

„ORAO“ A.D. za proizvodnju i remont Bijeljina, Republika Srpska, Bosna i Hercegovina

https://doi.org/10.65614/uisk_yucorr.2025.26.ch15

bokijevmejl@gmail.com

Abstract

In the aviation industry, in order to ensure the safe operation of jet engines in all modes and in all application conditions, the fuel and lubricants used must have a safe quality prescribed by relevant international standards. Conventional jet fuels are chemically complex mixtures consisting of four basic groups of hydrocarbons: paraffin, naphthene, aromatics and olefins. Their content in the fuel ranges from 98% to 99%, while the rest from 1% to 2% are non-hydrocarbon compounds: sulfur, nitrogen, oxygen and traces of various metals or compounds containing metals. In the last decades of the twentieth century, the development and use of sustainable alternative jet fuels emerged as a key factor in reducing the decarbonization of the airspace (reducing aviation-related CO_2 emissions). "Refuel Aviation" initiative promotes the development and use of sustainable aviation fuels. of SAFs (sustainable aviation fuels) for the decarbonization of air traffic, highlighting the obligation of suppliers to increasingly sell sustainable fuels at all airports within the EU.

Lubricants in aviation face serious challenges, the biggest of which is heat. Modern engine housings achieve lubricant temperatures in the range between 80 °C and 100 °C, while during purification this temperature rises to approximately 190 °C, with exposure to temperatures up to 300 °C and 400 °C along the metal wall in the chamber bearing.

The paper presents some physical and chemical characteristics of modern JET A-1 fuel and the characteristics and composition of some lubricants. Verification of the quality of the same at the end user is a necessary and legally binding condition for proper exploitation.

Keywords: *Jet fuel JET A-1; lubricants; turbojet engine; quality control*

Izvod

U vazduhoplovnoj industriji, u cilju obezbjeđivanja sigurnog rada mlaznih motora na svim režimima i u svim uslovima primjene upotrijebljeno gorivo i maziva moraju imati siguran kvalitet propisan relevantnim međunarodnim standardima. Konvencionalna mlazna goriva su po hemijskom sastavu složene smješe koje se sastoje se od osnovne četiri grupe ugljovodonika: parafina, naftena, aromata i olefina. Njihov sadržaj u gorivu kreće se od 98% do 99%, dok su ostatak od 1% do 2% neugljovodonična jedinjenja: sumpora, azota, kiseonika i u tragovima različiti metali ili jedinjenja koja sadrže metale. Posljednje decenije dvadesetog vijeka, razvoj i upotreba održivih alternativnih mlaznih goriva se javlja kao ključni faktor u smanjenju dekarbonizacije vazdušnog prostora (smanjenju emisija CO_2 vezanog za vazduhoplovstvo). „Refuel Aviation“ inicijativa promoviše razvoj i upotrebu održivih vazduhoplovnih goriva tzv. SAF-ova (sustainable aviation fuels) za dekarbonizaciju vazdušnog saobraćaja, ističući kao obavezu snabdjevača da sve više prodaju održiva goriva na svim aerodromima unutar EU.

Maziva se u vazduhoplovstvu suočavaju s ozbiljnim izazovima, od kojih je najveći izazov toplota. Moderna kućišta motora postižu temperature maziva u rasponu između 80 °C i 100 °C, dok se

prilikom prečišćavanja ta temperatura podiže i na približno 190°C, uz izlaganje temperaturama uz metalni zid u ležaju komora čak do 300 °C i 400 °C.
U radu su prikazane neke fizičko-hemijske karakteristike savremenog goriva JET A-1 i karakteristike i sastav nekih maziva. Verifikacija kvaliteta istih kod krajnjeg korisnika je neophodan i zakonski obavezujući uslov za pravilnu eksploataciju.
Ključne riječi: *mlazno gorivo JET A-1; maziva; turbomlazni motor; kontrola kvaliteta*

Uvod

Sa aspekta trenutnih mogućnosti i raspoloživih resursa, "ORAO" a.d. Bijeljina ima *osvojen i serijski izvršeni remont turbomlaznih motora* (motori Rolls-Royce): VIPER 22-6, VIPER 22-8, VIPER 531, VIPER 632-41, VIPER 632-46, VIPER 632-43 i VIPER 633-41 i *motora ruske proizvodnje:* R-13-300, R-25-300, RD-33, R-95Š i AI-*25TL i osvojenu i serijski izvršenu proizvodnju motora* VIPER 632/633 po licenci firme Rolls-Royce iz Engleske. U obezbjeđivanju sigurnog rada mlaznih motora na svim režimima i u svim uslovima primjene, goriva moraju imati siguran kvalitet. Pored opštih osobina, karakterističnih za sva tečna goriva, ovdje su posebno strogi zahtjevi za visokim stepenom kvaliteta specifičnih osobina. Ovako stroge zahtjeve postavljaju i opravdavaju uslovi upotrebe mlaznih goriva, kao što su veoma velike brzine i visine leta mlaznih aviona, a na njih utiču i termički najopterećeniji dijelovi mlaznog motora: komora sagorijevanja, gasna turbina i sl. kao i goriva instalacija. Pored navedenih, postoji i drugi niz problema zbog kojih gorivo za mlazne motore mora ispuniti određene zahtjeve.
Na našim prostorima u upotrebi je gorivo JET A-1, a to je kerozinska frakcija nafte sa temperaturom ključanja u temperaturnom intervalu od 170°C do 300°C. Ovo mlazno gorivo, po svom kvalitetu zadovoljava zahtjeve vojnog i civilnog vazduhoplovstva [1,2].
U cilju smanjenja emisija gasova staklene bašte, **IATA** *(International Aviation Transport Association*) je ažurirala strategiju kojoj je *osnovni cilj da avioni imaju 0% emisija gasova staklene bašte do 2050. godine.* Ta strategija se sastoji od četiri faze:

1) *unaprjeđenje tehnologije i visoka opredjeljenost ka gorivima sa niskim sadržajem ugljenika,*
2) *unaprjeđenje operacija aviona,*
3) *kvalitetnija infrastruktura u aerodromima,*
4) *ekonomske mjere, radi postizanja globalnog tržišta i pokrivanja ostalih emisija.*

Održivo vazduhoplovno gorivo *(Sustainable Aviation SAF)* je glavni naziv koji vazduhoplovna industrija koristi za predstavljanje nekonvencionanog vazduhoplovnog goriva.
Standard ASTM D7566 *(Standard za avionsko sintetizovano turbinsko gorivo koje sadrži ugljovodonike).* Ova oznaka definiše karakteristike i svojstva obje uredne sintetizovane komponente miješanja, *kao i miješani avionsko-turbinski ekvivalent goriva (mlazno gorivo JET A i JET A-1). Sintetizovane komponente* mogu biti izrađene iz mnogih izvora, kao što su prvenstveno biomasa (lignoceluloza, šećeri, masti, ulja i masti), otpadni tokovi, sintetički gas, itd.
Standard ASTM D1655 *(Standardna specifikacija za avio-turbinsko gorivo)* definiše specifične vrste avio-turbinskog goriva za civilnu upotrebu u radu i sertifikaciji aviona, opisuje gorivo za koje je *utvrđeno da je zadovoljavajuće obnovljivo vazduhoplovno gorivo* (zakonodavna primjena za rad aviona i motora).

Fizičko-hemijske karakteristike mlaznog goriva

Po hemijskom sastavu mlazna goriva su složene smješe a sastoje se od osnovne četiri grupe ugljovodonika: parafina, naftena, aromata i olefina. Njihov sadržaj u gorivu kreće se od 98% do 99%, dok su ostatak od 1% do 2% neugljovodonična jedinjenja: sumpora, azota, kiseonika i u tragovima različiti metali ili jedinjenja koja sadrže metale. Ovakav sastav mlaznih goriva uslovljen je strogim zahtjevima za što većom toplotnom moći i stabilnošću, a što manjim stvaranjem gareži, što upravo obezbjeđuju parafinski i naftenski ugljovidonici. U mlaznim gorivima najzastupljeniji su parafinski i

naftenski ugljovodonici (oko 70%). Sadržaj aromatskih ugljovodonika je manje poželjan zbog toga što oni imaju manju toplotnu moć (za oko 10%), smanjuju brzinu i potpunost sagorijevanja, povećavaju stvaranje gareži, uzrokuju progorijevanje komore za sagorijevanje i snižavaju termičku stabilnost. Olefini su hemijski nestabilni i skloni stvaranju smola a pogoršavaju termičku stabilnost goriva. U tabeli 1 prikazani su osnovni podaci o gorivu za mlazne motore JET A-1 [3,4,6].

Tabela 1. Osnovni podaci o gorivu za mlazne motore JET A-1

Red. broj	KARAKTERISTIKE	VRIJEDNOST
	Izgled	bistra prozračna tečnost bez slobodne vode i vidljivih mehaničkih nečistoća na temperaturi okoline
1	**Boja**	prijavljuje se
2	**Čestice, ukupan broj čestica, mg/l**	max 1.0
SASTAV		
3	**Ukupna kiselost, mg KOH/g**	max 0,015
4	**Sadržaj aromata, %v/v**	max 25
5	**Sadržaj ukupnih aromata, %v/v**	max 26.5
6	**Sadržaj ukupnog sumpora**	max 0.30
7	**Sadržaj merkaptanskog sumpora**	max 0,003
ISPARLJIVOST		
8	**Destilacija: početak, ^{0}C**	prijavljuje se
	10%v/v postotak predestilisanog, ^{0}C	205
	50%v/v postotak predestilisanog, ^{0}C	prijavljuje se
	90%v/v postotak predestilisanog, ^{0}C	prijavljuje se
	Kraj, ^{0}C	max 300
	Ostatak, %v/v	max 1.5
	Gubitak, %v/v	max 1.5
9	**Gustina kod 15^{0}C, kg/m^3**	max 775.0 do 840.0
OSOBINE TEČLJIVOSTI		
10	**Tačka mržnjenja, ^{0}C**	max – 47.0
11	**Kinematička viskoznost na -20^{0}C, mm^2/s**	max 8.000
TOPLOTNA MOĆ		
12	**Toplotna moć (donja), MJ/kg**	min 42.80
STABILNOST		
13	**Kontrolna temperatura, ^{0}C** **Razlika pritiska na filtru, mmHg** **Ocjena taloga na cijevi grijača (vizuelno), razred**	max 260 mmax 25.0 manje od 3
NEČISTOĆE, mg/100 ml		
14	**Postojeća smola, max** **S aditivom za poboljšanje provodljivosti** **Bez aditiva za poboljšanje provodljivosti**	max 7 min 70 min 85
15	**Električna provodljivost, pS/m**	50 do 600

Shodno međunarodnim standardima, u mlaznim gorivima dozvoljena je primjena samo propisanih sljedećih aditiva: *antioksidanasa, antistatičkih sredstava, inhibitora korozije, biocida i metalnih deaktivatora.*

Fizičko-hemijske karakteristike maziva za mlazne motore

Mlazni motori aviona, u principu su jednostavniji od klipnih motora u pogledu njihove kompleksnosti i izgradnje, pa su, shodno tome i jednostavniji kada se primjenjuju maziva za podmazivanje. U komori za sagorijevanje goriva nema pokretnih dijelova, te mazivo nije izloženo direktno temperaturama izgaranja. Kako su kompresor i turbina glavni pokretni dijelovi u stalnoj rotaciji, tako su izbjegnuti problemi s dinamičkim opterećenjem zbog povratnih rotacija elemenata. No i pored toga, maziva se i dalje suočavaju s ozbiljnim izazovima, od kojih je najveći izazov toplota. Moderna kućišta motora postižu temperature maziva u rasponu između 80 °C i 100 °C, dok se prilikom prečišćavanja ta temperatura podiže i na približno 190 °C, uz izlaganje temperaturama uz metalni zid u ležaju komora čak do 300 °C i 400 °C [4,5].
Kombinujući ovo s činjenicom i težnjom da se avioni u letu učine što je moguće izdržljivijima, kako bi se smanjili troškovi održavanja i produžilo vrijeme između velikih remonta, trenutno više od 40.000 radnih sati za neke civilne motore, onda je jasno, kako maziva moraju biti postojana kroz dugi vremenski period. Pojavljuje se problem vezan za teškoće maziva da toliko dugo ostanu funkcionalna. Maziva se tokom rada troše, potrebno ih je nadoknađivati svježim mazivima. Ne postoje proizvodi koji bi uklanjali talog nastao izgaranjem maziva (problem pojave redovnog formiranja naslaga taloga koksa usljed visokih temperatura tokom rada motora). Svaki stvoreni talog mora biti uklonjen, kako bi se spriječila začepljenja. Mazivo i dalje ima važnu ulogu u smanjivanju stvaranja naslaga i prema tome, mora biti ostvarena mogućnost efikasnog uklanjanja već stvorene naslage. Toplotna postojanost turbinskih maziva, vjerovatno, je najveći izazov, kako za proizvođače maziva, tako i za projektante mlaznih motora [5,6].

Sastav i osobine maziva za mlazne motore

U proizvodnji ulja za podmazivanje (maziva) u vazduhoplovnoj industriji, kao najefikasnijim su se pokazali *esteri, tj. di-ester temeljena maziva na bazi di-bazičnih kiselina*, kao što su [4]:
sebacijanska kiselina, HOOC–$(CH_2)_8$–COOH; azelainska kiselina, HOOC–$(CH_2)_7$ – COOH i adipinska kiselina, HOOC–$(CH_2)_4$–COOH. Ove kiseline, u reakciji sa alkoholima, grade di-estere. Izbor, kako kiseline, tako i alkohola ima značajan uticaj na osobine gotovog proizvoda. Na primjer, više lanaca di-kiseline poboljšava indeks viskoziteta, ali smanjenjuje temperature stinjavanja.
Sintetičko motorno ulje, Mobil Jet Oil 2, MIL PRF23699F je organska materija *visokosintetičkog baznog ulja (fluida) neopentil poliol estera*, slika 1. Sadrži dodatke – aditive za poboljšanje *oksidacionih, antikorozionih osobina kao i dodatke protiv habanja, tabela 2.* Ovo sintetičko motorno di-ester ulje je pogodno za maksimalnu temperaturu ulja u rezervoaru do 149°C i temperature u ležaju do 204 °C. Posjeduje odobrenje proizvođača za veliki broj motora: Honeywell turbine; Kompanija za motore Rolls-Royce/Alison; CMF-International; General Elctric kompanija; Međunarodni aeromotori; Pratt & Whitney grupa Kanada; Rolls-Royce Limited; CHECMA; Kompanija za turbinske motore Honeywell/Garrett i Turbomeca.

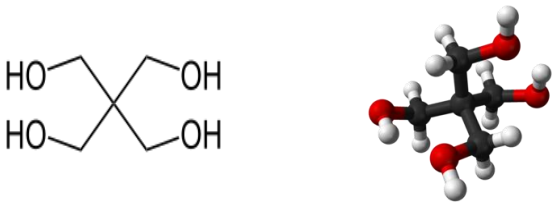

Slika 1. *Pentraeritritilol, $C_5H_{12}O_4$.*

Tabela 2. Sastav sintetičkog motornog ulja Mobil Jet Oil 2

Red. Broj*	Naziv	CAS broj
1	masne kiseline, C5-10 estri sa pentaeritritolom (*fatty acids, c5-10, esters with pentaerythritol)*	68424-31-7
2	masne kiseline, C5-10 estri sa dipentaeritritolom (*fatty acids, c5-10, esters with dipentaerythritol)*	70983-72-1
3	1-naftilamin, n-fenil, *(1-naphthylamine, n-phenyl-)*, PAN, $C_{16}H_{13}N$	90-30-2
4	bis(4-(1,1,3,3-tetrametilbutil)fenil)amin, *(bis(4-(1,1,3,3-tetramethylbutyl)phenyl)amine),* OPAN, $C_{28}H_4O$	15721-78-5
5	trikrezil fosfat *(tricresyl phosphate) TCP,* $C_{21}H_{21}O_4P$	1330-78-5
6	fosfor *(phosphorus),* P	7723-14-0

**1 i 2 – bazno ulje; 3-6- aditivi*

Jedna od najvažnijih osobina mazivih ulja je *promjena viskoznosti ulja s temperaturom* (sposobnost tečenja ili unutrašnjeg trenja slojeva). U vezi s tim, na osnovu ponašanja ulja na temperaturi 40°C, sva maziva su klasifikovana u 7 *ISO VG viskozitetnih gradacija* (ISO VG 15 do ISO VG 150, slika 3. Ulja za podmazivanje niže viskoznosti i potencijalno većeg otpora naprezanju moraju održavati dovoljnu debljinu uljnog filma, u suprotnom će porastom temperature doći do smanjenja ili nestanka uljnog filma i kontakta dviju metalnih površina. Tada se kaže da je došlo do „zaribavanja".

Osobine baznih ulja poboljšavaju se dodavanjem aditiva gotovom proizvodu. Osim *poliglikol zgušnjivača*, koji se koristi u *7,5 cSt diester - baznim mazivima*, za većinu vrsta koristi se i *poliol.*

Aero Shell Turbine Oil 750, DEF STAN 91-098 je sintetičko miješano estarsko ulje viskoznosti 7,5 cSt koje sadrži zgušnjivač i aditive koji pružaju permanentno podmazivanje u civilnim gasnim turbinama, posebno turbopropelerskim motorima (dobro ulje za prenos opterećenja za reduktor propelera).

Kod mlaznih motora, dodaci mazivu koji se najčešće koriste protiv oksidacije su *fenil-α-naftilamin, PAN, oktitfeml-α-naftilamin, OPAN i dioktifenilamin, DODPA i njihovi derivati.*

Optimalnu efikasnost maziva za mlazne motore, u smislu postizanja sinergističkog efekta, daju *dva anti-oksidansa* (veća sigurnost pri datoj koncentraciji zajedno nego pojedinačno). To je *kombinacija oligomernih i monomernih amina kao antioksidansa.* Druga inovacija je primjena *monomernog antioksidansa* koji čine oligomeri tokom oksidacije, čime se produžava dužina trajanja protu-oksidativnih osobina maziva. Jedan osnovni nedostatak modernih antioksidantnih kombinacija je njihova tendencija ka agresivnosti prema elastomerima.

Maziva se takođe, upotrebljavaju i za smanjenje trošenja dijelova aviona, pri čemu se najčešće koristi *trikrezil fosfat, TCP*, obično u koncentracijama između 1 i 3%. TCP reaguje s površinom metala, pri čemu se formira hemijski apsorbcioni sloj koji štiti elemente od međusobnog trenja.

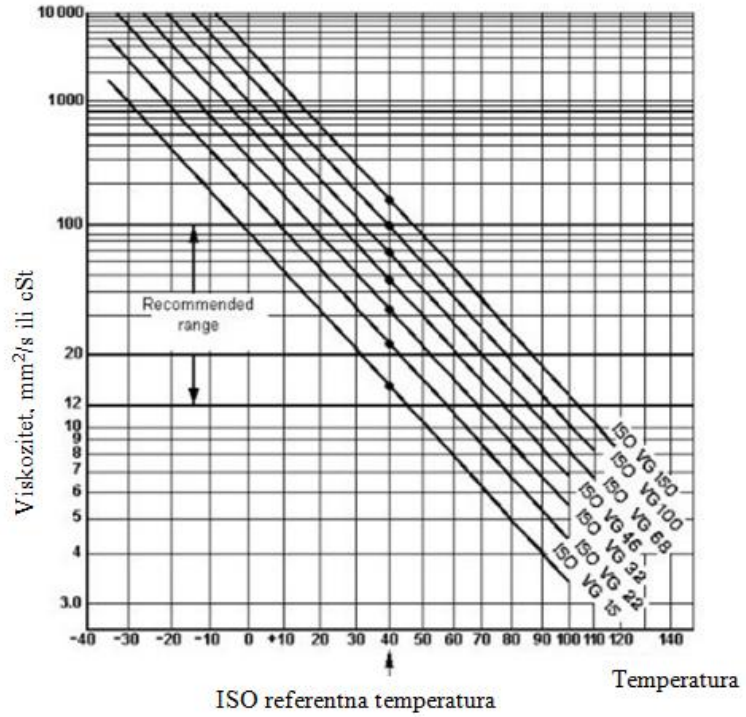

Slika 3. *Promjena viskoznosti ulja u zavisnosti od temperature (ISO VG gradacija ulja).*

Kada se radi o ekstremnim uslovima pritiska, kao što su kod prenosnika motora i kod helikoptera, mogu se koristiti *sredstva za podmazivanje koja sadrže fosfatne soli s aditivima* od *amina.* Iako se time postižu poboljšanja sposobnosti maziva, na taj način se *može mazivo učiniti agresivnijim prema određenim vrstama elastomera*, posebno silikonskom materijalu (povećanje sposobnosti koksovanja maziva). Drugi nedostatak je da u prisustvu vode, ova vrsta aditiva reaguje s nezaštićenom legurom magnezijuma koje se nalaze na površinama unutrašnjosti motora. Ako je sistem suv ili su magnezijumske legure na površinama dovoljno dobro zaštićene epoksidnom prevlakom, tada se reakcija ne odvija [4].

Upotreba maziva pri ispitivanju agregata

Paralelno sa procesom opravke turbomlaznih motora i komponenti aviona, kao i nazavisno od ovih procesa, u "ORAO" a.d. se vrši opravka svih gorivnih, hidro, uljnih i elektro agregata koji se razlikuju u zavisnosti od proizvođača i tipa turbomlaznog motora i aviona. Proces opravke agregata se obavlja u skladu sa zahtjevima orginalnih tehničkih specifikacija, tj. komplentan tehnološki proces je opisan u instrukcijama za remont agregata, urađenim od strane proizvođača. Svaki agregat ima svoju listu ispitivanja i ona je jedinstvena.
Za ispitivanje agregata, pored goriva za mlazne motore, JET A-1, koriste se različiti radni fluidi: kalibracioni fluid MIL-PRF-7024 tip II; Aero Shell Fluid 41 i sintetičko motorno ulje Mobil Jet Oil II, sa propisanim fizičko hemijskim karakteristikama, tabela 3 [5]. Uzimanje uzoraka radnog fluida se vrši prema standardu SRPS ISO 3170 "Ručno uzimanje uzoraka". Ispitivanje fizičko-hemijskih karakteristika radnih fluida se obavlja prema standardnim metodama i internim uputstvima sa standardnom laboratorijskom opremom i priborom.

Tabela 3. Fizičko-hemijske karakteristike mazivih ulja u eksploataciji instaliranih uređaja

Fizičko-hemijske karakteristike	**Kalibracioni fluid, tip 2[1)] MIL-PRF-7024**	**Aero Shell Fluid 41 MIL-H-5606F**	**Mobil Jet Oil 2 MIL-PRF-23699F**

Spoljni izgled	bistra tečnost	prozračna tečnost crvene boje	bistra narandžasta tečnost
Specifična težina na 15.6°C, g/cm³	0.770±0.005	0.870	ne uslovljava se ali se prijavljuje, type 1.0035
Kinematička viskoznost, 25°C, mm²/s	1.17±0.05	min 13.2[3)] min 4,90[4)]	min 23[7)] (4,9-5,4)[8)]
Kiselinski broj, mg KOH/g	-	max 0.20	max 1.0
Korozija, Cu traka, 3h 100°C, max	1	max 25[5)]	1 b
Tačka paljenja, otvoreni sud, °C	min 38[2)]	min 82[6)]	min 246
Sadržaj vode	ne sadrži	ne sadrži	ne sadrži
Sadržaj mehaničkih nečistoća	max 2,0 mg/l	ne sadrži	max 10,0 mg/l

[1)] – fluid za kalibraciju; [2,6)] – tačka paljenja (zatvoreni sud); [3,7)] – kinematička viskoznost na 40 °C; [4,8)] – kinematička viskoznost na 100 °C; [5)] – korozivnost na 135⁰C na 72 h.

Kvalitet radnog fluida u uređajima i agregatima, kao i osposobljenost uređaja za rad sa aspekta kvaliteta radnog fluida, verifikuje se sa tri verifikacione naljepnice, slika 4 [5].

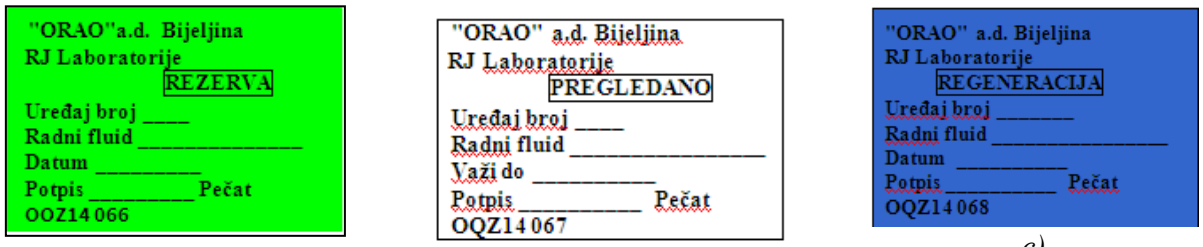

a) *b)* *c)*

***Slika 4**. Verifikacione naljepnice kvaliteta radnog fluida na uređajima i agregatima: zelena verifikaciona naljepnica za uređaj u rezervi, a) bijela verifikaciona naljepnica za važeći period zahtjevanog kvaliteta radnog fluida, b) i plava verifikaciona naljepnica za nezadovoljavajući kvalitet radnog fluida (zabrana ispitivanja na uređaju).*

Na slici 5 prikazani su uređaji za ispitivanje gorivnih agregata, Dawty, model 4400, slika 5a) i uređaj za ispitivanje pumpi ulja, AMS model BEP 1341/B, slika 5b.

a) *b)*

***Slika 5.** Uređaji za ispitivanje gorivnih agregata, Dawty, model 4400, slika 5a) i uređaj za ispitivanje pumpi ulja, AMS model BEP 1341/B, slika 5b).*
Radni fluidi u uređajima: 5a) Kalibracioni fluid, type 2 i 5b) Mobil Jet Oil 2

Zaključak

Posljednih nekoliko decenija mlazni motori aviona koriste mlazno gorivo Jet A-1. Razvoj i upotreba održivih alternativnih mlaznih goriva se javlja kao ključni faktor u smanjenju dekarbonizacije vazdušnog prostora. *„Refuel Aviation"* inicijativa promoviše razvoj i upotrebu *održivih vazduhoplovnih goriva tzv. SAF-ova (sustainable aviation fuels)* za dekarbonizaciju vazdušnog saobraćaja. *Goriva i maziva* koja se koriste u avijaciji razlikuju se od goriva i maziva koja se koriste u drugim oblicima prevoza, prvenstveno zbog različitih fizičkih sila, atmosferskih prilika i konstrukcija motora aviona i helikoptera, ali isto tako i zbog potrebe ostvarivanja maksimalne sigurnosti i uspješnosti pri djelovanju a sve u cilju minimaliziranja mogućnost bilo kakve greške (kvara).

Maziva se danas suočavaju, a i u budućnosti će se suočavati s ozbiljnim izazovima, od kojih je najveći izazov toplota. Moderna kućišta motora dostižu temperature maziva između 80 i 100 °C, dok se prilikom prečišćavanja ta temperatura podiže i na približno 190°C, uz dodatno izlaganje temperaturama uz metalni zid ležaja komore za sagorijevanje, čak do 300 i 400 °C.

Ne smije se zanemariti ni značajan uticaj izduvnih gasova sagorijevanja goriva u toku leta aviona na životnu sredinu, za koji se procjenjuje da se svakodnevno povećava sve većim brojem letova.

Literatura

1. B. Arsenović, E. Banjac: "ECOLOGICAL ASPECTS OF AIRCRAFT EXHAUST GASES AFFECT IN SUM OF GREEN-HOUSE ATMOSPHERE GASES"; International Conference on Innovative Technologies; INTECH 2011; BRATISLAVA; SLOVAKIA; (str 23 – 25)
2. B. Arsenović, Z. Janjuš, E. Banjac: "Uticaj izduvnih gasova aviona na sumu gasova staklene bašte atmosfere" XIV YUCORR, 2012.
3. Đ. Šilić, V. Stojković i D. Mikulić, Goriva i maziva, Veleučilište Velika Gorica, Velika Gorica, 2012.
4. R. M. Mortier, M. F. Fox i S. T. Orszulik, Chemistry and Technology of Lubricants, Springer, Sevenhampton, 2010.
5. B. Arsenović; D. Jovičić: „Ispitivanje fizičko-hemijskih karakteristika radnih fluida u uređajima-Periodična kontrola kvaliteta radnih fluida"; 052/5 –LQ-5; „ORAO" a.d. Bijeljina, 2023.
6. B. Arsenović; „Development of alternative jet fuels from the aspect of reducing CO_2 emissions (fuels for the future) Part 2; XXV YuCORR, Divčibare, Republika Srbija, 2024.
7. Global Aviation, Aviation Fuels Technical Review, Chevron Corporation, 2004.
8. G. E. Totten, Fuels and lubricants handbook: technology, properties, performance and testing, ASTM International, Glen Bumie, 2003.
9. Standardi: DEF STAN 91-91; ASTM D7566; ASTM D1655; MIL PRF23699F; MIL - C-7024; MILH 5606F.

Relationship between photosynthetic efficiency and total carotenoids and the content of Zn and Sr in *Aesculus hippocastanum* L.

Marija Matić*, Dragana Pavlović, Ksenija Jakovljević, Olga Kostić, Natalija Radulović, Miroslava Mitrović, Pavle Pavlović

Department of Ecology, Institute for Biological Research „Siniša Stanković" – National Institute of the Republic of Serbia, University of Belgrade, Bulevar Despota Stefana 142, 11108 Belgrade, Serbia

https://doi.org/10.65614/uisk_yucorr.2025.26.ch16

*marija.pavlovic@ibiss.bg.ac.rs

Abstract

Aesculus hippocastanum L., known as the European horse chestnut, is a deciduous tree naturally occurring in the mountainous regions of the Balkans and southeastern Europe, at altitudes between 700 and 1200 meters. Although it adapts well to different growing conditions, its resistance to pollution is limited, resulting in visible damage in urban environments and a decline in natural populations due to disease and environmental stress. Given its widespread occurrence, frequent planting, and the ease of monitoring physiological parameters, A. hippocastanum is often used as a bioindicator of pollution, particularly in urban environments. In this study, the influence of Zn, a cofactor of numerous enzymes involved in carotenoid and antioxidant synthesis, and Sr^{2+}, a chemical analog of Ca^{2+} that can interfere with thylakoid membrane stability and PSII enzyme function, was investigated for their effects on photosynthetic efficiency and total carotenoid content at a polluted - Pionirski Park, Belgrade and an unpolluted site – Kosmaj. The leaf samples were analysed using ICP-OES for Mn and Zn, chlorophyll fluorometry for photosynthetic efficiency (Fv/Fm), and spectrophotometry for total carotenoid content. The results showed that Sr concentrations at both sites exceeded levels considered toxic for plant tissues (>30 mg kg^{-1}; Shacklette et al., 1978), measuring 37.17 mg kg^{-1} at Belgrade and significantly higher at Kosmaj (62.41 mg kg^{-1}). In contrast, Zn concentrations were below the threshold required for normal physiological functioning of plants (<20 mg kg^{-1}; Kabata-Pendias and Pendias, 2001), with values of only 11.81 mg kg^{-1} in A.hippocastanum leaves at both Belgrade and Kosmaj. Consequently, photosynthetic efficiency values were lower than optimal at both sites—0.671 in Pionirski Park and 0.692 at Kosmaj, as well as the total carotenoid content (1.59 mg g^{-1} and 1.87 mg g^{-1}, respectively), probably due to the combined effects of toxic Sr concentrations, which can disrupt thylakoid membrane integrity and PSII activity, and Zn deficiency, which impairs antioxidant defence and enhances oxidative pigment degradation.

The results confirm that A. hippocastanum responds to Zn deficiency and toxic Sr accumulation through reduced photosynthetic efficiency and lower carotenoid content, indicating sensitivity to both micronutrient imbalance and excess metal exposure. This highlights its potential as a reliable bioindicator for assessing the impact of trace element availability in different environments.

Keywords: *trace elements; Aesculus hippocastanum; photosynthetic efficiency; carotenoids; urban pollution; bioindicator*

Acknowledgment

This work was supported by the Ministry of Education, Science, and Technological Development of the Republic of Serbia, grant no. 451-03-136/2025-03/200007.

Urban trees as bioindicators and mitigators of PTEs: the case of *Acer platanoides* L.

Urbano drveće kao indikatori i faktori za smanjenje PTEs: slučaj Acer platanoides L.

Dragana Pavlović*, Marija Matić, Ksenija Jakovljević, Dragan Čakmak, Veljko Perović, Miroslava Mitrović, Pavle Pavlović

Department of Ecology, Institute for Biological Research "Siniša Stanković"-National Institute of the Republic of Serbia, University of Belgrade, Bulevar despota Stefana 142, 11000 Belgrade, Serbia

https://doi.org/10.65614/uisk_yucorr.2025.26.ch17

*dragana.pavlovic@ibiss.bg.ac.rs

Abstract

Trees in urban ecosystems not only improve the microclimatic conditions and aesthetic value of urban spaces, but also contribute to the accumulation and redistribution of potentially toxic elements (PTEs), thereby mitigating ecological risks and supporting urban sustainability. In this study, the phytoremediation potential of Acer platanoides L. was assessed by analysing B, Cu, Sr and Zn in soil, roots and leaves from three urban parks in Belgrade. The element concentrations were determined by ICP-OES after microwave digestion (CEM Mars 6). The measured concentrations of B and Sr in leaves reached toxic levels, indicating a potential risk of phytotoxicity of A. platanoides. Bioconcentration and translocation factors confirmed an efficient uptake and transfer of B, but a limited uptake of Cu, Sr and Zn from the soil. The results show that the species is very good at accumulating and translocating B, while it has limited uptake and redistribution of other elements into plant tissue. Due to its relatively rapid growth, stress tolerance and ability to accumulate certain PTEs (especially B), A. platanoides can be considered as an efficient and cost-effective species to improve the resilience and ecological functions of urban green spaces.

Keywords: *Urban ecosystems; Acer platanoides L; phytoremediation; potentially toxic elements (PTEs); biological factors*

Izvod

Drveće u urbanim ekosistemima ne samo da poboljšava mikroklimatske uslove i estetsku vrednost urbanih prostora, već i doprinosi akumulaciji i redistribuciji potencijalno toksičnih elemenata (PTEs), čime smanjuju ekološke rizike i podržava urbanu održivost. U ovoj studiji procenjivan je fitoremedijacioni potencijal vrste Acer platanoides L. analizom sadržaja B, Cu, Sr i Zn u zemljištu, korenu i listovima iz tri gradska parka u Beogradu. Koncentracije elemenata određene su ICP-OES metodom nakon mikrotalasne digestije (CEM Mars 6). Izmerene koncentracije B i Sr u listovima dostizale su toksične nivoe, što ukazuje na potencijalni rizik od fitotoksičnosti kod A. platanoides. Vrednosti biokoncentracionog i translokacionog faktora su potvrdile efikasno usvajanje i transport B, ali ograničeno usvajanje Cu, Sr i Zn iz zemljišta. Rezultati pokazuju da je ova vrsta veoma dobra u akumulaciji i translokaciji B, dok za ostale elemente ima ograničeno usvajanje i redistribuciju u biljnom tkivu. Zbog relativno brzog rasta, otpornosti na stres i sposobnosti akumulacije određenih PTEs (posebno B), A. platanoides se može smatrati efikasnom i ekonomičnom vrstom za unapređenje otpornosti i ekoloških funkcija urbanih zelenih površina.

Ključne reči: *Urbani ekosistemi; Acer platanoides L; fitoremedijacija; potencijalno toksični elementi (PTEs); biološki faktori*

Acknowledgment

This work was supported by the Ministry of Education, Science, and Technological Development of the Republic of Serbia, grant no. 451-03-136/2025-03/200007.

Influence of the nature of the support on the photocatalytic activity of silver-modified catalysts for fluorescein removal and hydrogen generation in the presence of simulated solar radiation

Teodora Vidović, Ivana Jagodić, Nemanja Banić*

University of Novi Sad, Faculty of Sciences, Department of Chemistry, Biochemistry and Environmental Protection, Trg D. Obradovića 3, 21000 Novi Sad, Serbia

https://doi.org/10.65614/uisk_yucorr.2025.26.ch18

*nemanja.banic@dh.uns.ac.rs

Abstract

The growing attention to energy and environmental challenges has sparked increased interest in the development and application of clean and renewable energy sources. In particular, photocatalytic water splitting as a method for obtaining hydrogen has been highlighted as a promising alternative to fossil fuels due to its renewable and environmentally friendly nature, based on solar energy. On the other hand, the increase in industrial activity, which involves the intensive production, application, and discharge of various chemicals, often leads to significant pollution of water resources. The main challenge is how to reduce the generation and harmful effects of pollutants, so improved methods have been developed to remove certain pollutants from the aquatic environment. Organic dyes are widely used in various industrial sectors, such as textile production, the food industry, and the cosmetics and pharmaceutical sectors. It is important to note that about 10-15% of the dyes used in the dyeing process end up in wastewater, which poses a risk of pollution of aquatic ecosystems. The photocatalytic method is one of the methods for removing organic dyes and is an effective method for purifying water systems, as it manages to mineralize stable pollutants that cannot be removed by other methods. It can be applied in combination with solar radiation, which is an available and environmentally friendly source of energy. To achieve a certain efficiency in removing organic dyes, photocatalysts, which are semiconductor materials, are used. Six materials (Ag : commercial support of 2.5% (w/w)) were synthesized by the photochemical reduction method of Ag on different commercial supports. The photocatalytic efficiency of these nanopowders for hydrogen production and fluorescein removal under simulated solar irradiation was investigated. The highest efficiency in terms of hydrogen generation rate was demonstrated by Ag/TiO_2 Reaktiv (14.8 μmol/hg H_2), while the other catalysts had lower efficiency in terms of hydrogen generation rate in the time interval of 300 min. The kinetics of fluorescein removal using the above-mentioned photocatalysts was monitored photometrically. Under simulated solar irradiation, the 2.5%Ag/ZnO catalyst proved to be the most efficient, with a photodegradation efficiency of 96.9% after 120 min. The synthesized materials did not show significant fluorescein adsorption efficiency, with adsorption ranging from 0.3% for 2.5%Ag/ZnO to 24.9% for 2.5%Ag/TiO_2 Hombikat after 120 min

Acknowledgements

This study was supported by the Ministry of Science, Technological Development, and Innovation of the Republic of Serbia (Grants No. 451-03-137/2025-03/ 200125 & 451-03-136/2025-03/ 200125). The authors are especially grateful to the Srbijagas company, which enabled the realization of this research possible by donating a gas chromatograph.

Eco-friendly synthesis and application of magnetite nanocomposites for the purification of dye-contaminated water

Ivana Basarić, Teodora Vidović, Nemanja Banić*

University of Novi Sad, Faculty of Sciences, Department of Chemistry, Biochemistry and Environmental Protection, Trg Dositeja Obradovića 3, 21000 Novi Sad, Serbia

https://doi.org/10.65614/uisk_yucorr.2025.26.ch19

*nemanja.banic@dh.uns.ac.rs

Abstract

A large number of industries use dyes in their production processes, consuming substantial amounts of water and consequently generating large volumes of wastewater. Methylene blue is one of the most widely used dyes in various industrial applications, and its presence at elevated concentrations can cause serious health and environmental problems; therefore, its removal from wastewater is of extreme importance. Advanced oxidation processes, which decompose pollutants into biodegradable products, represent a promising approach for the efficient treatment of dye-contaminated water. However, one of the main challenges remains the development of photocatalysts that combine high photocatalytic efficiency, recyclability, and effective utilization of solar energy.

In this study, newly synthesized Fe_3O_4/PVC composites were investigated as photocatalysts for the removal of methylene blue ($c_o = 2.45 \times 10^{-2}$ mM) under simulated solar radiation and dark conditions. Magnetite (Fe_3O_4) was synthesized via an electrosynthesis method using a rotating cylindrical electrode. Fe_3O_4 and commercial PVC were used in the preparation of the composites. Fe_3O_4/PVC composites were prepared with different mass ratios of Fe_3O_4 to PVC (1%, 2.5%, and 5% w/w). The composites were shaped into tablets with a diameter of 5 mm and a thickness of 2 mm. The highest methylene blue removal efficiency (99.72%) under simulated solar radiation was achieved using the 2.5%Fe_3O_4/PVC photocatalyst. The degradation kinetics was monitored by UV/Vis spectrophotometry.

Acknowledgements

The authors gratefully acknowledge financial support from State University of Novi Pazar, Novi Pazar, Republic Serbia.

Monitoring the electrochemical behavior of a modified Ti-Ni alloy in an artificial saliva solution

Monitoring elektrohemijskog ponašanja modifikovane Ti-Ni legure u rastvoru veštačke pljuvačke

Đenđi Vaštag[1,*], Peter Majerič[2,3], Rebeka Rudolf [2,3]

[1] *University of Novi Sad, Faculty of Sciences, Novi Sad, Serbia*

[2] *University of Maribor, Faculty of Mechanical Engineering, Slovenia*

[3] *Zlatarna Celje d.o.o., Slovenia*

https://doi.org/10.65614/uisk_yucorr.2025.26.ch20

[*]*djendji.vastag@dh.uns.ac.rs*

Abstract

Modern people are increasingly faced with a situation in which their body fluids, such as sweat, saliva, lymph or blood, come into temporary or long-term contact with metal objects. Contact, which occurs with dental materials, orthopedic implants, prostheses or fashion jewelry, can trigger various electrochemical processes, which can have dual consequences: it can change the structure and properties of the metals, and at the same time cause harmful reactions in the human tissue with which they come into contact. Titanium-nickel alloys (Ti-Ni) are among the most used alloys to produce both fashion accessories and various implants (dental, orthopedic). In addition to many good properties, Ti-Ni alloys have one major drawback, which is that nickel ions that are formed during the electrochemical reaction of the alloy with human electrolyte cause various allergic reactions in an increasing number of people. For the above reason, there is a great desire to find a way to prevent or minimize the release of nickel ions from the alloy. Therefore, the focus of this work was monitoring the electrochemical characteristics of the thermally modified Ti-Ni alloy. The electrochemical behavior of the thermally modified Ni-Ti alloy was monitored in an artificial saliva solution as a function of the exposure time.

Keywords: *Ti-Ni alloy; electrochemical properties; artificial saliva*

Izvod

Savremeni čovek sve se češće susreće sa situacijom da njegove telesne tečnosti, kao što su znoj, pljuvačka, limfa ili krv dolaze u privremeni ili dugotrajan kontakt sa metalnim predmetima. Navedeni kontakti koji se javljaju kod stomatoloških materijala, ortopedskih implanata, proteza ili modnog nakita, mogu pokrenuti različite elektrohemijske procese, koji imaju dvostruke posledice: mogu narušiti strukturu i svojstva samih metala, a istovremeno izazvati štetne reakcije u humanom tkivu sa kojim dolaze u kontakt. Legure titana i nikla (Ti-Ni) spadaju u najčešće primenjene legure za izradu kako modnih dodataka tako i različitih implanta (stomatoloških, ortopdeskih). Pored velikog broja dobrih osobina, legure Ti-Ni imaju jedan veliki nedostatak, a to je da joni nikla nastali u toku elektrohemisjke reakcije legure sa humanim elektrolitom kod sve većeg broja ljudi izazivaju različite alergijske reakcije. Iz navedenog razloga, postoji velika težnja da se da se nađe način da se ispuštanje jona nikla iz legure spreči ili svede na minimum. Stoga je fokus ovog rada bio monitoring elektrohemijskih karakteristika termički modifikovane Ti-Ni legure. Elektrohemijskog ponašanja termički modifikovane Ni-TI legure je praćeno u rastvoru veštačke pljuvačke u funkciji vremena ekspozicije rastvoru humanog elektrolita.

Ključne reči: *Ti-Ni legura; elektohemijske osobine; veštačka pljuvačka*

Electrochemical Characterization of Glucose Oxidase Immobilized in Intrinsically Conducting Polymers: Polyaniline vs. Self-Doped and Substituted Polyaniline

Elektrohemijska karakterizacija glukoza-oksidaze imobilisane u elektroprovodnim prolimerima poređenje polianilina sa samodopovanim i substituisanim polianilinom

Milica Gvozdenović[1,*], Branimir Jugović[2], Aleksandar Kojović[1], Zorica Knežević-Jugović[1]

[1] *Faculty of Technology and Metallurgy,University of Belgrade, Karnegijeva 4, 11120 Belgrade, Serbia*

[2] *Institute of Technical Science, SASA, Knez Mihajlova 35, 11 000 Belgrade, Serbia*

https://doi.org/10.65614/uisk_yucorr.2025.26.ch21

[*]*popovic@tmf.bg.ac.rs*

Abstract

This study investigates the electrochemical behaviour of glucose oxidase (GOx) immobilized in: polyaniline (PANI), self-doped polyaniline (SD-PANI), and poly(o-toluidine) (POT), a substituted aniline derivative. All polymeric materials were synthesized electrochemically via galvanostatic polymerization on graphite electrodes. SD-PANI was obtained by copolymerizing aniline with meta-aminobenzoic acid, introducing internal proton-donating groups to enhance conductivity and enzyme compatibility. The presence of –OH groups increases the hydrophilicity of the polymer, facilitating interactions with aqueous solutions and biological molecules such as enzymes, thereby improving immobilization efficiency. GOx was immobilized by cross-linking via glutaraldehyde. Amperometric measurements in the presence of glucose were used to evaluate the bioelectrocatalytic response. Michaelis-Menten kinetic parameters — the apparent Michaelis constant (Km) and maximum current response (Imax) — were extracted from steady-state current responses using the Lineweaver-Burk method. Although the most favorable kinetic parameters were obtained for PANI, followed by POT and SD-PANI, the highest storage stability of GOx was observed with SD-PANI due to its conductivity in neutral media. These findings highlight the influence of polymer structure and functionalization on enzymatic activity and biosensor efficiency.

Keywords: *polyaniline; self-doped polyaniline; poly(o-toluidine); enzyme immobilization; Michaelis-Menten kinetics*

Izvod

U ovom radu ispitivano je elektrohemijsko ponašanje glukoza oksidaze (GOx) imobilisane u elektroprovodnim polimerima: polianilinu (PANI), samodopovanom polianilinu (SD-PANI) i poli(o-toluidinu) (POT), koji su dobijeni elektrohemijskom sintezom na grafitnoj elektrodi u galvanostatskim uslovima. Imobilizacija enzima u elektrodnim mateerijalima izvršena je umrežavanjem glutaraldehidom. SD-PANI je izabran zbog provodljivosti u neutralnoj sredini, dok –OH grupe u POT-u povećavaju hidrofilnost i olakšavaju interakciju sa enzimima. Amperometrijska merenja u prisustvu glukoze korišćena su za određivanje parametara enzimske kinetike primenom Lineweaver-Burk metode. Najpovoljniji kinetički parametri dobijeni su za PANI, dok je SD-PANI pokazao najveću stabilnost u neutralnoj sredini. Rezultati ukazuju na značaj strukture i funkcionalizacije polimera u efikasnosti elektrohemijskih biosenzora.

Ključne reči: *polianilin*; *samodopovani polianilin*; *poli(o-toluidin); imobilizacij*; *Mihaelis Mentenova kinetika*

Influence of morphology of electrodeposited copper on the electrochemical regeneration of nicotinamide adenine dinucleotide (1,4-NADH)

Uticaj morfologije elektrohemijski istaloženog bakra na elektrohemijsku regeneraciju nikotinamid adenin dinukleotida (1,4-NADH)

Mohammed Ali Saif Al-Shaibani[1], Monisha Sivasankaran[1], Ivana O. Mladenović[2], Jelena D. Lović[2], Sanja I. Stevanović[2], Nebojša D. Nikolić[2,*], Tanja Vidaković-Koch[1]

[1] *Max Planck Institute for Dynamics of Complex Technical Systems, Sandtorstraße 1, 39106 Magdeburg, Germany*

[2] *University of Belgrade, Institute of Chemistry, Technology and Metallurgy, Njegoševa 12, 11000 Belgrade, Serbia*

https://doi.org/10.65614/uisk_yucorr.2025.26.ch22

[*]*nnikolic@ihtm.bg.ac.rs*

Abstract

This study investigates how copper electrode morphology influences the electrochemical regeneration of 1,4-NADH. Bioelectrochemical systems that couple enzymatic catalysis with electrochemical redox reactions are emerging as promising platforms for developing sustainable industrial processes, and efficient NADH regeneration is central to their performance. Electrochemical deposition (ED) offers a low-cost, rapid, and environmentally friendly route to fabricate metal electrodes with tailored surface morphologies. By adjusting deposition parameters—current density or overpotential, temperature, time, electrolyte type and composition, additives (levelers/brighteners), and agitation—as well as employing constant or periodically pulsed deposition regimes, the morphology of deposited copper can be precisely tuned. We show that the resulting copper morphologies markedly impact the efficiency and selectivity of 1,4-NADH electroregeneration, identifying copper as a promising electrocatalyst for bioelectrochemical applications.

Keywords: *bioelectrochemical systems; electrodeposition; copper; morphology*

Izvod

Ova studija istražuje kako morfologija bakarnih elektroda utiče na elektrohemijsku regeneraciju 1,4-NADH. Bioelektrohemijski sistemi koji spajaju enzimsku katalizu sa elektrohemijskim redoks reakcijama pojavljuju se kao obećavajuće platforme za razvoj održivih industrijskih procesa, a efikasna regeneracija NADH je ključna za njihove performanse. Elektrohemijsko taloženje (ED) nudi jeftin, brz i ekološki prihvatljiv način za izradu metalnih elektroda sa prilagođenim površinskim morfologijama. Podešavanjem parametara taloženja - gustine struje ili prenapetosti, temperature, vremena, vrste i sastava elektrolita, aditiva (sredstva za poravnavanje/sjaj) i mešanja - kao i primenom konstantnih ili periodično pulsnih režima taloženja, morfologija istaloženog bakra može se precizno podesiti. Pokazali smo da rezultujuće morfologije bakra značajno utiču na efikasnost i selektivnost elektroregeneracije 1,4-NADH, identifikujući bakar kao perspektivni elektrokatalizator za bioelektrohemijske primene.

Ključne reči: *bioelektrohemijski sistemi; elektrohemijsko taloženje; bakar; morfologija*

Acknowledgements

This investigation was supported by the bilateral research project between the Ministry of Science, Technological Development and Innovation of the Republic of Serbia and German Academic Exchange Service (DAAD), Project No. 337-00-253/2023-05/4.

Electrochemical characterization of PtCu catalyst for methanol electrooxidation

Elektrohemijska karakterizacija PtCu katalizatora za elektooksidaciju metanola

Sanja Stevanović*, Dragana Milošević, Dušan Tripković

[1] *University of Belgrade, Institute of Chemistry, Technology and Metallurgy, National Institute of the Republic of Serbia, Njegoševa 12, 11000 Belgrade, Serbia*

https://doi.org/10.65614/uisk_yucorr.2025.26.ch23

*sanjas@ihtm.bg.ac.rs

Abstract

Direct methanol fuel cells (DMFCs) have ignited significant interest due to their straightforward design, efficient energy conversion, and eco-friendly emission characteristics. Creating efficient and long-lasting platinum-based catalysts is vital for advancing DMFCs. However, the most difficult concerns in the fuel cell sector are cost, efficiency, and lifetime. Because platinum is the most expensive component of DMFCs, it is most important to produce catalysts with higher activity and stability while reducing the content of expensive platinum. By integrating non-precious metals, such as copper, with platinum, we can significantly decrease reliance on costly platinum while enhancing catalytic efficiency, paving the way for a highly effective and versatile solution for a wide range of electrocatalytic applications. Recently, PtCu alloy catalysts have attracted particular attention because the formed bimetallic structures of Pt and Cu could enhance platinum activity and tolerance to CO poisoning, a common byproduct of the reaction. The synergistic effect between platinum and copper increases the overall catalytic activity, which lies in enhanced CO tolerance, bifunctional and electronic effects. Additionally, it is well-known that an optimized catalyst synthesis procedure could reduce the noble catalyst consumption and enhance its electrocatalytic performance. In this work, microwave-assisted polyol method was used to obtain PtCu/C catalyst for effective methanol oxidation reaction. The electrocatalytic activity of PtCu/C catalyst was examined in 0.5 M H_2SO_4 + 0.5 M CH_3OH solution. Catalyst stability was examined by long-term potential cycling.

The results from cyclic voltammetry experiments indicate enhanced catalytic activities for methanol oxidation reaction and improved resistance ability to CO inhibition, after addition of Cu to Pt catalyst.

Keywords: *fuel cels; platinum catalysts; PtCu alloy; methanol oxidation*

Izvod

Direktne gorivne ćelije sa metanolom kao gorivom (DMFC) izazvale su značajno interesovanje zbog svog jednostavnog dizajna, efikasne konverzije energije i ekološki prihvatljivih karakteristika emisije. Stvaranje efikasnih i dugotrajnih katalizatora na bazi platine je od vitalnog značaja za unapređenje DMFC-a. Međutim, najteža pitanja u sektoru gorivnih ćelija su troškovi, efikasnost i vek trajanja. Pošto je platina najskuplja komponenta PEMFC-a, potrebno je proizvesti katalizatore sa većom aktivnošću i stabilnošću, uz smanjenje sadržaja skupe platine. Integracijom neplemenitih metala, kao što je bakar, sa platinom, možemo značajno smanjiti zavisnost od skupe platine, a istovremeno poboljšati katalitičku efikasnost, otvarajući put ka veoma efikasnom i svestranom rešenju za širok spektar elektrokatalitičkih primena. Nedavno su katalizatori u obliku PtCu legura privukli posebnu pažnju jer formirane bimetalne strukture Pt i Cu mogu poboljšati aktivnost platine i toleranciju na trovanje CO, koji je nepoželjni međuproizvod reakcije. Sinergijski efekat između platine i bakra dovodi do povećanja ukupne katalitičke aktivnosti, što leži u poboljšanoj toleranciji na CO,

bifunkcionalnim i elektronskim efektima. Pored toga, dobro je poznato da optimizovana procedura sinteze katalizatora može smanjiti potrošnju plemenitog katalizatora i poboljšati njegove elektrokatalitičke performanse. U ovom radu, korišćena je mikrotalasna poliolna metoda za dobijanje PtCu/C katalizatora za efikasnu reakciju oksidacije metanola. Elektrokatalitička aktivnost PtCu/C katalizatora ispitana je u rastvoru 0,5 M H2SO4 + 0,5 M CH3OH. Stabilnost katalizatora ispitana je dugoročnim cikliranjem potencijala. Rezultati eksperimenata ciklične voltametrije ukazuju na poboljšanu katalitičku aktivnost za reakciju oksidacije metanola i poboljšanu otpornost na inhibiciju CO, nakon dodavanja Cu u Pt katalizator.
Ključne reči: *gorivne ćelije; platinski katalizatori; PtCu legura; elektooksidacija metanola*

Acknowledgments

This research has been financially supported by the Ministry of Science, Technological Development and Innovation of the Republic of Serbia (Contract No. 451-03-136/2025-03/200026).

Evaluation of Aronia Pomace Extract as a Green Corrosion Inhibitor

Anđela Simović[1,*], Aleksandra Ivanovska[2], Jelena Bajat[3]

[1] *University of Belgrade, Institute of Chemistry, Technology and Metallurgy, National Institute of the Republic of Serbia, Belgrade, Serbia*

[2] *University of Belgrade, Innovation Center of the Faculty of Technology and Metallurgy in Belgrade, Belgrade, Serbia*

[3] *University of Belgrade, Faculty of Technology and Metallurgy, Belgrade, Serbia*

https://doi.org/10.65614/uisk_yucorr.2025.26.ch24

[*] *andjela.simovic@ihtm.bg.ac.rs*

Abstract

In this study, the effectiveness of Aronia pomace extract as an environmentally friendly corrosion inhibitor for carbon steel in 1 M HCl was investigated. Electrochemical measurements, including electrochemical impedance spectroscopy (EIS) and polarization studies, revealed a significant reduction in the corrosion rate in the presence of the extract, with a maximum inhibition efficiency of 96.7% at the optimal concentration of 100 ppm after 24 hours. EIS results indicated an increase in charge transfer resistance over time for all tested concentrations and the formation of a stable protective film on the steel surface. Polarization measurements suggested that the extract acts as a mixed-type inhibitor, with a predominant effect on the cathodic reaction. Scanning electron microscopy (SEM) analysis showed a smooth and compact surface for the inhibited samples, while contact angle measurements confirmed increased compaction of the organic protective layer over time. X-ray photoelectron spectroscopy (XPS) identified the presence of organic functional groups from phytochemicals in the extract on the steel surface, confirming the adsorptive protection mechanism. These results demonstrate that aronia extract is an efficient, environmentally friendly inhibitor of carbon steel corrosion in acidic media, with potential applications in industrial processes and green metal protection technologies.

Keywords: *corrosion; carbon steel; green inhibitor; plant extract*

Izvod

U ovoj studiji ispitivana je efikasnost ekstrakta aronije (Aronia pomace) kao ekološki prihvatljivog inhibitora korozije ugljeničnog čelika u 1 M HCl. Elektrohemijska ispitivanja, uključujući elektrohemijsku impedansnu spektroskopiju (EIS) i polarizacione analize, pokazala su značajno smanjenje brzine korozije u prisustvu ekstrakta, sa maksimalnom inhibitorskom efikasnošću od 96,7% pri optimalnoj koncentraciji od 100 ppm nakon 24 sata. EIS rezultati ukazali su na povećanje otpornosti prenosa naelektrisanja tokom vremena za sve testirane koncentracije i formiranje stabilnog zaštitnog sloja na površini čelika. Polarizacione analize sugerisale su da ekstrakt djeluje kao inhibitor mješovitog tipa, sa dominantnim uticajem na katodnu reakciju. Analiza skenirajućom elektronskom mikroskopijom (SEM) pokazala je glatku i kompaktnu površinu inhibiranih uzoraka, dok su mjerenja kontaktnog ugla potvrdila povećanu kompaktnost organskog zaštitnog sloja tokom vremena. Analiza fotoelektronskom spektroskopijom rendgenskih zraka (XPS) identifikovala je prisustvo organskih funkcionalnih grupa fitohemikalija iz ekstrakta na površini čelika, čime je potvrđen mehanizam adsorpcije. Dobijeni rezultati pokazuju da ekstrakt aronije predstavlja efikasan, ekološki prihvatljiv inhibitor korozije ugljeničnog čelika u kiseloj sredini, sa potencijalnom primjenom u industrijskim procesima i zelenim tehnologijama zaštite metala.

Ključne reči: *korozija; ugljenični čelik; zeleni inhibitor; biljni ekstrakt*

Formic acid electrooxidation on carbon-supported PtCu catalyst

Elektrooksidacija mravlje kiseline na PtCu katalizatoru na ugljeničnom nosaču

Dragana L. Milošević*, Dušan V. Tripković, Sanja I. Stevanović

University of Belgrade - Institute of Chemistry, Technology and Metallurgy, Njegoševa 12, 11000 Belgrade, Republic of Serbia

https://doi.org/10.65614/uisk_yucorr.2025.26.ch25

*dragana.milosevic@ihtm.bg.ac.rs

Abstract

Over the last decade, fuel cell (FC) technology has grown in potential as an alternative energy source. Platinum (Pt)- based electrocatalysts, deposited over high surface area carbon, are often used as anodic catalysts in the formic acid oxidation (FAO) reaction. However, the most significant problem with utilizing Pt as an anodic catalyst for FAO is the creation of intermediate carbon monoxide (CO), which poisons the Pt surface by blocking the active sites and thus reduces the overall fuel cell performance.

Since Pt is an expensive and rare precious metal, recent research has focused on lowering the amount of Pt present in the catalyst by forming alloys, wherein a portion of platinum is substituted with more affordable metals such as Sn, Ni, Cu or Co. High catalytic activity and especially stability of catalysts are dependent on the quality of supporting material used. Carbon (Vulcan XC-72R) is still one of the most widely utilized commercial carbon supports because of its high surface area, porosity, and superior electrical conductivity, the essential features ensuring homogeneous catalyst dispersion.

In this work, a PtCu/C catalyst was synthesized by the microwave-assisted polyol method. The produced catalyst was electrochemically characterized using cyclic voltammetry and the oxidation of the adsorbed CO monolayer. Activity and stability of synthesized catalysts for the formic acid oxidation reaction in 0.5 M sulfuric acid were investigated. The obtained result indicates that the activity of the synthesized catalyst was improved, in comparison to the pure Pt/C catalyst, thanks to the synergistic effects caused by the addition of Cu, through bifunctional and electronic effects.

Keywords: *Fuel Cell; Platinum Catalysts; Formic acid electrooxidation*

Izvod

Tokom poslednje decenije, tehnologija gorivnih ćelija (FC) beleži značajan napredak i pokazuje sve veći potencijal kao alternativni izvor energije. Elektrokatalizatori na bazi platine (Pt), deponovani na ugljeniku velike specifične površine, često se koriste kao anodni katalizatori u reakciji oksidacije mravlje kiseline (FAO). Međutim, najveći problem pri korišćenju Pt kao anodnog katalizatora za FAO je stvaranje međuprodukta reakcije - ugljen-monoksida (CO), koji truje površinu Pt blokiranjem aktivnih mesta i time smanjuje ukupne performanse gorivne ćelije.

S obzirom na to da je platina skup i redak plemeniti metal, savremena istraživanja usmerena su na smanjenje njenog sadržaja u katalizatoru formiranjem legura, u kojima se deo platine zamenjuje jeftinijim metalima kao što su Sn, Ni, Cu ili Co. Visoka katalitička aktivnost i posebno stabilnost katalizatora zavise od vrste korišćenog nosača. Ugljenik (Vulcan XC-72R) je i dalje jedan od najčešće korišćenih komercijalnih ugljeničnih nosača zbog svoje velike specifične površine, poroznosti i izuzetne električne provodljivosti, što su bitne karakteristike koje omogućavaju homogenu disperziju katalizatora.

U ovom radu sintetisan je PtCu/C katalizator poliol postupkom u mikrotalasnoj pećnici. Dobijeni katalizator je elektrohemijski okarakterisan korišćenjem ciklične voltametrije i oksidacije adsorbovanog monosloja CO. Ispitana je aktivnost i stabilnost sintetisanog katalizatora za reakciju oksidacije mravlje kiseline u 0,5 M sumpornoj kiselini. Dobijeni rezultati su ukazali da je aktivnost

sintetisanog katalizatora poboljšana u poređenju sa Pt/C katalizatorom, zahvaljujući sinergetskom efektu izazvanom dodavanjem Cu, poput bifunkcionalnog i elektronskog efekta.
Ključne reči: *Gorivne ćelije; Platinski katalizatori; elektrooksidacija mravlje kiseline*

Acknowledgments

This work was financially supported by the Ministry of Science, Technological Development and Innovation of the Republic of Serbia (contract No 451-03-136/2025-03/200026).

Activated carbon from hazelnut bark-based biomaterial as an electrode material for supercapacitors

Aktivirani ugljenik dobijen iz biomaterijala na bazi kore lešnika kao elektrodni materijal za superkondenzatore

Vanja Gujaničić[1,2], Danica Bajić[3,2], Mirjana Krstović[3,2], Marija Baltić[4], Aleksandar Knežević[5], Radovan Karkalić[3], Milica Košević[6,*]

[1] *Technical Test Center, Vojvode Stepe 445, 11000 Belgrade, Serbia,*

[2] *University of Defence, Military Academy, Veljka Lukića Kurjaka 33, 11040 Belgrade, Serbia*

[3]*Military Technical Institute, Ratka Resanovića 1, 11030 Belgrade, Serbia*

[4] *University of Belgrade, Faculty of Mechanical Engineering, Kraljice Marije 16, 11120 Belgrade, Serbia*

[5] *University of Belgrade, Faculty of Biology, Studentski trg 16, 11000 Belgrade, Serbia*

[6] *University of Belgrade, Institute of Chemistry, Technology and Metallurgy - National Institute of the Republic of Serbia, Njegoševa 12, 11000 Belgrade, Serbia*

https://doi.org/10.65614/uisk_yucorr.2025.26.ch26

[*]*milica.kosevic@ihtm.bg.ac.rs*

Abstract

The growing demand for sustainable energy storage solutions drives the search for eco-friendly and low-cost electrode materials for supercapacitors. This study presents a sustainable approach for converting discarded hazelnut bark-based biocomposite into activated carbon (AC). The biocomposite was chemically activated with KOH at a mass ratio of 1:3. The mixture was then thermally treated under a nitrogen atmosphere in two stages: initially heated at 2 °C/ min to 500 °C and held for 1 h, followed by heating at 5 °C min^{-1} to 800 °C with an additional 1 h retention time. Electrochemical performance was investigated by cyclic voltammetry (CV) at various scan rates in 0.5 M H_2SO_4. The CV curves show a nearly rectangular shape, indicating that the charge storage mechanism is predominantly governed by electric double-layer capacitance. These findings demonstrate that hazelnut bark-based biocomposite represents a sustainable and efficient precursor for producing high-performance activated carbons, offering a promising alternative to conventional electrode materials in supercapacitors and contributing to environmentally responsible energy storage technologies.

Keywords: *Biomass-derived carbon; porous carbon; KOH activation*

Izvod

Rastuća potražnja za održivim rešenjima za skladištenje energije podstiče razvoj ekološki prihvatljivih i ekonomičnih elektrodnih materijala za superkontenzatore. U ovom radu je prikazan održiv pristup za konverziju odbačenog biokompozita na bazi kore lešnika u aktivirani ugljenik (AC). Biokompozit je hemijski aktiviran pomoću KOH u masenom odnosu 1:3, a zatim termički tretiran u atmosferi azota u dva koraka: u prvom koraku je zagrevan brzinom od 2 °C/min do 500 °C uz zadržavanje od 1 h, a potom zagrevan brzinom od 5 °C/min do 800 °C uz dodatno zadržavanje od 1 h. Elektrohemijska svojstva su ispitivana metodom ciklične voltametrije (CV) pri različitim brzinama skeniranja u rastvoru 0,5 M H_2SO_4. CV krive pokazuju približno pravougaoni oblik, što ukazuje na to da je mehanizam skladištenja naelektrisanja pretežno zasnovan na kapacitivnosti dvojnog sloja. Ovi nalazi pokazuju da biokompozit na bazi kore lešnika predstavlja održiv i efikasan prekurzor za

dobijanje aktiviranih ugljenika, koji mogu služiti kao obećavajuća alternativa konvencionalnim elektrodnim materijalima u superkondenzatorima i doprineti razvoju ekološki odgovorne tehnologije skladištenja energije.
Ključne reči: *ugljenik dobijen iz biomase; porozni ugljenik; aktivacija sa KOH*

Introduction

The increasing global demand for efficient and sustainable energy-storage solutions has become a major driving force behind contemporary research in electrochemical materials [1]. Among the available technologies, supercapacitors, also known as electric double-layer capacitors (EDLCs), are particularly promising due to their high power density, outstanding cycling stability, and rapid charge–discharge capability [2]. These attributes make them well-suited for applications requiring instantaneous energy delivery, including electric vehicles, hybrid propulsion systems, and regenerative energy technologies.

Activated carbons (ACs) currently dominate the commercial supercapacitor market as electrode materials because of their high specific surface area, well-developed porosity, and relatively low production cost [3]. Nevertheless, conventional methods for producing ACs often depend on non-renewable precursors and chemically intensive processes that are not fully aligned with the principles of green chemistry or sustainable manufacturing. Consequently, the search for environmentally friendly and economically viable precursors for high-performance carbon materials has intensified in recent years [4].

Biomass has emerged as a highly attractive renewable resource for the synthesis of activated carbon, offering advantages such as reduced environmental burden and decreased fabrication costs [5]. Agricultural residues are especially promising due to their abundance, low cost, and status as significant agronomic waste. Their valorization not only mitigates environmental pollution but also supports circular-economy principles [6].

This study presents a sustainable and efficient strategy for converting hazelnut bark-based derived biowaste into high-performance activated carbon. The approach involves carbonization followed by potassium hydroxide (KOH) activation at 800 °C, aimed at producing a highly developed microporous structure [7]. This method enables the fabrication of porous carbon materials with high specific surface area and tunable pore distribution, which are key determinants of electrochemical performance in EDLC electrodes.

Previous studies have demonstrated that various biomass-derived carbon materials can exhibit outstanding electrochemical performance [7,8]. These findings clearly indicate that carbon materials synthesized from agricultural waste streams can be highly competitive with, and in some cases superior to, conventional electrode materials.

Although materials such as reed and kapok have been explored, hazelnut biocomposite, as a widely available agricultural waste, remains an underexplored resource for the synthesis of AC electrodes. Building on this foundation, the present work focuses on developing a sustainable and efficient pathway for converting hazelnut biocomposites into high-performance activated carbon (AC). A straightforward yet effective synthesis approach was employed, consisting of carbonization followed by potassium hydroxide (KOH) activation at 800 °C. This route promotes the formation of a well-developed microporous network, which is essential for achieving effective electric double-layer charge storage [9].

Materials and Methods

Preparation of the activated carbon

Activated carbon (AC) was synthesized through chemical activation of discarded hazelnut-based biomass generated during the production of biomass-based bricks (Figure 1), using potassium

hydroxide (KOH, Sigma-Aldrich), followed by high-temperature carbonization. The milled biocomposite precursor was mixed with KOH at an optimal mass ratio of 1:3 (biocomposite:KOH). The mixture was thoroughly homogenized and subsequently dried at 100 °C for 6 h to remove residual moisture and promote uniform alkali impregnation. The impregnated precursor was placed in a tubular furnace and subjected to thermal treatment under a constant flow of high-purity nitrogen to maintain an inert atmosphere and carry away volatile decomposition products [10]. The temperature was increased at a heating rate of 5 °C min^{-1} up to 800 °C, followed by an isothermal hold for 1 h to complete carbonization and chemical activation. After natural cooling to room temperature under N_2, the resulting black powder was washed thoroughly to remove residual KOH and associated inorganic species. The washing procedure involved treatment with 0.1 M HCl, followed by repeated rinsing with distilled water until the filtrate reached a neutral pH (approximately 6.5). The final product was dried at 105 °C to constant mass.

Figure 1. *Discarded hazelnut-based biomass used as a precursor for activated carbon.*

Electrochemical studies

The basic electrochemical characteristics of the synthesized samples were investigated using cyclic voltammetry (CV). The electrochemical analysis was conducted in a three-electrode system comprising a platinum wire (counter electrode), a saturated calomel electrode (SCE) (reference electrode), and the working electrode, all immersed in an aqueous 0.5 M H_2SO_4 electrolyte at ambient temperature. Measurements were performed using a Bio-Logic SP200 potentiostat/galvanostat (Bio-Logic SAS, Grenoble, France). The working electrode was prepared by first dispersing 3 mg of the alkali-treated carbon per 1 mL H_2O, which was subsequently homogenized via ultrasonic treatment (40 kHz, 70 W) for 1 h. A volume of 7 µl of this suspension was drop-cast onto a glassy carbon (GC) disk electrode (diameter 0.5 cm) and dried at room temperature (24 °C). To ensure structural stability and adhesion of the active layer, the dried film was covered with a protective layer of Nafion binder, prepared from a 1:100 volume ratio dilution of 10 mass % Nafion solution in isopropanol/water with water. Cyclic voltammetry was performed at various scan rates (400, 300, 200, 100, 20 and 5 mV s^{-1}) to assess rate capability.

Results and Discussion

The CV curves recorded for the activated carbon at various scan rates are shown in Figure 3.

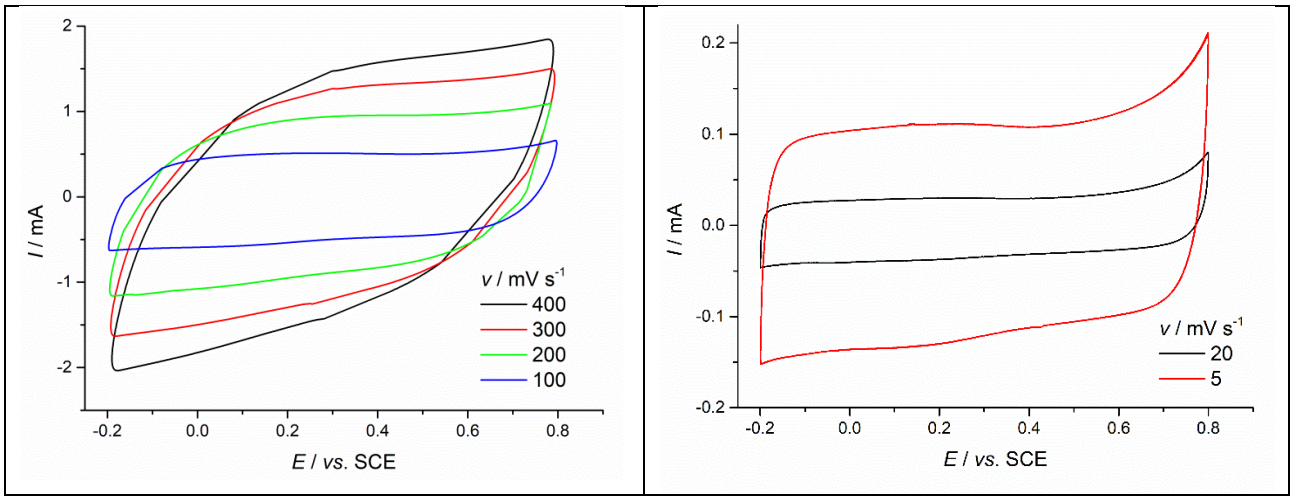

Figure 3. *CVs of activated carbon at a) high and b) low scan rates. Electrolyte: N_2-deaerated 0.5 M H_2SO_4*

The CV curves recorded for the activated carbon at both low and high scan rates (Figure 3) exhibit a characteristic quasi-rectangular profile, typical for carbon-based materials dominated by the electric double-layer capacitance (EDLC) mechanism [2]. Such a shape indicates the predominance of rapid and reversible ion adsorption/desorption processes occurring at the electrode–electrolyte interface, with minimal contribution from faradaic reactions. As the scan rate rises, the current values correspondingly become higher, reflecting the linear relationship expected for ideal capacitive behavior. At higher sweep rates, a slight tilting of the curves becomes evident, indicating increased resistive contributions and some limitations in ion transport within the pore structure. Nevertheless, the overall quasi-rectangular contour is largely preserved, suggesting that the pore structure of the activated carbon, particularly its accessible surface area and well-developed network of micro- and mesopores, remains sufficiently open to enable fast ion movement. The maintenance of the curve shape under dynamic conditions indicates that the electrode material is capable of rapid charge propagation within its porous framework. This is a key indicator of good rate capability, implying that ions can efficiently diffuse throughout the pore channels without severe diffusion limitations, even when the system is subjected to high polarization rates. In practical terms, such behavior is desirable for high-power supercapacitor applications, where the device must respond quickly to fluctuations in current demand.

Furthermore, the absence of pronounced redox peaks across all scan rates confirms that the capacitance arises predominantly from electrostatic charge storage rather than pseudocapacitive surface reactions. This purity of the EDLC response is consistent with highly porous, chemically stable carbon materials and suggests that the activation process has generated a surface chemistry favorable for efficient double-layer formation without introducing significant electroactive functional groups.

Conclusion

In this study, activated carbon derived from discarded hazelnut bark-based biocomposite was successfully synthesized through KOH activation and high-temperature carbonization. The resulting material exhibited a well-developed porous structure capable of supporting efficient electric double-layer charge storage, as evidenced by the quasi-rectangular CV curves. These electrochemical results, together with the sustainable and low-cost origin of the precursor, demonstrate that hazelnut bark-based biocomposite is a highly promising feedstock for producing high-performance activated carbons. By converting agricultural and biomass waste into efficient supercapacitor electrode materials, this approach not only reduces environmental impact but also supports the development of

greener energy storage technologies. Overall, the findings validate the potential of this bio-derived activated carbon as an effective and environmentally responsible alternative to conventional carbonaceous electrodes in modern supercapacitor systems.

Acknowledgments

This work was supported by the Ministry of Science, Technological Development and Innovation of the Republic of Serbia (Contract No. 451-03-137/2025-03/200325, 451-03-136/2025-03/200026, No 451-03-136/2025-03/200105, 451-03-136/2025-03/200178 and University of Defense, Military Academy, Proj. No. VA-TT/1/22-24). The work is aligned with the United Nations Sustainable Development Goals #7 - Ensure access to affordable, reliable, sustainable and modern energy for all.

References

1. P. Simon, Y. Gogotsi, Materials for electrochemical capacitors, Nat. Mater., 7(11), 845-854, 2008.
2. S. V. Bhosale, S. H. Sheshanath, Advancements in supercapacitors: breaking barriers and enabling amazing applications, Chem. Sci., 16:10159–10227, 2025
3. L. Miao, Z. Song, D. Zhu, L. Li, L. Gan, M. Liu, Recent advances in carbon-based supercapacitors, Mater. Adv., 1(5), 945-966, 2020.
4. M. Ayaz, S. S. Shah, M. Younas, U. Safder, I. Khan, M. A. Aziz, A. Adnan, M. Oyama, J. H. Rice, M. N. Tahir, M. Ashraf, Green synthesis of activated carbon from biomass waste of date palm seeds: A sustainable solution for energy storage and environmental impact, J. Energy Storage, 110, 115291, 2025.
5. A. Sevilla, R. Mokaya, Energy storage applications of activated carbons from biomass, Energy Environ. Sci., 7(4), 1250-1280, 2014.
6. P. Dzikunu, E. S. Appiah, E. K. Arthur, S. O. Akinwamide, E. Gikunoo, E. A. K. Fangnon, K. Mensah-Darkwa, A. Andrews, P. Vilaça, Waste-to-carbon-based supercapacitors for renewable energy storage: progress and future perspectives, Mater. Renew. Sustain. Energy, 14(8), 2025.
7. P. Ozpinar, C. Dogan, H. Demiral, U. Morali, S. Erol, C. Samdan, D. Yildiz, I. Demiral, Activated carbons prepared from hazelnut shell waste by phosphoric acid activation for supercapacitor electrode applications and comprehensive electrochemical analysis, Renew. Energy, 189, 535-548, 2022.
8. Y.-L. Bai, C.-C. Zhang, F. Rong, Z.-X. Guo, K.-X. Wang, Biomass-Derived Carbon Materials for Electrochemical Energy Storage, Chemistry, 30(23), 2024.
9. M. Härmas, T. Thomberg, H. Kurig, T. Romann, A. Jänes, E. Lust, Microporous–mesoporous carbons for energy storage synthesized by activation of carbonaceous material by zinc chloride, potassium hydroxide or mixture of them, J. Power Sources, 326, 624-634, 2016.

Corrosion Resistance of Fluorapatite Nanoparticles: A Brief Review with a Focus on Biomedical Applications

Otpornost nanočestica fluorapatita na koroziju: Kratki pregled sa fokusom na biomedicinske primene

Dušan Milojkov[1,*], Miroslav Sokić[1], Vukosava Živković-Radovanović[2], Gvozden Jovanović[1], Vaso Manojlović[3]

[1] *Institute for Technology of Nuclear and Other Mineral Raw Materials, Belgrade, Serbia*

[2] *Faculty of Chemistry, University of Belgrade, Serbia*

[3] *Faculty of Technology and Metallurgy, University of Belgrade, Serbia*

https://doi.org/10.65614/uisk_yucorr.2025.26.ch27

[*] *d.milojkov@itnms.ac.rs*

Abstract

Fluorapatite (FAP), a calcium phosphate compound, has gained significant attention as a promising material for various biomedical applications due to its excellent biocompatibility, osteoconductivity, and resistance to corrosion. The incorporation of fluoride ions into the crystal lattice of FAP enhances its structural stability, making it less susceptible to degradation in biological environments. FAP nanoparticles exhibit increased surface activity, improved adhesion, and a pronounced barrier effect compared to microparticles, which makes them highly suitable for use in protecting metal implants from corrosion. This review provides an overview of corrosion resistance of FAP nanoparticles, focusing on the mechanisms that contribute to this property and its implications for biomedical applications. Key aspects such as FAP synthesis methods, bioactivity, and its role in bone regeneration, dental materials, and implant coatings are explored. Additionally, the mechanisms of corrosion protection offered by FAP, including surface passivation and the role of fluoride ions, are discussed in detail. Finally, the biomedical significance of these properties is evaluated, with an emphasis on their potential to improve the longevity and performance of implantable biomaterials.
Keywords: *fluorapatite; corrosion; biomedical applications; implants; bioactivity*

Izvod

Fluorapatit (FAP), jedinjenje kalcijum-fosfata, privuklo je značajnu pažnju kao obećavajući materijal za različite biomedicinske primene zbog svoje izuzetne biokompatibilnosti, osteokonduktivnosti i otpornosti na koroziju. Uključivanje fluoridnih jona u kristalnu rešetku FAP-a poboljšava njegovu strukturalnu stabilnost, čineći ga manje podložnim degradaciji u biološkim sredinama. FAP nanočestice pokazuju povećanu površinsku aktivnost, bolju adheziju i izraženiji barijerini efekat u odnosu na mikročestice, što ih čini veoma pogodnim za primenu u zaštiti implantata od korozije. Ovaj pregled razmatra otpornost na koroziju FAP nanočestica, sa fokusom na mehanizme koji doprinose ovoj osobini i njenim implikacijama za biomedicinske primene. Ključni aspekti, kao što su metode sinteze FAP-a, bioaktivnost i njegovu ulogu u regeneraciji kostiju, dentalnim materijalima i premazima za implantate, istraženi su u ovom radu. Takođe, detaljno su razmatrani mehanizmi zaštite od korozije koje FAP nudi, uključujući pasivaciju površine i ulogu fluoridnih jona. Na kraju, biomedicinski značaj ovih osobina je evaluiran, sa naglaskom na njihov potencijal da poboljšaju dugovečnost i performanse implantabilnih biomaterijala.
Ključne reči: *fluorapatit; korozija; biomedicinske primene; implantati; bioaktivnost*

Introduction

The field of biomaterials has undergone significant advancements in recent decades, driven by the increasing demand for medical implants and tissue regeneration solutions. Bone and dental implants, which must integrate well with the surrounding tissue and function reliably over time, are key areas where materials science plays a crucial role. To meet these demands, researchers have focused on developing materials that are biocompatible, bioactive, and possess long-term stability in physiological environments. Among the various materials being explored, calcium phosphate ceramics, especially fluorapatite (FAP), have emerged as promising candidates for biomedical applications.

Fluorapatite ($Ca_{10}(PO_4)_6F_2$) is a calcium phosphate compound that is structurally similar to natural bone and tooth mineral [1, 2]. What sets FAP apart from other calcium phosphate materials, such as hydroxyapatite (HA), is the substitution of hydroxyl groups with fluoride ions in the crystal lattice [3]. This substitution has a significant impact on the stability of the material, particularly in environments where the pH decreases, such as the oral cavity during acidic reactions caused by bacterial activity [4, 5]. Fluorapatite's unique properties make it an attractive material for use in dental and orthopedic implants, as well as for applications in bone tissue regeneration.

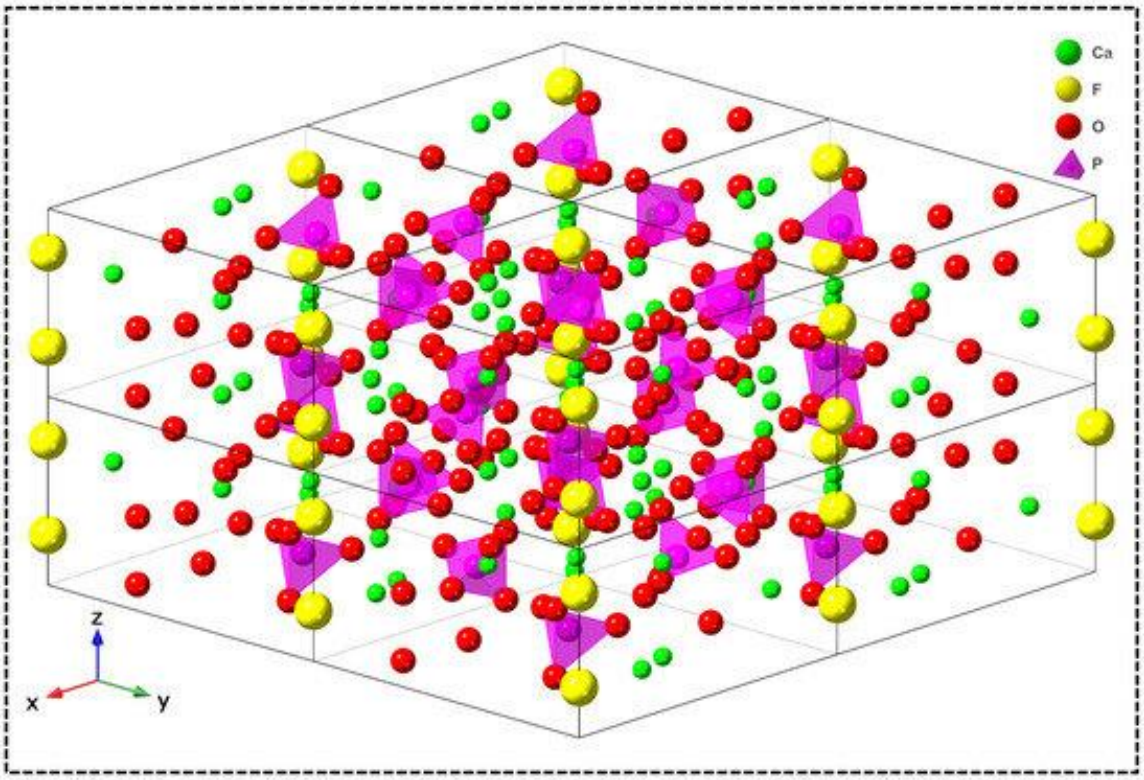

Figure 1. *Crystal structure of FAP. Reprinted from [3] under CC BY 4.0.*

One of the key challenges in the long-term success of medical implants is their corrosion resistance. Implantable materials must maintain their integrity when exposed to biological fluids, which can be corrosive. The degradation of implant materials not only compromises their mechanical strength but can also result in the release of ions that might cause inflammatory responses or even lead to implant failure [6, 7]. Titanium and its alloys, as well as stainless steels, are commonly used in medical implants but are susceptible to various forms of degradation in the presence of body fluids containing chloride ions [6, 7]. The corrosion of metallic materials represents one of the key challenges in materials engineering, particularly in biomedical applications, where implant damage can lead to serious health complications. Therefore, corrosion resistance is one of the critical criteria for evaluating biomaterials for use in clinical settings.

This review aims to explore the corrosion resistance of fluorapatite nanoparticles, focusing on the mechanisms that contribute to this stability and the material's biomedical relevance. By examining the chemical structure, synthesis methods, and biomedical applications of FAP, this paper will provide a comprehensive understanding of why FAP is a suitable candidate for long-term use in the human body. The review will also address how the fluoride ion substitution contributes to enhanced corrosion resistance and the material's overall biocompatibility.
Furthermore, we will discuss the significant biomedical applications of FAP in bone regeneration, dental materials, and implant coatings, with particular emphasis on its role in maintaining stability under physiological conditions. As research in this field continues to advance, understanding the interplay between structure, corrosion resistance, and bioactivity in FAP will be critical for developing improved biomaterials for medical use.

Characteristics of Fluorapatite Influencing Corrosion Resistance

Fluorapatite (FAP) exhibits a unique set of properties that contribute significantly to its corrosion resistance and overall stability as a biomaterial. The key feature that differentiates FAP from other calcium phosphate materials is the presence of fluoride ions within the crystal structure, which replaces the hydroxyl groups typically found in hydroxyapatite (HA). This substitution has profound implications on the chemical stability and dissolution behavior of the material.
Fluoride substitution in the FAP crystal lattice strengthens the ionic bonding between calcium and phosphate ions. This structural modification reduces the material's solubility, particularly in acidic conditions [8, 9]. In biological fluids, which can range in pH from slightly acidic to neutral, the fluoride ions help maintain the integrity of the material by preventing the rapid dissolution that is observed in materials like HA under similar conditions [10, 11]. This enhanced stability makes FAP less susceptible to pH fluctuations, which is particularly advantageous for its use in the human body, where acidic environments can lead to degradation of other biomaterials.
The fluoride ion substitution also has a thermodynamic effect, reducing the free energy of dissolution and, consequently, the tendency of FAP to undergo solubilization when exposed to simulated body fluids (SBF). This makes FAP an ideal candidate for long-term use in environments where other materials would experience significant degradation.
In addition to fluoride substitution, the surface chemistry of FAP plays a crucial role in its corrosion resistance. When used as a coating on metal implant materials, FAP forms a protective layer that acts as a passivating barrier between the metal and surrounding biological fluids. This layer reduces ion exchange and prevents corrosion of the underlying metal, while its biocompatible nature ensures long-term stability and reliability of the implant.
FAP's high chemical stability also allows it to maintain its bioactive properties, such as the ability to stimulate bone growth and promote the formation of mineralized tissue. These properties make it suitable for bone implants and dental applications, where stability and bioactivity are essential for successful integration with the body.

Synthesis of FAP for Biomedical Applications

Fluorapatite can be synthesized using a variety of methods, each of which impacts its structural properties, particle size, and surface characteristics. The method of synthesis plays a pivotal role in determining the material's suitability for different biomedical applications. Some of the most commonly used synthesis techniques for FAP are precipitation, sol-gel, and hidrothermal metohod [8, 11].
One of the most widely used techniques for synthesizing FAP is precipitation [11]. In this method, calcium and phosphate salts are mixed in an aqueous solution containing fluoride ions. This approach allows for the formation of FAP nanoparticles, which can be further processed to enhance their size,

shape, and surface properties. Precipitation is a cost-effective and scalable method, making it suitable for large-scale production of FAP for biomedical applications.
The sol-gel process is another common method used to synthesize FAP [8]. This technique involves the transition of a sol (a colloidal solution) into a gel-like substance, which is then heated to form a stable FAP network. The sol-gel process allows for precise control over the nanostructure of FAP, including particle size and surface area, making it particularly useful for applications where fine control over these characteristics is crucial.
The hydrothermal method involves synthesizing FAP under high-pressure and high-temperature conditions [8]. This method is particularly advantageous for producing high-purity FAP with superior crystallinity and mechanical properties. FAP synthesized through hydrothermal methods tends to have a more stable structure, which is essential for use in demanding biomedical applications such as implant coatings and bone scaffolds.
Fluorapatite has a broad range of biomedical applications due to its bioactive nature and corrosion resistance. Some of the most prominent applications include:

- *Bone Regeneration*: FAP is frequently used in the development of bone scaffolds and grafts. Due to its chemical similarity to natural bone, FAP promotes osseointegration and supports the growth of new bone tissue. It is used in orthopedic implants to enhance healing in fractures and bone defects.
- *Dental Materials*: In dental medicine, FAP is used in dental implants, fillings, and coatings. FAP's ability to bond with natural tooth enamel and resist corrosion in the mouth makes it ideal for long-lasting dental restorations.

Implant Coatings: FAP is often applied as a coating on metallic implants, such as titanium and stainless steel, to improve their biocompatibility and corrosion resistance. This coating helps prevent the release of metal ions into the surrounding tissue, reducing the risk of inflammatory reactions and implant failure.

Mechanisms of Corrosion Protection and Biomedical Significance

Fluorapatite's resistance to corrosion is governed by several key mechanisms that ensure its stability and biocompatibility in the body.
The surface passivation of FAP plays a crucial role in its corrosion resistance. When exposed to biological fluids, a passivating layer forms on the surface of the material, preventing further degradation. This passivation reduces the solubility of FAP in physiological environments, ensuring that the material maintains its structural integrity over time.
Fluoride ions significantly enhance the chemical stability of FAP by reducing its solubility in acidic environments. This is particularly important for long-term implants that may be exposed to acidic body fluids. Fluoride also plays a key role in promoting surface protection, making FAP highly stable even in aggressive biological conditions.
The corrosion resistance of FAP ensures that implants made from this material maintain their mechanical strength and bioactivity over time. This stability is critical for the long-term success of implants, as it prevents the release of harmful ions into the surrounding tissue. FAP's ability to withstand degradation while promoting bone regeneration makes it a reliable material for use in bone implants, dental materials, and orthopedic prostheses.
Table 1 summarizes selected studies investigating the corrosion behavior of FAP, its composites, and coatings on metallic substrates. These studies collectively demonstrate the strong potential of FAP for enhancing corrosion resistance in biomedical devices.
Recent studies have further demonstrated that substituting additional cations (e.g., Mg^{2+}) or combining FAP with metallic or carbon-based reinforcements can substantially enhance corrosion resistance, mechanical stability, and bioactivity. Such hybrid systems exhibit multi-functional

performance, providing both mechanical robustness and chemical protection under physiological conditions [12–17].

Table 1. Summary of recent studies on corrosion resistance of FAP-based materials

Authors	Year	Material/System	Main Findings	Ref.
Sharifnabi A., et al.	2014	Mg-substituted fluorapatite coating on 316L SS	Mg–FAP coating reduced corrosion rate and metal ion release, enhancing corrosion resistance and biocompatibility.	[12]
Razavi M., et al.	2010	Mg–fluorapatite nanocomposite (AZ91–20FA)	FAP nanoparticles decreased corrosion rate and promoted apatite layer formation, improving protection and osteoconductivity.	[13]
Fathi M.H., et al.	2009	Fluorapatite/niobium (FA/Nb) composite coating	FAP/Nb coating showed lower corrosion current and improved biocompatibility compared with FAP alone.	[14]
Khani M., et al.	2022	Mg–Mn–Ca/FA + GNP hybrid biocomposite	Reinforcements enhanced mechanical strength and corrosion resistance, achieving over 15× higher impedance.	[15]
Zang M., et al.	2024	Fluorine-substituted HA coating on Ti–6Al–4V	Optimal 9 wt% CaF_2 substitution yielded highest crystallinity, strength, and lowest corrosion rate.	[16]
Razavi M., et al.	2010	AZ91–FA nanocomposites (10–30 wt% FA)	Increasing FAP content improved hardness and corrosion resistance, with 20 wt% FAP giving best overall performance.	[17]

Conclusion

Fluorapatite nanoparticles and their composites are emerging as highly promising materials for biomedical applications, primarily due to their outstanding corrosion resistance, biocompatibility, and bioactivity. The presence of fluoride ions within the crystal lattice enhances chemical stability and minimizes degradation in physiological environments. Recent research consistently demonstrates that FAP-based coatings and composites can significantly improve the corrosion resistance of metallic substrates while maintaining or even enhancing biological performance. Continued development of optimized synthesis methods and hybrid FAP systems is expected to further advance their use in next-generation medical implants, contributing to safer, longer-lasting, and more reliable biomaterials. Future research should focus on tailoring the surface functionalization of FAP nanoparticles to further enhance their corrosion resistance and biological response.

Acknowledgments

Ministry of Science, Technological Development and Innovation of the Republic of Serbia, institutional funding - (Contract No. 451-03-136/2025-03/200023).

References

1. Leroy, N., & Bres, E. (2001). Structure and substitutions in fluorapatite. *European Cells and Materials, 2*, 36–48.. doi: 10.22203/ecm.v002a05.

2. Kazimierczak, P., Wessely-Szponder, J., Palka, K., Barylyak, A., Zinchenko, V., & Przekora, A. (2023). Hydroxyapatite or fluorapatite—Which bioceramic is better as a base for the production of bone scaffold? A comprehensive comparative study. *International Journal of Molecular Sciences, 24*(6), 5576. doi: 10.3390/ijms24065576.
3. Li, C., Wang, G., Wang, S., Shen, W., Zhang, Y., Kang, J., & Xiao, Z. (2025). Fluorapatite glass-ceramics in dentistry: Synthesis, properties, forming technology, applications, challenges, and future perspectives. *Materials, 18*, 804. https://doi.org/10.3390/ma18040804
4. Aoba, T. (1997). The effect of fluoride on apatite structure and growth. *Critical Reviews in Oral Biology & Medicine, 8*(2), 136–153. doi:10.1177/10454411970080020301
5. Legeros, R. Z., Kijowska, R., Jia, W., & Legeros, J. P. (1988). Fluoride-cation interactions in the formation and stability of apatites. *Journal of Fluorine Chemistry, 41*, 53–64.
6. Prakasam, M., Locs, J., Salma-Ancane, K., Loca, D., Largeteau, A., & Berzina-Cimdina, L. (2017). Biodegradable materials and metallic implants—A review. *Journal of Functional Biomaterials, 8*(4), 44. https://doi.org/10.3390/jfb8040044
7. Eliaz, N. (2012). Degradation of Implant Materials, Springer New York, NY. https://doi.org/10.1007/978-1-4614-3942-4
8. Borkowski, L., Przekora, A., Belcarz, A., Palka, K., Jozefaciuk, G., Lübek, T., Jojczuk, M., Nogalski, A., & Ginalska, G. (2020). Fluorapatite ceramics for bone tissue regeneration: Synthesis, characterization and assessment of biomedical potential. *Materials Science and Engineering: C, 116*, 111211. https://doi.org/10.1016/j.msec.2020.
9. Song, H., Cai, M., Yuan, P., et al. (2024). Effect of fluoride on the ion-association of calcium phosphate and crystallization of hydroxyapatite. *Journal of Wuhan University of Technology-Materials Science Edition, 39*, 831–838. https://doi.org/10.1007/s11595-024-2943-1
10. Borkowski, L., Jojczuk, M., Belcarz, A., Pawlowska-Olszewska, M., Kruk-Bachonko, J., Radzki, R., Bienko, M., Slowik, T., Lübek, T., Nogalski, A., & Ginalska, G. (2023). Comparing the healing abilities of fluorapatite and hydroxyapatite ceramics in regenerating bone tissue: An in vivo study. *Materials, 16*(17), 5992. https://doi.org/10.3390/ma16175992
11. Milojkov, D. V., Sokić, M., Radosavljević-Mihajlović, A., Stanić, V. D., Manojlović, V., Mutavdžić, D. R., & Milanović, M. (2021). Influence of Pr3+ and CO32− Ions Coupled Substitution on Structural, Optical and Antibacterial Properties of Fluorapatite Nanopowders Obtained by Precipitation. Metals, 11(9), 1384. https://doi.org/10.3390/met11091384
12. Sharifnabi, A., Fathi, M. H., Eftekhari Yekta, B., & Hossainalipour, M. (2014). The structural and bio-corrosion barrier performance of Mg-substituted fluorapatite coating on 316L stainless steel human body implant. *Applied Surface Science, 288*, 331–340. https://doi.org/10.1016/j.apsusc.2013.10.029
13. Razavi, M., Fathi, M. H., & Meratian, M. (2010). Bio-corrosion behavior of magnesium–fluorapatite nanocomposite for biomedical applications. *Materials Letters, 64*(22), 2487–2490. https://doi.org/10.1016/j.matlet.2010.07.079
14. Fathi, M. H., Mohammadi Zahrani, E., & Zomorodian, A. (2009). Novel fluorapatite/niobium composite coating for metallic human body implants. *Materials Letters, 63*(13–14), 1195–1198. https://doi.org/10.1016/j.matlet.2009.02.040
15. Khani, M., Ebrahimi, G., & Ezatpour, H. R. (2022). Accumulative extrusion bonding of Mg–Mn–Ca/FA + GNP hybrid biocomposite: On microstructure evaluation, mechanical and corrosion properties. *Materials Today Communications, 33*, 104426. https://doi.org/10.1016/j.mtcomm.2022.104426
16. Zang, M., Li, L., Sun, X., Niu, Z., Bai, X., & Liu, X. (2024). Characterization, mechanical properties, corrosion behavior and bone-like apatite formation ability of fluorine substituted hydroxyapatite coating. *Journal of the Mechanical Behavior of Biomedical Materials, 151*, 106364. https://doi.org/10.1016/j.jmbbm.2023.106364
17. Razavi, M., Fathi, M. H., & Meratian, M. (2010). Microstructure, mechanical properties and bio-corrosion evaluation of biodegradable AZ91–FA nanocomposites for biomedical applications. *Materials Science and Engineering: A, 527*(26), 6938–6944. https://doi.org/10.1016/j.msea.2010.07.063

Application of MIPAR Software in the Quantitative Analysis of Corroded Surfaces

Primena MIPAR softvera u kvantitativnoj analizi korodirane površine

Gvozden Jovanović[1,*], Stefan Dikić[2], Aleksandra S. Popović[2], Nikola S. Vuković[1], Branimir N. Grgur[2], Miroslav Sokić[1]

[1] *Institute for Technology of Nuclear and Other Mineral Raw Materials, Franchet d'Esperey 86, Belgrade, Serbia*

[2] *Faculty of Technology and Metallurgy University of Belgrade, Karnegijeva 4, Belgrade, Serbia*

https://doi.org/10.65614/uisk_yucorr.2025.26.ch28

[*] *g.jovanovic@itnms.ac.rs*

Abstract

Corrosion is a common failure mechanism in steel and its structural components, often compromising their mechanical integrity and service life. One widely used method of protection is the application of functional coatings (organic, inorganic, or hybrid) that are tailored to perform specific roles under various environmental conditions. This study investigates the use of MIPAR, a powerful image analysis software, in the quantitative evaluation of corroded surfaces to assess the performance of such coatings. Composite coatings were prepared by incorporating 5 wt.% of polyaniline into a commercial alkyd-based paint and applied onto carbon steel substrates. The polyaniline emeraldine salt was synthesized following the IUPAC-recommended procedure, involving deprotonation with ammonium hydroxide and subsequent reprotonation with sulfamic, succinic, citric, and acetic acids. The base coating and four composite coatings were then exposed to a corrosive environment (3% NaCl solution), and surface degradation was monitored through digital imaging. MIPAR analysis was employed to quantify surface corrosion coverage, enabling a detailed evaluation of coating performance and corrosion progression. This approach demonstrates how digital image analysis enhances the accuracy and efficiency of corrosion studies by providing measurable, reproducible data on coating performance. The results highlight the potential of integrating digital imaging and advanced software tools like MIPAR in the development of next-generation functional coatings, including those with self-healing properties. Furthermore, future applications of MIPAR may involve leveraging its machine learning capabilities and multi-layer imaging to analyze complex coating systems, corroded and healed surfaces. This integration can significantly streamline research workflows and accelerate the discovery of more effective corrosion protection technologies.

Keywords: *corrosion; image software; surface analysis; MIPAR*

Izvod

Korozija je čest mehanizam degradacije kod čelika i čeličnih konstrukcija, što značajno utiče na njihov mehanički integritet i radni vek. Jedna od najčešće korišćenih metoda zaštite jeste primena funkcionalnih prevlaka (organskih, neorganskih ili hibridnih) koje se mogu prilagoditi da obavljaju određene funkcije u različitim uslovima radne sredine. Ova studija istražuje upotrebu softvera MIPAR, efikasnog alata za analizu digitalnih slika, u kvantitativnoj evaluaciji korozije i efikasnosti zaštitnih prevlaka. Kompozitne prevlake su pripremljene dodatkom 5% polianilina u komercijalnu alkidnu boju i nanete su na podloge od ugljeničnog čelika. Polianilin smaragdna so je sintetizovana prema IUPAC-ovoj proceduri, koja podrazumeva deprotonaciju sa amonijum hidroksidom, a zatim reprotonaciju sa sulfaminskom, sukcinskom, limunskom i sirćetnom kiselinom. Bazni premaz i četiri kompozitna premaza su zatim izloženi korozivnoj sredini (3% rastvor NaCl), a degradacija površine je praćena digitalnim snimanjem. Za kvantifikaciju korodirane površine korišćena je MIPAR analiza,

što je omogućilo detaljnu evaluaciju performansi premaza i napredovanja korozije. Ovakav pristup pokazuje kako digitalna analiza slika može unaprediti preciznost i efikasnost istraživanja u oblasti korozione zaštite, pružajući merljive i ponovljive rezultate. Rezultati ukazuju na veliki potencijal integracije digitalnog snimanja i naprednih softverskih alata poput MIPAR-a u razvoju novih generacija funkcionalnih prevlaka, uključujući samopopravljajuće prevlake. Dodatno, buduća primena softvera MIPAR mogla bi obuhvatiti upotrebu njegovih naprednih mogućnosti u oblasti mašinskog učenja i višeslojne analize slika za detaljno ispitivanje kompleksnih prevlaka, korodirane i regenerisane površine. Ova integracija može značajno ubrzati istraživačke procese i doprineti razvoju efikasnijih tehnologija zaštite od korozije.
Ključne reči: *korozija; program za obradu slika; analiza površine; MIPAR*

Introduction

Corrosion is a pervasive failure mechanism in steel structures, causing significant economic losses and compromising structural integrity [1]. Localized forms, such as pitting and crevice corrosion, are particularly difficult to predict due to their dependence on environmental and material factors [2]. The consequences of corrosion are not only financial but can also threaten safety and reduce the service life of critical infrastructure.

Functional and smart coatings, including polyaniline-based systems, are widely used to protect metals by enhancing surface stability and delaying corrosion propagation [3]. These coatings can be tailored to provide multiple functionalities, such as barrier protection, hydrophobicity, or self-healing capability, depending on the application. Evaluating their performance requires reliable and quantitative assessment methods that go beyond traditional visual inspection, which is often subjective and time-consuming [4].

Digital imaging combined with automated analysis offers a powerful approach for such evaluations. MIPAR software enables the creation of automated analysis “recipes” to segment and quantify corroded surfaces efficiently, reducing manual effort while maintaining precision [5]. By integrating high-resolution imaging with computational analysis, MIPAR allows researchers to track corrosion progression, compare coating performance, and support the development of more effective protection strategies.

Material and Methods

As already described in our previously published paper, polyaniline in a powdered form was produced using the chemical synthesis route [6, 7]. Composite coatings were prepared by incorporating 5 wt.% of polyaniline into a commercial alkyd-based paint and applied onto carbon steel substrates. The polyaniline (PANI) emeraldine salt was synthesized following the IUPAC-recommended procedure [8], involving deprotonation with ammonium hydroxide and subsequent reprotonation with sulfamic, succinic, citric, and acetic acids. The base coating and four composite coatings were then exposed to a corrosive environment (3% NaCl solution). The image of surfaces of the samples was made using a PANASONIC DC-FZ82 digital camera (Panasonic Corporation, Kadoma, Osaka, Japan). A digital image analysis using MIPAR v.4.50 (MIPAR Image Analysis, Columbus, Ohio, USA) was employed to quantify surface corrosion coverage, enabling a detailed evaluation of coating performance and corrosion progression [9].

The method of selecting the pixels that correspond to the corroded surface was within the specified hue, saturation, and pixel value ranges according to the settings presented in figure 1.

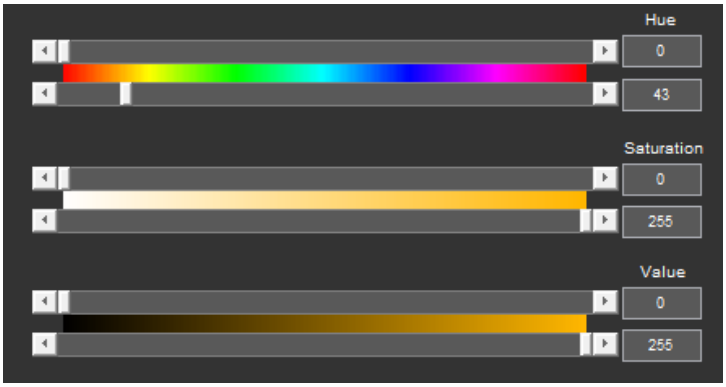

Figure 1. *Illustration of the settings of selecting colors from the image [10].*

The selection of pixels was performed by eyedropper function, additively expanding the range of hue, saturation, and value. Six recipes were developed using the color selection feature, five were tailored to their respective images for the tested samples, while one was developed to be used on all five corroded images. The overarching recipe used for all the images was modified to exclude the dark and gray areas at the corner of the images as well as the marked numbers. All the color selection data for the recipes are given in table 1.

Table 1. Color selection ranges for the recipes used on the images of corroded surfaces

Recipe	Hue	Saturation	Pixel value
I	17 48	12 161	123 255
II	0 65	3 255	74 255
III	17 49	13 255	100 255
IV	0 48	33 255	83 255
V	0 360	22 255	56 255
All*	0 360	12 255	66 255

*modified to exclude gray and black surfaces

Results and Discussion

The surface area of the tested samples was measured to be 11.074 cm^2 and the non-corroded sample coated with the composite of polyaniline and sulfamic acid is shown in figure 2. The polyaniline particles are visible as black dots while the improper dispersion could be seen as a bluish hue. By use of MIPAR software, the particles were highlighted in pink and the unapplied or uneven coating in green, while the product of the overarching recipe on the non-corroded surface is given in red.

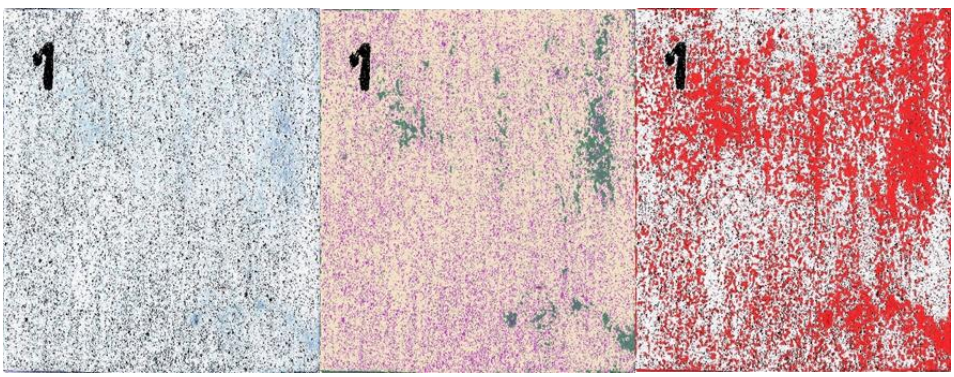

Figure 2. *Non-corroded sample (left), MIPAR selection of particles and coating (middle), result of recipe „All" on non-corroded sample (left).*

The main difficulty when applying the same recipe on the corroded surfaces stems from their differences in brightness, contrast, and exposure when the photos were taken. In order to uniformly identify the intensity of the corrosion on the tested surface it is crucial to keep the changes in these settings to a minimum when acquiring the photographs. If that is unavoidable, it is recommended to take a reference photo of a non-corroded sample under the same conditions. The differences in these settings in the original images are seen in their image pixel histograms (figure 3). These can be altered by utilizing the pre-processing functions like *Flatten Background* or *Histogram equalization* and *Smart Clusters;* however, these are not recommended since the dark coating particles can be confused with the corroded surfaces, thus *Color Selection* was the only function employed.

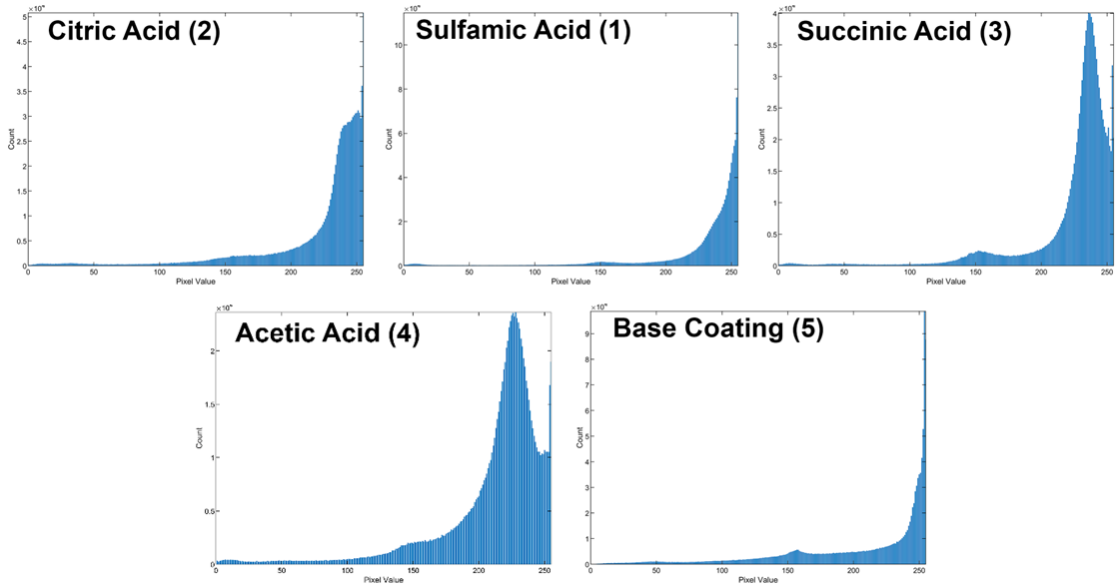

Figure 3. *Image pixel histograms of original image.*

The peak in pixels values between 120 and 180, or more specifically the peak from 150 to 160, corresponds to both the gray areas at the edge of the samples as well as the mild brown rusted corroded surface, that can be seen across all the coated samples in figure 3.

The results of each corroded surface for every recipe are presented in table 2 as percentage of the covered surface within the whole image. The lower the value the more efficient the composite coating is, making the best composite coating those of polyaniline doped with sulfamic acid, and succinic acid to a lesser extent. Among all samples, the base polyaniline coating exhibited the lowest performance. We can observe how the differences in recipe approaches are reflected on the results of area measurements.

Table 2. Percentages of the corroded surface area measured by different recipes

Coating type (Sample No.)	Recipe					
	I	**II**	**III**	**IV**	**V**	**All**
Sulfamic Acid (1)	**9.59**	27.53	0.005	1.67	4.43	11.17
Citric Acid (2)	15.79	**24.62**	16.09	13.73	17.27	20.94
Succinic Acid (3)	11.06	22.01	**10.90**	4.82	8.57	13.29
Acetic Acid (4)	28.93	58.13	28.76	**19.32**	24.45	31.18
Base Coating (5)	51.11	83.34	52.65	47.00	**58.18**	68.77

The values for the tailored recipes on their respective sample surfaces, as well as the overarching recipe next to the original images, are shown in figure 4. The most significant discrepancy between the tailored and the overarching recipe results was observed for the composite with acetic acid (11.86 %), while the minimal difference was observed for the least corroded sample with sulfamic acid composite (1.58%).

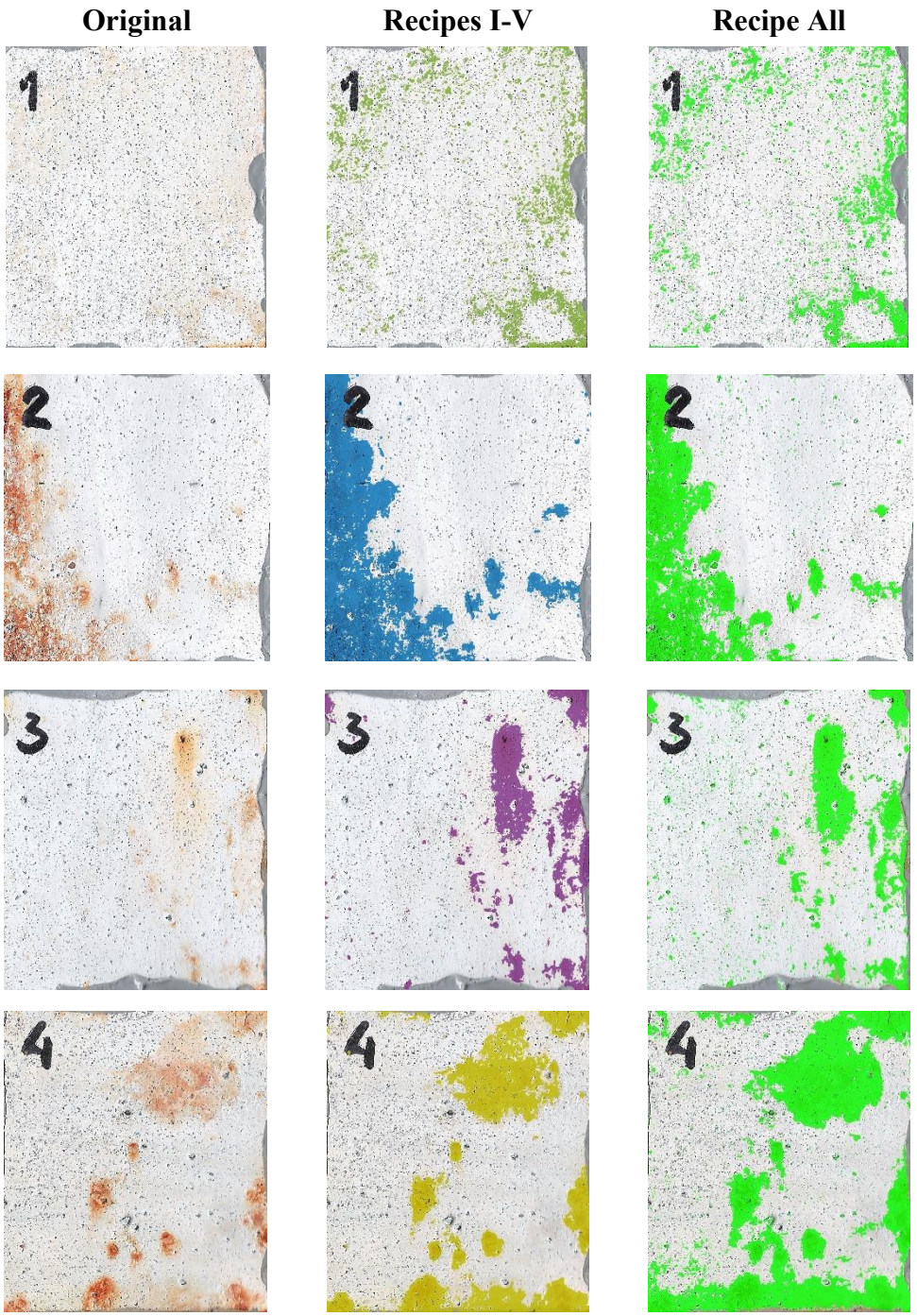

Figure 4. *Results of MIPAR analysis with reference images: original corroded surface (left), recipes tailored for each image (middle), overarching recipe (right).*

Combining the percentages of the corroded areas from respective recipes with the total image surface of 11.074 cm^2, the corroded area for each sample is obtained (table 3). Furthermore, assuming that the tailored recipes are more accurate and representative, in comparison to the overarching recipe, the absolute error can be calculated. The average absolute error (E_{abs}) is 0.553 cm^2, which is equal to 4.99 % of the total image surface.

Table 3. Recalculated corroded surface area (in cm^2) of the coated samples

Recipe	Sample No.				
	1	**2**	**3**	**4**	**5**
I-V	1.062	2.727	1.207	2.707	6.443
All	1.237	2.319	1.472	3.453	7.615
E_{abs}	0.175	0.408	0.265	0.746	1.172

In order to improve the applicability of MIPAR and to create an overarching recipe that can accurately estimate the corroded area on various samples, a much larger sample set should be studied. Moreover, the *Color Selection* function can be used to correlate the pixel color with the degree of corrosion on the studied surfaces. However, for the purpose of this paper, the software's capabilities proved to be quite appropriate.

Conclusion

Overall, the use of software programs for digital image analysis, such as MIPAR, has shown to be accurate and reliable in order to estimate the corroded surface area. However, in order to make a recipe that can work uniformly and that can identify the intensity of the corrosion on the tested surface, it is crucial to establish a minimal set of sample images to train the recipe. On the other hand, it is also helpful to avoid changes in brightness, contrast, and exposure between the images as much as possible. In this instance, five recipes were developed for their respective images and one recipe was developed to work on all five images. If we take the tailored recipes as representative, than the overarching recipe has an average absolute error of 0.553 cm^2, which is equal to 4,99 % of the total image surface. In the future applications, MIPAR can be employed to analyze the efficiency of coating application on the sample surface. The uniformity of the coating before the corrosion process can be compared to the distribution of the corroded areas, so their overlap can be quantified. However, in order to successfully employ MIPAR software, the coated samples need to have a small area of pristine surfaces. In summary, MIPAR is a versatile software program with multiple tools for image analysis, which can be utilized in various manners in order to better understand and evaluate the corrosion process.

Acknowledgements

This work was supported by the Ministry of Science, Technological Development and Innovation of the Republic of Serbia (Contract No. 451-03-136/2025-03/200023 and 451-03-136/2025-03/200135).

References

1. M. Khayatazad, L. De Pue, W. De Waele, "Detection of corrosion on steel structures using automated image processing," *Developments in the Built Environment*, 3, 100022, 2020.
2. M. J. Quinn, M. G. Bailey, B. M. Dceda, D. W. Shoesmit, *Image-Analysis Techniques for Investigating Localized Corrosion Processes*, Whiteshell Laboratories, Pinawa, Manitoba, 1993.
3. M. F. Montemor, "Functional and smart coatings for corrosion protection: A review of recent advances," *Surface & Coatings Technology*, 258, 17–37, 2014.
4. M. P. Bento, F. N. S. de Medeiros, I. C. de Paula Jr., *Image Processing Techniques applied for Corrosion Damage Analysis*, Universidade Federal do Ceará, Fortaleza-CE, Brasil, 2010.
5. C. A. Garcia, V. Prasad, T. C. Gamblin, "MIPAR and ImageJ FIJI as Tools for Electron Microscopy Quantification of Amyloid Fibrils," *Biochemistry*, 64, 1907–191, 2025.
6. B. N. Grgur, A. S. Popović, A. Salem, "Influence of Alkyd Composite Coatings with Polyaniline Doped with Different Organic Acids on the Corrosion of Mild Steel," *Metals*, 13, 1364, 2023.
7. A. J. Salem, B. N. Grgur, "The influence of the polyaniline initial oxidation states on the corrosion of steel with composite coatings," *Prog. Org. Coat.*, 119, 138, 2018.
8. J. Stejskal, R. G. Gilbert, "Polyaniline: Preparation of a conducting polymer (IUPAC Technical Report)," *Pure Appl. Chem.*, 74, 857, 2002.
9. Sosa, J.M., Huber, D.E., Welk, B. *et al.* Development and application of MIPAR™: a novel software package for two- and three-dimensional microstructural characterization. *Integr Mater Manuf Innov* **3**, 123–140 (2014). https://doi.org/10.1186/2193-9772-3-10
10. "MIPAR 4.50 Manual > Image Processor > Functions > Color > Color Select," *MIPAR User Manual v4.5*. [Online]. Available: https://www.manula.com/manuals/mipar/user-manual/v4.5/en/topic/color-select

Conversion of Tree Leaf Biowaste into a Promising Material as Energy source

Konverzija otpada lišća drveta u potencijalni energetski material

Marija Koprivica[1,*], Jelena Dimitrijević[1], Jelena Petrović[1], Marija Simić[1], Marija Ercegović[1], Ivana Mikavica[1], Aleksandar Jovanović[1]

[1] *Institute for Technology of Nuclear and Other Mineral Raw Materials, Belgrade, Serbia*

https://doi.org/10.65614/uisk_yucorr.2025.26.ch29

[*]*m.koprivica@itnms.ac.rs*

Abstract

This study investigates the conversion of Paulownia tree leaf biomass (LP) into biochar (BLP) through slow pyrolysis at 400 °C under low-oxygen conditions. The research aims to elucidate the influence of the pyrolysis process on the chemical composition, structural characteristics, and combustion behavior of the resulting biochar. Thermogravimetric and Differential Thermal Analysis (TG/DTA), along with proximate and elemental analyses, were employed to provide comprehensive insights into the physicochemical and thermal properties of the biochar, which are crucial for assessing its potential as an energy material. The process yielded a significant increase in fixed carbon (from 8.72 ± 0.23% to 41.96 ± 0.28%) and total carbon content (from 45.49 ± 0.21% to 64.11 ± 0.42%), accompanied by a marked decrease in oxygen content (from 38.05 ± 0,09% to 9.68 ± 0.01%), resulting in a reduced O/C ratio (from 0.63 to 0.11). The higher heating value increased from 18.98 MJ/kg to 26.44MJ/kg, with improvements in fuel ratio (FR) and lower heating value (LHV), collectively enhancing the biochar's energy potential. Thermal analysis confirmed the formation of new aromatic structures, reflecting enhanced thermal stability and improved combustion characteristics. Overall, Paulownia leaves represent a promising biomass feedstock for sustainable biochar production, contributing to waste valorization, pollution mitigation, and the development of alternative energy resources.

Keywords: *tree leaf biochar; fuel properties; biochar - feedstock comparison; TG/DTA analysis*

Izvod

Ova studija istražuje konverziju biomase lišća drveta Paulownia (LP) u biočađ (BLP) putem spore pirolize sprovedene na 400 °C u uslovima ograničenog prisustva kiseonika. Cilj istraživanja je da se razjasni uticaj procesa pirolize na hemijski sastav, strukturne karakteristike i sagorevajuće ponašanje dobijenog biočađ. Za detaljnu karakterizaciju fizičkohemijskih i termičkih svojstava biočađi, koja su ključna za procenu njegovog potencijala kao energetskog materijala, primenjene su termogravimetrijska (TG) i diferencijalna termička analiza (DTA), zajedno sa tehničkom i elementarnom analizom. Proces pirolize doveo je do značajnog povećanja sadržaja fiksnog ugljenika (sa 8,72 ± 0,23 % na 41,96 ± 0,28 %) i ukupnog ugljenika (sa 45,49 ± 0,21 % na 64,11 ± 0,42 %), uz istovremeno izraženo smanjenje sadržaja kiseonika (sa 38,05 ± 0,09 % na 9,68 ± 0,01 %), što je rezultiralo smanjenjem odnosa O/C (sa 0,63 na 0,11). Viša toplotna vrednost (HHV) povećana je sa 18,98 MJ/kg na 26,44 MJ/kg, uz poboljšanje gorivnog odnosa (FR) i niže toplotne vrednosti (LHV), čime je ukupno unapređen energetski potencijal biočađi. Termička analiza potvrdila je formiranje novih aromatičnih struktura, što ukazuje na povećanu termičku stabilnost i poboljšane karakteristike sagorevanja. Sveukupno, lišće Paulownia drveta pokazuje se kao perspektivna biomasa za održivu proizvodnju biočađi, doprinoseći valorizaciji otpada, smanjenju zagađenja i razvoju alternativnih izvora energije.

Ključne reči: *biočađ lista drveta; gorivne karakteristike; poređenje biočađi sa početnom biomasom; TG/DTA analiza*

Monitoring Heavy Metal Mobilisation in Acid Leaching of Coal

Praćenje oslobađanja teških metala pri kiselinskom luženju uglja

Katarina Pantović Spajić[1,*], Milica Mišić[1], Katarina Mihajlović, Dimitrije Anđić[1], Nikola Vuković[1], Branislav Marković[1], Miroslav Sokić[1]

[1] *Institute for Technology of Nuclear and Other Mineral Raw Materials, 11000 Belgrade, Serbia*

https://doi.org/10.65614/uisk_yucorr.2025.26.ch30

[*]*k.pantovic@itnms.ac.rs*

Abstract

Acid leaching was applied to coal samples from the Bogovina basin, located in eastern Serbia, in order to evaluate its effectiveness in reducing sulphur and ash content and to monitor the mobilisation of heavy metals into the leachate. The experiments were conducted under controlled laboratory conditions, with a leaching time of 30 minutes, employing three different temperatures and various acid concentrations. Two acid reagents were tested, and the resulting leachates were analysed for concentrations of heavy metals, including Cr, Cu, Co, and Pb.

The analytical results, obtained using an Atomic Absorption Spectrophotometer (AAS) and Eschka method, showed that acid leaching significantly reduced the sulphur and ash content of the coal while simultaneously mobilising varying amounts of heavy metals into the aqueous phase. The extent of metal mobilisation depended on the type of acid used, indicating that reagent composition plays a key role in determining both desulphurisation efficiency and environmental impact.

This study confirms the presence of toxic heavy metals in coal from the Bogovina region and demonstrates that acid leaching can effectively improve coal quality, although it may increase the mobility of certain metals. These findings highlight the need to balance coal upgrading with appropriate management in order to minimise environmental risks.

Future research will focus on comparing the concentrations and behavior of heavy metals in leachate and sediments from the Bogovina area, to gain a deeper understand of metal distribution and potential pathways within the local environment.

Keywords: *acid leaching; coal; desulphurization; deashing; leachate monitoring*

Acknowledgements

This work was supported by the Ministry of Science, Technological Development and Innovation of the Republic of Serbia (Contract No. 451-03-136/2025-03/200023).

Comparison of the functional properties of ilite clay/ TiO_2 and kaolinite clay/TiO_2 coatings

Poređenje funkcionalnih svojstava premaza od ilit gline/TiO_2 i kaolinit gline/TiO_2

Vojo Jovanov[1,*], Snežana Vučetić[2], Biljana Angjusheva[1], Jonjaua Ranogajec[2], Emilija Fidanchevski[1]

[1] *Ss. Cyril and Methodius University in Skopje, Faculty of Technology and Metallurgy, Ruger Bosković 16, 1000 Skopje, Republic of N. Macedonia*

[2] *University of Novi Sad, Faculty of Technology, bul. Cara Lazara 1, 21000 Novi Sad, Serbia*

https://doi.org/10.65614/uisk_yucorr.2025.26.ch31

[*]*vojo@tmf.ukim.edu.mk*

Abstract

Ilite/ TiO_2 and kaolinite/TiO_2 coatings, impregnated with 10 wt.% nano TiO_2 using mild conditions, was applied to and investigated on three types of substrates: porous (clay roofing tiles), highly porous (clay-fly ash composite), and non-porous (window glass). The coatings were analyzed for their capillary water absorption and surface properties, including roughness, micro-hardness, and hydrophilicity. The functional properties of self-cleaning and photocatalytic activity were evaluated by measuring the initial contact angle and the photodegradation of the model pollutant Rhodamine B, which was assessed during UV/VIS irradiation.

The study suggests that the applied synthesis by mechanical activation methodology resulted in a homogenous distribution of TiO_2 as an active component in the photocatalytic coating, leading to better surface and functional properties. Novel natural clay/TiO_2-based coatings are advantageous due to their low cost and simple preparation, ensuring high photo-degradation efficiency.

Keywords: *nano-TiO_2; kaolinite clay; illite clay; mechanical activation; photocatalytic coating*

Izvod

Premazi ilit/TiO_2 i kaolinit/TiO_2, impregnirani sa 10 tež.% TiO_2 korišćenjem nove metode pod blagim uslovima, naneti su i ispitani na tri vrste podloga: poroznim (glineni crepovi), visoko poroznim (kompozit gline i pepela) i neporoznim (prozorsko staklo). Premazi su analizirani na osnovu njihove kapilarne apsorpcije vode i površinskih svojstava, uključujući hrapavost, mikrotvrdoću i hidrofilnost. Funkcionalna svojstva samočišćenja i fotokatalitičke aktivnosti procenjena su merenjem početnog kontaktnog ugla i fotodegradacije modelnog zagađivača rodamina B, koja je procenjena tokom UV/Vis zračenja.

Studija sugeriše da je primenjena sinteza metodologijom mehaničke aktivacije rezultirala homogenom raspodelom TiO_2 kao aktivne komponente u fotokatalitičkom premazu, što je dovelo do boljih površinskih i funkcionalnih svojstava. Novi premazi na bazi prirodne gline/TiO_2 su predni zbog svoje niske cene i jednostavne pripreme, obezbeđujući visoku efikasnost fotodegradacije.

Ključne reči: *nano-TiO_2; kaolinitna glina; ilitna glina; mehanička aktivacija; fotokatalitički premaz*

Introduction

The surfaces of exposed building materials, such as ceramic tiles, roofing tiles, glass, and facades, are exposed to environmental conditions that can result in the deposition of pollutants onto them, so that cleaning, which is connected to a high consumption of energy, labor, and detergents, is needed, resulting in high maintenance costs. To reduce costs and enhance the long-term aesthetic appearance of the exposed surfaces of building materials, photocatalytic and self-cleaning coatings can be applied

[1,2]. Among various semiconductor catalysts, titanium dioxide (TiO_2) has garnered significant attention for this application due to its efficient photocatalytic activity, high stability, low cost, and non-toxicity [3]. One of the possibilities to increase its photocatalytic activity is the impregnation of TiO_2 nanoparticles into the clay mineral structure [8,9]. Clay minerals have unique layered structures, a large specific surface area, and high adsorption capacity [10,11]. The incorporation of TiO_2 into their structure enhances photocatalytic efficiency by providing a durable support structure and improving adsorption characteristics [12,13,14].
Many studies indicate that incorporating TiO_2 into clay minerals through mechanical activation offers several benefits. These include a uniform distribution of TiO_2 as an active component, increased reactivity due to reduced particle size, and a larger surface area, which improves absorption properties This study aimed to develop photocatalitically active coatings based on kaolinite and illite clays serving as supports for the incorporation of 10 wt.% nano-TiO_2. The impregnation was carried out through mechanical activation using an attritor and a planetary mill under controlled conditions. The effects of the coatings on three types of substrates with varying porosities were evaluated in terms of capillary water absorption, surface properties (roughness, microhardness, and hydrophilicity), and functional properties (self-cleaning and photocatalytic activity).

Experimental

Materials

Illite and kaolinite clay were used in this study. Illite caly originates from the eastern part of Republic of North Macedonia, while kaolinite was commercial refractory clay from Republic of Poland.
The nano TiO2, sourced from the Degussa company in Germany, acted as the photocatalytic precursor. The suspension consisted of 30.0 ± 1.0 wt.% dry matter, primarily comprising 80 wt.% anatase and 20 wt.% rutile, with particle sizes under 100 nm and a neutral pH of 7.

Preparation of illite clay/nano TiO_2 coating

The impregnation of nano TiO_2 in content of 10 wt.% into the illite clay was performed using mechanical activation in an attritor mill for 90 minutes at a speed of 1500 rpm. The impregnation in kaolinite clay was performed in two ways: in an attritor mill under the same conditions as those for illite clay, and as a second way in a planetary mill during 180 minutes at a speed of 200 rpm. The material-to-ball ratio was set at 1:5, and the pH value was maintained between 9 and 9.5. This pH level was adjusted using $NaCO_3$ solution with a concentration of 0.67 mol/dm^3. The resulting powders were then dried at 105°C for 24 hours. The coatings were prepared by diluting 0.5 g of the synthesized powder in 100 mL of demineralized water, followed by the stabilization procedure procedure [10, 14]. This coating suspensions were then applied using a spray technique onto three different types of model substrates: porous, highly porous and non-porous. Industrial clay roofing tile (CRT) was used for the porous substrate, a composite of fly ash and clay (CFA) was employed as the highly porous substrate and window glass (WG) served as the non-porous substrate. The capillary water absorption coefficients for these substrates were as follows, [kg/m² min$^{1/2}$]: CRT - 8.22, CFA - 1.04 x 10^{-6} and WG - 0.73[10]. The coding system for the samples used in this investigation is as follows: uncoated reference substrates are marked with the suffix "R" (e.g., CRT-R, CFA-R, WG-R). Substrates coated with an Ilite clay/TiO_2 suspension are labeled with the suffix "H2A" (e.g., CRT-H2A, CFA-H2A, WG-H2A). Those coated with a kaolinite clay/TiO_2 suspension are designated with the suffix "E2A" (e.g., CRT-E2A, CFA-E2A, WG-E2A) when impregnated in an attritor mill, or "E2P" (e.g., CRT-E2P, CFA-E2P, WG-E2P) when processed in a planetary mill.

Characterization methods

The capillary water absorption of the reference and coated substrates was evaluated according to the standard SRPS U. M8.300, 1985 – EN [15].
Surface roughness (Surtronic 25, Taylor Hobson) of the coatings was evaluated based on the Ra parameter. The obtained data were calculated according to the standard cited in ISO 4287.
Vickers micro-hardness for the reference and coated samples was measured using the Vickers micro-hardness technique (Micro hardness tester model HVS 1000A, ZZV Precision Tool Supply) with a load of 0.3 kg.
To assess self-cleaning efficiency, the initial contact angle was measured using the Surface Energy Evaluation System (Advex Instruments, Brno, Czech Republic), following the procedure described in [10].
The photocatalytic activity of the coatings was assessed following the procedure described by Jovanov et al. [7], and the values were measured using UV/VIS spectroscopy (EVOLUTION 600 spectrophotometer).

Results and discussions

Characterization of reference and illite clay/TiO_2 and kaolinite clay/TiO_2 coated substrates

The capillary water absorption coefficients (A) of the three reference substrates, as well as those coated with illite/nano-TiO_2 and kaolinite/nano-TiO_2, are presented in Table 1. All coated substrates exhibited a decrease in the capillary water absorption coefficient compared to their respective references, regardless of the clay type or impregnation method used. The greatest reduction in the coefficient (A) for all three substrates was achieved with the illite/nano-TiO_2 coating prepared by mechanical activation in the attritor mill. The extent of reduction was strongly influenced by substrate porosity. Namely, it was the most pronounced for the highly porous CFA substrate, moderate for CRT, and negligible for the non-porous WG, consistent with previous findings [7]. Overall, the comparison of capillary water absorption coefficients suggests that the coatings successfully reduce water absorption in the mineral substrates.

Table 1. Capillary water absorption coefficients (A) of the reference – R substrate and substrates with illite/nano TiO_2 and kaolinite/nano TiO_2 coating

Mineral substrate	A, [$kg/m^2min^{1/2}$]
CRT-R	0.73
CRT-H2A	0.54
CRT-E2A	0.59
CRT-E2P	0.63
CFA-R	8.22
CFA-H2A	5.72
CFA-E2A	6.22
CFA-E2P	6.43
WG-R	$1.04x10^{-6}$
WG-H2A	$1.02x10^{-6}$
WG-E2A	$1.03x10^{-6}$

WG-E2P	$1.03x10^{-6}$

The surface properties, including surface roughness and Vickers microhardness of the reference substrates and substrates with illite/nano TiO_2 and kaolinite/nano TiO_2 coating, are presented in Tables 2 and 3, respectively.

The surface roughness (Ra parameter), Table 2, for the coated substrates exhibits an increase in the WG substrate, a negligible increase in the CRT substrate, and a slight decrease in the CFA substrate, after the deposition of all three different coatings. The minor changes in roughness for CRT and CFA are due to these substrates already being rough because of their porosity [14]. Therefore, the coatings did not significantly affect the surface roughness of the two porous substrates. In contrast, when the coating was applied to the WG substrate, the Ra value increased, with the most pronounced effect observed for the E2P coating.

Table 2. Surface roughness (Ra parameter) of the reference -R and substrates with illite/nano TiO_2 and kaolinite/nano TiO_2 coating

Mineral substrate	Ra [μm]
CRT-R	2.45
CRT-H2A	2.53
CRT-E2A	2.50
CRT-E2P	2.55
CFA-R	12.31
CFA-H2A	12.25
CFA-E2A	12.24
CFA-E2P	12.26
WG-R	0.09
WG-H2A	0.20
WG-E2A	0.21
WG-E2P	0.27

The Vickers micro-hardness (HV), results, Table 3, indicate that the hardness of the substrates increased only negligibly after coating with all three different coatings, most likely due to the presence of additional crystalline particles on the surface [16].

Regarding the type of clay used as a coating carrier and the conditions of mechanical impregnation of the active component, the E2A coating, made of kaolin clay impregnated with 10% TiO_2 in an attritor mill, shows better values for Vickers microhardness, compared to the H2A and E2P coatings, when applied to all three types of substrates.

Table 3. Vickers micro-hardness (HV) values of the reference -R and coated substrates

Mineral substrate	Vickers micro-hardness (HV) values
CRT-R	45.0
CRT-H2A	46.4

CRT-E2A	45.8
CRT-E2P	45.5
CFA-R	13.3
CFA-H2A	13.6
CFA-E2A	13.7
CFA-E2P	13.4
WG-R	453.0
WG-H2A	455.5
WG-E2A	456.3
WG-E2P	455.7

The average initial contact angles (θci) for both the reference and coated substrates are shown in Table 4. The θci values for the reference substrates were below 90°, indicating that the substrates used were hydrophilic. After coating, the θci values decreased further, indicating improved hydrophilicity. The most pronounced reduction was observed for the E2A coating, with the θci decrease of nearly 60% on the WG substrate.

Table 4. Average values of initial contact angles (θci) of the reference -R and coated substrates

Mineral substrate	Average initial contact angle values θci, (°)
CRT-R	54.7
CRT-H2A	43.24
CRT-E2A	36.99
CRT-E2P	38.97
CFA-R	52.56
CFA-H2A	38.35
CFA-E2A	35.29
CFA-E2P	37.92
WG-R	67.02
WG-H2A	28.13
WG-E2A	27.40
WG-E2P	28.73

Self-cleaning and photocatalytic properties of the coated substrates

The self-cleaning capabilities of the coated substrates were assessed by measuring θci after 24 hours of UV/VIS irradiation, as shown in Figure 1. All three different types of substrates, coated with three types of coatings demonstrated a reduction in θci during UV/VIS exposure. The most significant decrease occurred within the first four hours, after which the contact angles of the substrates

continued to decline at a slower pace. This pattern reinforces the coating's effectiveness in promoting self-cleaning properties across the different substrate types (highly porous, porous, and non-porous).

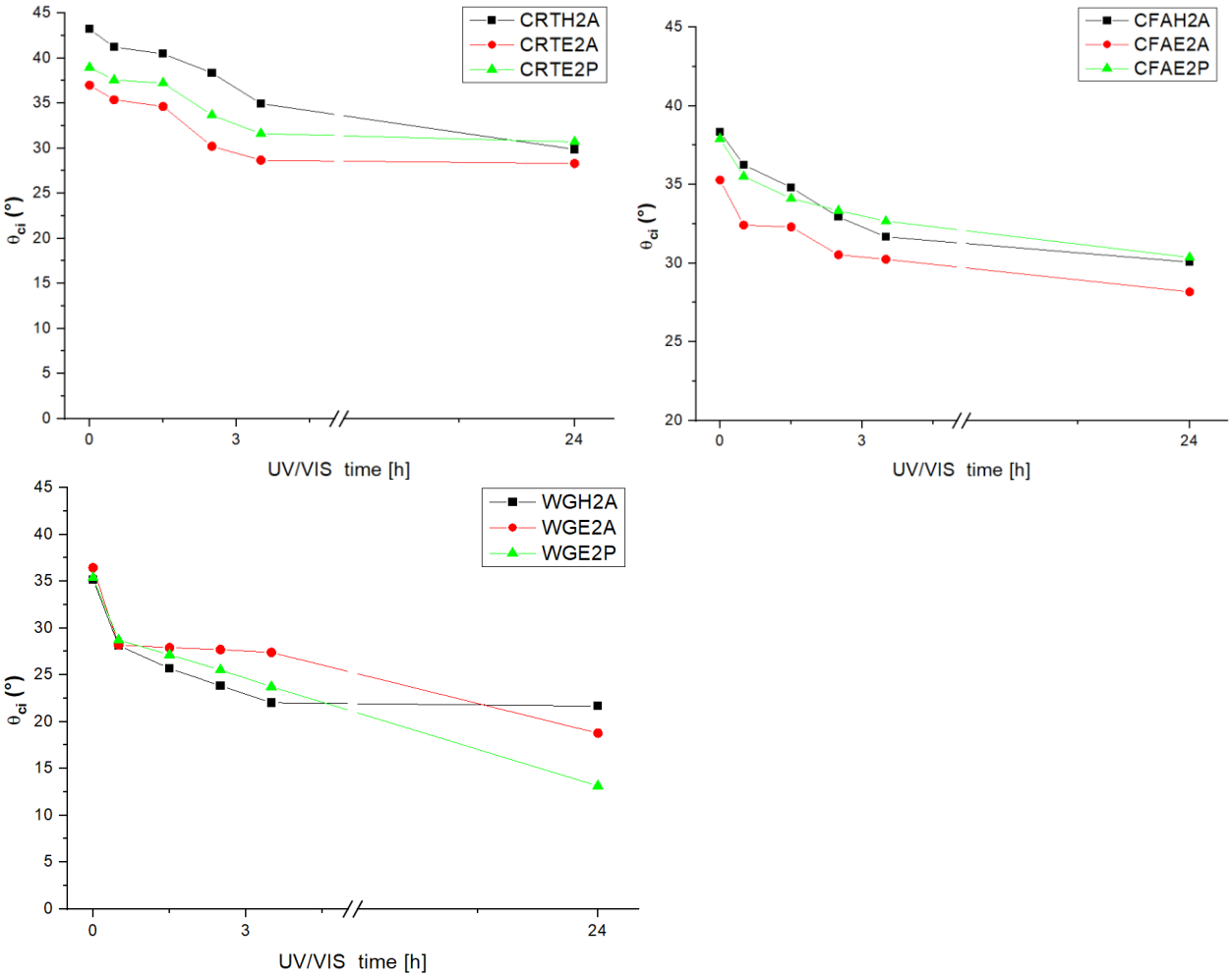

Figure 1. *Initial contact angle (θci) of coated substrates (CRT, CFA and WG) as a function of UV/VIS radiation time.*

The photocatalytic effectiveness was evaluated by measuring the degradation rate of rhodamine B (RhB) after 24 hours of UV/VIS light exposure, illustrated in Figure 2. The CRT substrate achieved around 43% photocatalytic effectiveness with the E2A coating and roughly 26% with the H2A and E2P coatings. In comparison, the CFA-coated substrate showed minimal activity across all three coatings. Conversely, the WG-coated substrate samples displayed remarkable photocatalytic performance, reaching a 90% degradation rate after 24 hours when treated with all three coatings.
The differences in photocatalytic performance can be linked to the varying surface characteristics and porosity of the substrates, as explained presented in Tables 1, 2, and 3. The CFA substrate, characterized by high porosity and significant capillary water absorption, allowed the active suspensions to penetrate deeper into the material, limiting their availability on the surface for light activation. Consequently, only a small amount of the suspension remained on the surface, which restricted the photocatalytic reaction.

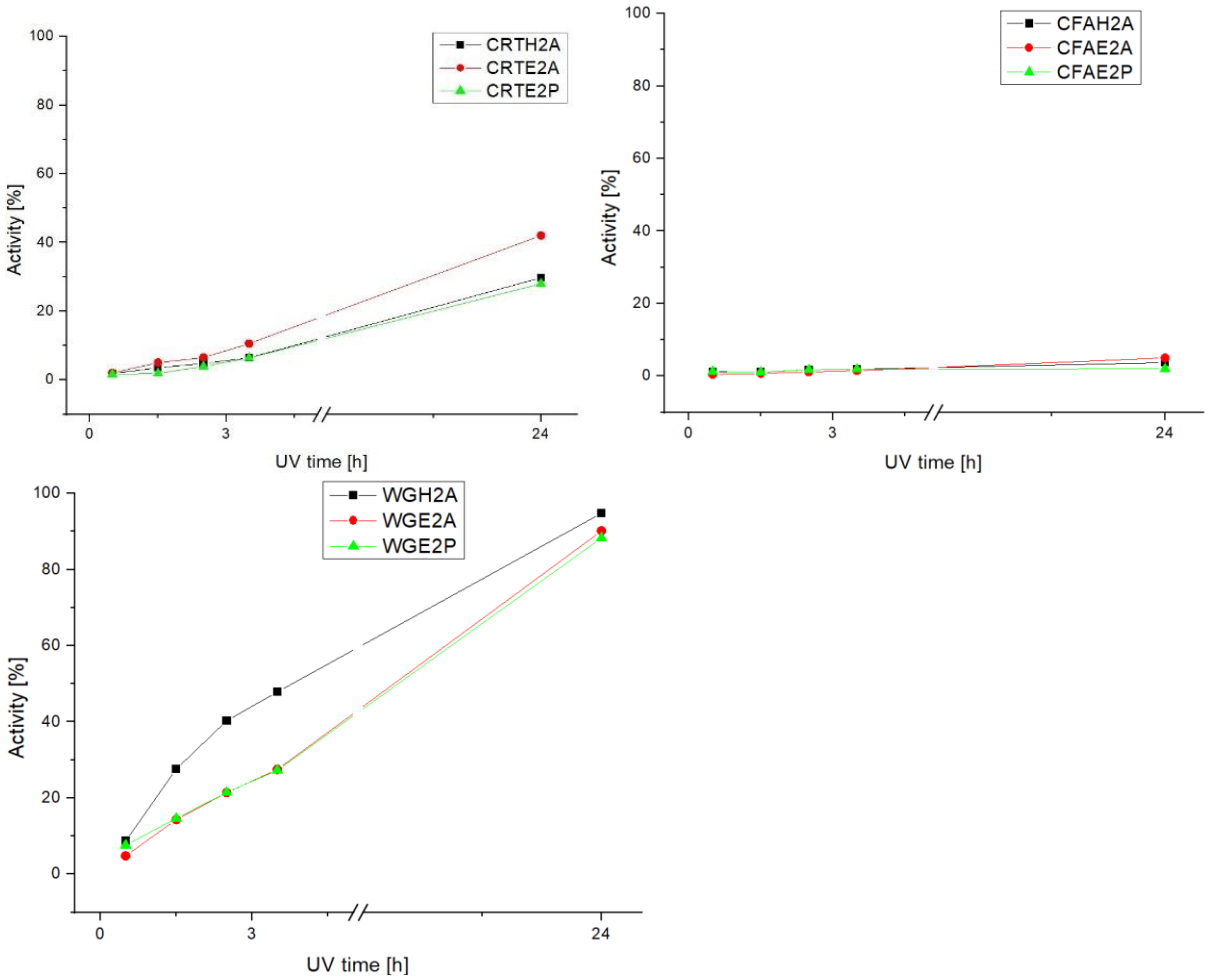

Figure 2. *Photocatalytic activity of coated substrates (CRT, CFA, and WG) as a function of UV/VIS radiation time.*

Conclusion

The study presents the potential of applying two types of clay, illite and kaolinite, as support for impregnation 10wt. % nano TiO_2 to create coatings with self-cleaning and photocatalytic properties. Nano TiO_2 was successfully impregrated on both clays by mechanical activation. The effect of coatings was studied on three different substrates (porous, highly porous, and non-porous) and the coatings have potencial to be applied on porous and non-porous substrate based on the results obtined for capillary water absorption and surface properties (roughness, micro-hardness, and hydrophilicity), as well as functional properties (self-cleaning and photocatalytic) were followed on the applied illite/TiO_2 and kaolinite/TiO_2 coating. Kaolinite/TiO_2 coatings obtained by atrittor mill showed favorable properties. The study shows the potential of using low-cost natural clays as supports for TiO_2 impregnation to create composite photocatalyst coatings, and it offers valuable insights for guiding future research efforts.

Acknowledgement

This research was supported by the Ministry of Education and Science of the Republic of North Macedonia, Grant no. 15-6171/34.

References

1. Rabajczyk A, Zielecka M, Klapsa W, et al. Self-Cleaning Coatings and Surfaces of Modern Building Materials for the Removal of Some Air Pollutants. *Materials* 2020; 14(9), 2161. https://doi.org/10.3390/ma14092161
2. Ranogajec J, Vučetić S, Milan J, et al. Photocatalytic Protection of Building Materials in Real Environmental Conditions. *Microscopy and Microanalysis* 2018; *24*(S1), 1698-1699. https://doi.org/10.1017/S1431927618008978
3. Manzoor Q, Sajid A, Ali Z, et al. Toxicity spectrum and detrimental effects of titanium dioxide nanoparticles as an emerging pollutant: A review. *Desalination and Water Treatment* 2023; *317*, 100025. https://doi.org/10.1016/j.dwt.2024.100025
4. Du X, Men K, Xu Y, et al. Enhanced capacitance performance of Al2O3–TiO_2 composite thin film via sol–gel using double chelators. *Journal of Colloid and Interface Science* 2015;*443*, 170-176. https://doi.org/10.1016/j.jcis.2014.11.038
5. 5. Mishra A, Mehta A, Basu S. Clay supported TiO_2 nanoparticles for photocatalytic degradation of environmental pollutants: A review. *Journal of Environmental Chemical Engineering* 2018; *6*(5), 6088-6107. https://doi.org/10.1016/j.jece.2018.09.029
6. Ozawa M, Matui H, Setsuhara Y. Microstructure and surface/interface characterization of TiO_2-pillared mica for photocatalytic acetaldehyde degradation. Hybrid Advances 2025; 10, 100435 https://doi.org/10.1016/j.hybadv.2025.100435
7. Jovanov V, Rudic O, Ranogajec J, et al. Synthesis of nanocompositecoating based on TiO_2/ ZnAl layer double hydroxides, Materiales de Construcción 2017; 67, 112–120. https://doi.org/10.3989/mc.2017.07215
8. Cardona Y, Korili SA, Gil A. Use of clays and pillared clays in the catalytic photodegradation of organic compounds in aqueous solutions. *Catalysis Reviews* 2023; *66*(5), 2063–2110 https://doi.org/10.1080/01614940.2023.2178736
9. Szczepanik B. Photocatalytic degradation of organic contaminants over clay-TiO_2 nanocomposites: A review. *Applied Clay Science* 2017; 141, 227-239. https://doi.org/10.1016/j.clay.2017.02.029
10. Jovanov V, Zečević V, Vulić T, et al. Preparation and characterization of protective self-cleaning TiO_2/kaolin composite coating, *Materiales de Construcción* 2018; 68, 163 https://doi.org/10.3989/mc.2018.08517
11. Qi Y, Zhao S, Shen Y, et al. A Critical Review of Clay Mineral-Based Photocatalysts for Wastewater Treatment. *Catalysts* 2024; *14*(9), 575. https://doi.org/10.3390/catal14090575
12. Tole I, Delogu F, Qoku E, et al. Enhancement of the pozzolanic activity of natural clays by mechanochemical activation. *Constr. Build. Mater.* 2022; 352, 128739. https://doi.org/10.1016/j.conbuildmat.2022.128739
13. Baláž P. Mechanochemistry in nanoscience and minerals engineering, *Springer Berlin Heidelberg* 2008; pp. 257-296
14. Jovanov V, Vučetić S, Ranogajec J, et al. Photocatalytic illite clay/TiO_2 composite powder synthesized by mechanical activation, GREEN CIRC 2025 PROCEEDINGS https://congress.sctm.mk/event/6/book-of-abstracts.pdf
15. SRPS U.M8.300:1985, Determination of the Capillary Water Absorption of Building Material and Coatings, 1985.
16. Rudic O, Ranogajec J, Vulic T, et al. Photo-induced properties of TiO_2/ZnAl layer double hydroxide coating onto porous mineral substrates, *Ceramic International* 2014; 40(7) 9445-9455. https://doi.org/10.1016/j.ceramint.2014.02.017

Influence of the Process Parameters on Physical Properties of CuMCs

Marko Simić[1,2*], Emilija Nidžović[1,2], Vladimir Pavkov[1,2], Jovana Ružić[1,2]

[1] *Department of Materials,"Vinča" Institute of Nuclear Sciences - National Institute of the Republic of Serbia, University of Belgrade, Serbia*

[2] *Center of Excellence "CEXTREME LAB", Vinča Institute of Nuclear Sciences – National Institute of the Republic of Serbia, University of Belgrade, Belgrade, Serbia*

https://doi.org/10.65614/uisk_yucorr.2025.26.ch32

[*] *marko.simic@vinca.rs*

Abstract

Copper matrix composites (CuMCs) are advanced materials that combine the superior electrical and thermal conductivity of copper with the enhanced strength, hardness, and wear resistance of the reinforcing phases. Due to this unique combination of properties, CuMCs are widely used in electrical contacts, heat sinks, braking systems, and aerospace components. The samples manufactured in this study were obtained after 30h of mechanical alloying, at a 10:1 ball-to-powder ratio. After the powders were mechanically alloyed, they were subjected to three different powders' consolidation techniques: (i.) cold pressing followed by sintering, (ii.) hot pressing and (iii.) spark plasma sintering (SPS). Obtained results of dislocation densities (DD) revealed that highest DD values are recorded at SPS samples, then for hot-pressed samples and lowest at sintered samples for both pure copper and Cu based composites. These findings are in agreement with determined macro hardness results. The lowest values of electrical and thermal conductivities are recorded after sintering at both pure copper and CuMCs samples. On the other hand, values of electrical and thermal conductivities of pure copper show the highest values after hot pressing while highest values of observed CuMCs are reached after SPS. Furthermore, values of electrical and thermal conductivities of pure copper show the highest values after hot pressing while highest values of observed CuMCs are reached after SPS. Deviation that the hot-pressed pure copper sample exhibits slightly better conductivity compared to the sample after SPS could be a consequence of lower electron scattering at grain boundaries and lower porosity.

Keywords: *Cu matrix composites; dislocation density; electrical conductivity; thermal conductivity*

Acknowledgements

This work was funded by the Ministry of Science, Technological Development and Innovations of the Republic of Serbia (Contract No. 451-03-136/2025-03/200017) and by the Science Fund of the Republic of Serbia, Grant No. 7365, Development of dispersion-strengthened metal-based materials for applications in fusion reactor - DisSFusionMat.

Adsorption/photocatalytic Degradation of Congo Red Using UiO-66 MOF and Activated Carbon Under Natural Solar Irradiation

Marija Egerić[1,*], Ljiljana Matović[1,2,3,4], Radojka Vujasin[1], Emilija Nidžović[1,2], Yi-nan Wu[3,4], Djordje Petrović[1], Aleksandar Devečerski[1]

[1] *Vinča Institute of Nuclear Sciences – National Institute of the Republic of Serbia, University of Belgrade, Mike Petrovića Alasa 12-14, Vinča, Belgrade, Serbia*

[2] *Center of Excellence "CEXTREME LAB", Vinča Institute of Nuclear Sciences – National Institute of the Republic of Serbia, University of Belgrade, Mike Petrovića Alasa 12-14, Vinča, Belgrade, Serbia*

[3] *College of Environmental Science and Engineering, State Key Laboratory of Pollution Control and Resource Reuse, Tongji University, Shanghai 200092, P.R. China*

[4] *Shanghai Institute of Pollution Control and Ecological Security, Shanghai 200092, P.R. China*

https://doi.org/10.65614/uisk_yucorr.2025.26.ch33

[*]*egericmarija@vin.bg.ac.rs*

Abstract

The presence of synthetic dyes in industrial effluents poses a significant environmental concern due to their high stability and toxicity. This study investigates the removal of Congo Red (CR) dye from aqueous solution using UiO-66 metal–organic framework (MOF), activated carbon (AC), and their composite under natural solar irradiation. The composite was synthesised by simple mechanical mixing of equal (50 wt.%) proportions of MOF and AC powders in a porcelain mortar, a cost-effective and mild synthesis approach that preserves the MOF structure while enabling large-scale preparation. The adsorption/photocatalytic mechanism was evaluated through UV–Vis spectroscopy to assess dye degradation efficiency, while FTIR, Raman, and XRD analyses provided insight into the interaction mechanisms. After four hours of natural sun irradiation, the MOF/AC composite exhibited superior CR removal efficiency (95%) compared to both individual components (≈75%), confirming the synergistic role of MOF and AC in photocatalytic degradation, where AC acts as an electron sink. XRD, FTIR, and Raman spectroscopy revealed that CR interacts with the Zr–O nodes of MOF through its S=O groups, indicating chemisorptive bonding. Additionally, all samples achieved a removal efficiency more than 50% higher than in dark conditions. The reusability study indicated that pure MOF maintained the highest stability over multiple cycles, while composites gradually lost activity due to AC surface saturation. These findings demonstrate that combining MOF with AC provides a sustainable and energy-efficient strategy for dye removal under natural solar conditions.

Acknowledgements

This research was funded by The Ministry of Science, Technological Development and Innovation of the Republic of Serbia under registration number: 451-03-136/2025-03/ 200017.

Development and Characterization of Basalt-Based Glass-Ceramic Composites for Extreme Environment

Aleksa Luković[1], Diana Carolina Lago[2], Jozef Kraxner[2], Branko Matović[1], Dušan Galusek[2], Bratislav Todorović[3], Sanja Petrović[3], Jelena Maletaškića[1]

[1] *Vinča Institute of Nuclear Sciences - National Institute of The Republic of Serbia, University of Belgrade, Mike Petrovića Alasa 12-14, Belgrade 11000, Serbia*

[2] *FunGlass, Alexander Dubček University of Trenčín, Študentská 2, 911 50, Trenčín, Slovakia*

[3] *Faculty of Technology, University of Niš, P.O. Box 79, 16000 Leskovac, Serbia*

https://doi.org/10.65614/uisk_yucorr.2025.26.ch34

Abstract

This study presents the synthesis and characterization of durable basalt-based glass-ceramic materials and composites tailored for chemically and mechanically aggressive conditions. Utilizing basalt rock from the Vrelo deposit in Serbia as the primary precursor and iron mine tailings from the Bor mining region as a sustainable additive, glass-ceramics were produced via high-temperature melting, quenching, and controlled thermal treatment. Comprehensive analyses, including DTA, XRD, HT-XRD, FTIR, and SEM/EDS, confirmed the formation of fine-grained pyroxene-type silicates, predominantly diopside and augite, with no compromise in microstructural integrity due to tailings incorporation. Chemical durability was assessed through immersion tests in aqueous solutions at pH 3, 7, and 12 for up to 30 hours. ICP-OES analysis revealed minimal elemental leaching, and SEM/EDS verified no surface degradation or compositional changes post-corrosion, underscoring exceptional chemical resistance. These findings highlight the potential of basalt-based glass-ceramics, enhanced by industrial waste, for applications in geotechnical barriers, chemical reactor linings, and waste containment systems, offering a sustainable and high-performance solution for demanding industrial and environmental challenges.

Keywords: *Basalt glass-ceramics; chemical durability; sustainable materials; mine tailings; extreme environments*

Nano Composite Coating on Titanium with Anti-Cancer Activity: A Strategy for Preventing Oral Cancer Recurrence

Evelina Herendija[1,*], Milica Jakšić Karišik[2], Marijana R. Pantović Pavlović[3], Miroslav M. Pavlović[3], Olivera Mitrović-Ajtić[4], Nenad L. Ignjatović[5], Miloš Lazarević[2]

[1] *University of Belgrade, Multidisciplinary PhD Studies, Biomedical Engineering and Technology, Studentski Trg 1, 11000, Belgrade, Serbia*

[2] *University of Belgrade, Faculty of Dental Medicine, Dr Subotića 8, 11000 Belgrade, Serbia*

[3] *University of Belgrade, Institute of Chemistry, Technology and Metallurgy, Department of Electrochemistry, Njegoševa 12, 11000, Belgrade, Serbia*

[4] *University of Belgrade, Institute for Medical Research, Department of Molecular Oncology, Dr. Subotića 4, 11129, Belgrade, Serbia*

[5]*Institute of Technical Sciences of the Serbian Academy of Science and Arts, Knez Mihailova 35/IV, 11000 Belgrade, Serbia*

https://doi.org/10.65614/uisk_yucorr.2025.26.ch35

[*]*nherendija@yahoo.com*

Abstract

The chemical modification of titanium implant surfaces significantly influenced their biological interactions. A novel surface design was developed that transitions from anticancer-inert to highly bioactive against oral squamous cell carcinoma (OSCC) cells. Titanium samples were coated using a combined anodizing and anaphoretic electrodeposition technique. The biological responses of coated (Ti/Coating) versus uncoated (Ti) titanium were evaluated in SCC-25 cells. Flow cytometry assessed apoptosis, cellular uptake, ROS generation, and cell cycle progression, while gene and protein expression were analyzed using qPCR and Western blot. The Ti/Coating surface significantly reduced cell viability, induced early apoptosis (via BAX upregulation and BCL2 downregulation), and caused G2/M cell cycle arrest. Increased ROS production contributed to cytotoxicity. Expression of EMT markers (VIM, SNAIL, SLUG) was inhibited, while CDH1 was upregulated, correlating with reduced cell migration. Furthermore, Ti/Coating suppressed AKT/mTOR and Wnt/β-catenin signaling pathways. These findings demonstrate that engineered titanium coatings can actively suppress OSCC cell proliferation and migration, offering a promising approach for bioactive implant surfaces with dual structural and therapeutic functions.

Keywords: *chitosan; coatings-cell interaction; nano-hydroxyapatite; oral cancer cells; selenium; surface-chemical modification*

SPONSORS

SPONZORI


JADRAN


INTERNATIONAL SOCIETY OF ELECTROCHEMISTRY
ISE

Кнеза Милоша 7
11000 Београд

Савез инжењера и техничара Србије

Union of Engineers and Technicians of Serbia


KANSAI
HELIOS

Firestop®
INTERNACIONAL

Inovativni protivpožarni premazi za sigurnu budućnost

Kompanija **Firestop Internacional** je sa svojim brendom **FIRESTOP** izbor broj 1 na tržištu Srbije i regiona u oblasti ekspandujućih protivpožarnih premaza za zaštitu čelika i drveta.

U svom portfoliju ima i **Tinto color** osnovne i završne premaze za zaštitu metala, koji se mogu koristiti samostalno ili u sklopu Firestop sistema zaštite.

Korišćenjem ovog inovativnog sistema premaza postiže se kompletna antikorozivna i protivpožarna zaštita.

Firestop Internacional d.o.o.
Gavrila Principa 20, 22330 Nova Pazova
Tel. 022 321 030, 326 342, 323 134 / Fax. 022 325 002
office@internacional.rs / www.firestopinternacional.rs

ALFATERM

ALFATERM d.o.o. je osnovano 1993. kao specijalizovano preduzeće za termotehnička postrojenja i uređaje površinske zaštite.
Zaposleni u preduzeću imaju tridesetogodišnje iskustvo u razvoju tehnologija i postrojenja površinske zaštite.
Okrenuti smo u smeru pronalaženja kreativnih rešenja i usluga koja su osmišljena da zadovolje veoma različite potrebe naših kupaca.

Ventilacija
- Generatori toplog vazduha i ložišta
- Otprašivanje
- Ventilatori

Plastifikacija metala
- Uređaji za predtretman radnih komada
- Kabine za nanošenje premaza u prahu
- Sušare za vlagu
- Peći za pečenje premaza u prahu

Mokro lakiranje i farbanje
- Kabina za lakiranje sa suvim filterom
- Fini filter
- Zagrejači svežeg vazduha,
- Kolica
- Pomoćna i prateća oprema

Transporteri

Zastupništvo

GRACO
www.graco.com
KEWESTA
www.kewesta.de
Liquid Control
www.liquidcontrol.co.uk

ALFATERM
Njegoševa 6, 32103 Čačak • Srbija
• e-mail: office@alfaterm.rs • www.alfaterm.rs
tel: +381 32 320 645 • fax: +381 32 226 222

Protection upgraded

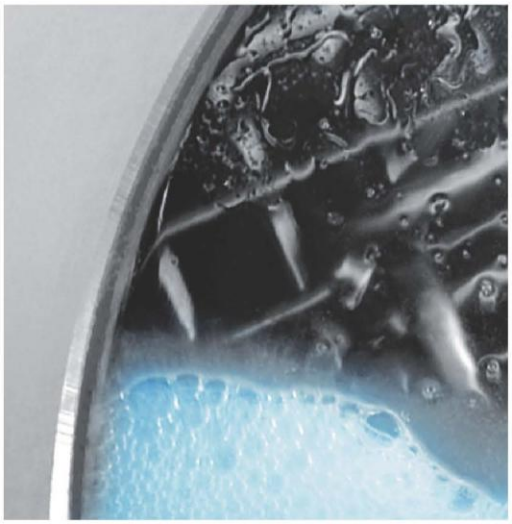

Custom Made Chemical Specialities for Surface Treatment

- Optimal solutions for all key applications of surface finishing
  - **Industrial Parts Cleaning**
  - **Metal Pre-treatment**
  - **Functional and Decorative Electroplating**
- Worldwide representatives in more than 50 countries
- A company of Freudenberg Group since 2011

SurTec doo Serbia

sales.serbia@surtec.com
www.SurTec.com

Preljinska baluga bb
32000 Cacak, Srbija

Tel. +381 32 538 1569
Fax. +381 32 538 1569

Institut za preventivu

zaštitu na radu, protivpožarnu zaštitu i razvoj d.o.o.

21000 Novi Sad • Kraljevića Marka 11 • tel/fax: 021 / 420-571, 420-572, 420-573
institut@izp.rs • www.izp.rs

ATC 04-010
АКРЕДИТОВАНО СЕРТИФИКАЦИОНО ТЕЛО
SRPS EN 45011:2004

ATC 06-013
АКРЕДИТОВАНА КОНТРОЛНА ОРГАНИЗАЦИЈА
SRPS ISO/IEC 17020:2002

ATC 01-069
АКРЕДИТОВАНА ЛАБОРАТОРИЈА ЗА ИСПИТИВАЊЕ
SRPS ISO/IEC 17025:2006

- bezbednost i zdravlje na radu
- zaštita od požara i eksplozije
- zaštita životne sredine
- tehnički pregledi objekata
- izrada projektno tehničke dokumentacije
- katodna zaštita
- akreditovana tela
- sertifikacija i ispitivanje opreme u "Ex" izvedbi

ИНСТИТУТ ЗА ПУТЕВЕ
АД БЕОГРАД


PPG

ИНСТИТУТ ЗА ОПШТУ И ФИЗИЧКУ ХЕМИЈУ
INSTITUTE OF GENERAL AND PHYSICAL CHEMISTRY